ELECTRONIC SPECTRA

OF SOME

DIATOMIC MOLECULES

Abstract of a thesis presented for the degree

of

D.Phil. in the University of Oxford

by

G.G. Chandler

Exeter College

Physical Chemistry
Laboratory

July 1965

BODLEIAN LIBRARY OXFORD
DEPOSITED
THESIS
18.1.66

ABSTRACT

The work presented in this thesis is divided into two chapters, each being devoted to a study of the band system of a diatomic molecule of Group VI elements. The molecules studied were Se_2 and TeO, and their choice depended on the feasibility of the experimental work and on some current trends in theoretical thinking. To gain useful information about these molecules from their spectra it was essential that rotational analyses should be done and thus the experimental work was directed towards achieving high dispersion and maximum resolution, using isotopically pure samples. The theoretical interest in Se_2 and TeO arises from the differences to be found in the molecules formed from the Group VI elements with increasing nuclear charge. Thus much of the earlier work on Se_2 has been shown to be wrong because of the misunderstanding of the nature of a $^3\Sigma$ state for a heavy molecule.

1. Se_2

Earlier work by the author on the emission spectrum has shown that the main system arises from the transition $^3\Sigma_u^- - {}^3\Sigma_g^-$, in which the spin-splitting constants λ are so large that two widely separated components are given, F_1 and F_2,F_3 for each state. The present work gives the results of a complete study of the absorption spectrum of the F_1-F_1 components of the separated isotopic species $^{78}Se_2$ and $^{80}Se_2$.

The numerous upper state perturbations confuse the analysis but, by studying the bands of both isotopes arising from all the stable upper state levels, 0 to 21, it has been found possible to derive accurate rotational and vibrational constants. The upper state has a potential maximum and the observation of several predissociations prompted a reinvestigation of the emission spectrum. Two limiting curves of predissociation are found and the atomic products have been identified. The value of the ground state dissociation energy, obtained from these, is in fair agreement with the latest mass spectroscopic figure but is much more precise.

The derived constants, in $cm.^{-1}$, for $^{80}Se_2$ are as follows: F_1

$T_{ee} = 25980.36$

$\omega'_e = 246.291$	$\omega''_e = 385.3028$
$x_e\omega'_e = 1.016$	$x_e\omega''_e = 0.96363$
$y_e\omega'_e = -5.49 \times 10^{-3}$	$y_e\omega''_e = -8.184 \times 10^{-4}$
$B'_e = 0.07048$	$B''_e = 0.08992$
$\alpha'_e = 0.000345$	$\alpha''_e = 0.000288$
	$\gamma''_e = -6.10 \times 10^{-7}$
$D = 4 \times 10^{-8}$	$D_v = 2.4 \times 10^{-8} - 0.023 \times 10^{-8}(v+\frac{1}{2})$
$r'_e = 2.4464$ Å	$r''_e = 2.1661$ Å

$$D_0^0 = 24974 \pm 20 \text{ cm.}^{-1} = 71.39 \pm 0.03 \text{ k.cal.mole}^{-1}$$

At the same time the observation of some $F_2,F_3 - F_2,F_3$ absorption bands has enabled the vibrational numbering, previously unknown, to be confirmed by the isotope effect. The splitting between the three components of $^3\Sigma^-$ is such that the ground state appears to be in case-c while the upper state retains some case-b character.

The derived constants, in cm^{-1}, for $^{80}Se_2$ are as follows: F_2,F_3

$T_{ee} = 25545.85 + 2\lambda''$ $\qquad 2\lambda''-2\lambda' = 434.51$

$\omega_e' = 246.42$ $\qquad \omega_e'' = 386.43$

$x_e\omega_e' = 1.225$ $\qquad x_e\omega_e'' = 0.9058$

$y_e\omega_e'' = -13.13 \times 10^{-4}$

$B_e'(F_2) = 0.07067$ $\qquad B_e''(F_2) = B_e''(F_3) = 0.09012$

$B_e'(F_3) = 0.07105$ $\qquad \alpha''(F_2) = \alpha''(F_3) = 0.000297$

$\alpha'(F_2) = \alpha'(F_3) = 0.000553$

$r_e'(F_2,F_3) = 2.4400$ Å $\qquad r_e''(F_2,F_3) = 2.1631$ Å

2. TeO

The ground states, $^3\Sigma^-$, of all the molecules of the Group VI elements so far analysed, O_2, SO, S_2, SeO, have been described in terms of Hund's case-b with an increasing value of the spin-splitting constant λ'' as the nuclear charge increases. For Se_2 the transition to case-c

is almost complete and the study of the main system of TeO was designed to determine whether the ground state is $^3\Sigma^-$ and, if so, how the increase in nuclear charge has affected the value of λ''.

As in the case of Se_2, the problems involved in the analysis of the spectrum of TeO have been largely due to the presence of numerous isotopic species. In the present work the use of highly separated isotopes has again so clarified the spectrum that the analysis is indisputable, and it shows that the spin-splitting in the $^3\Sigma^-$ states of TeO has become so large that they have gone over into case-c, that is into 0^+ and 1 states. The difference in the behaviour of a $^3\Sigma^-$ state in case-b with a large value of λ (for example, in SeO) and in case-c (for example, in TeO) is discussed.

The derived constants, in $cm.^{-1}$, for ^{128}TeO are as follows:

	T_{00}	ω_e	$x_e\omega_e$
A 1	$27641.83 + 2\lambda''$	-	-
A 0^+	28036.48	$\Delta G_{\frac{1}{2}} = 445.25$	
X 1	$2\lambda''$	798.70	4.00
X 0^+	0	797.69	4.00

$2\lambda'' \sim 2750$

	B	$10^3\alpha$	r, Å
$A\ ^{1+}$	$B_0 = 0.2779$	-	$r_0 = 2.066$
$A\ ^{1-}$	$B_0 = 0.2775$	-	
$A\ 0^+$	$B_e = 0.2763$	5.5	$r_e = 2.071$
$X\ ^{1+}$	$B_e = 0.3575$	2.379	$r_e = 1.821$
$X\ ^{1-}$	$B_e = 0.3572$	2.368	
$X\ 0^+$	$B_e = 0.3560$	2.375	$r_e = 1.825$

The upper state is perturbed and is also predissociated in $A0^+$ at v=9. The dissociation energy D_0'' is estimated to be about 90 k.cal.mole^{-1}.

In Appendices are given details of (A) a reinvestigation of the emission spectrum of XeO, in which a new assignment of the diffuse rotational lines, based on the isotope effect, is proposed; (B) the theoretical performance of an Ebert spectrograph and of an order-sorter; (C) Algol computer programmes for the settings of a Jarrell-Ash 3.4 metre grating spectrograph, and for the determination of potential curves by the Klein method.

ELECTRONIC SPECTRA
OF SOME
DIATOMIC MOLECULES

A thesis presented for the degree

of

D.Phil. in the University of Oxford

by

G.G. Chandler

Exeter College

Physical Chemistry
Laboratory

July 1965

CONTENTS

	page
Chapter I. The $B^3\Sigma_u^- - X^3\Sigma_g^-$ Main System of Se_2	1
Introduction	2
Experimental	5
Rotational Analysis	8
F_1-F_1 Sub-bands	13
Determination of Rotational Constants	33
Vibrational Analysis	40
F_1-F_1 Sub-bands	43
Potential Energy Curves	54
Perturbations & Predissociations in F_1 component of $B^3\Sigma_u^-$	60
F_2,F_3-F_2,F_3 Sub-bands	74
Rotational Analysis	74
Vibrational Analysis	79
Triplet Splitting	84
States of Se_2	87
Dissociation Energy	89
Discussion	100
Chapter II. The $A^3\Sigma^+$-$X^3\Sigma^-$ Main System of TeO	103
Introduction	104
Experimental	105
Rotational Analysis	109
Vibrational Analysis	117
Perturbations	121
Dissociation Energy & $X0^+$-$X1$ Splitting	123
Discussion	124
Appendix A. The Spectrum of XeO	128
Introduction	129
Experimental	131
Analysis	135
Discussion	140

...continued

		Page
Appendix B.	Theoretical Order-sorting for an Ebert Spectrograph	142
Appendix C.	Two Algol Computer Programmes	150
Appendix D.	Vacuum wave numbers of lines for analysed bands of Se_2	156
Appendix E.	Vacuum wave numbers of lines for analysed bands of TeO	201
References		222
Acknowledgement		227

LIST OF TABLES

Chapter I. Se_2

1. Rotational constants for F_1 component of $X^3\Sigma_g^-$, $^{80}Se_2$ 36
2. " " " " " " " $^{78}Se_2$ 37
3. " " " " " " $B^3\Sigma_u^-$, $^{80}Se_2$ 38
4. " " " " " " " $^{78}Se_2$ 39
5. Origins of absorption F_1-F_1 bands 49
6. " " emission " " 50
7. Vibrational constants for F_1-F_1 sub-system 51
8. Vibrational isotope effect for F_1-F_1 absorption bands 52
9. " " " " " emission " 53
10. Rotational constants for F_2,F_3 components of $B^3\Sigma_u^-$ 77
11. " " " " " " $X^3\Sigma_g^-$ 78
12. Band origins and vibrational constants for F_2,F_3-F_2,F_3 82
13. Vibrational term values & isotope effect " " 83

Chapter II. ^{128}TeO

14. Rotational constants for $A0^+$-$X0^+$ 115
15. " " " A1 - X1 116
16. Vibrational isotope effect 119
17. Band origins and vibrational constants 120

LIST OF FIGURES

		page
Chapter I.	**Se_2**	
1.	Plots of B'_v (obs.-calc.) against v' for F_1 component	35
2.	Plots of $T'_{v,e}$ (obs.-calc.) against v' for F_1 component	47
3.	Potential curves for F_1 component of ground state	58
4.	Potential curves for F_1 component of upper state	59
5.	Schematic effective potential curves for case c^+ of predissociation	64
6.	Enlargement of part of Fig. 5.	64
7.	Limiting curves of predissociation for F_1 component of upper state	68
8.	Correlation of atomic J with molecular	95
9.	Atomic products and their energies for the possible configurations II and III	96
Chapter II.	**TeO**	
10.	Correlation of rotational symmetries for transition from case-b (large λ) to case-c	112

LIST OF PLATES

			page
Chapter I.		Se_2	
1.	16-0	F_1-F_1 absorption band of $^{78}Se_2$	14
2.	15-0	" " " " "	17
3.	12-0	" " " " "	21
4.	6-2	F_1-F_1 emission band of $^{78}Se_2$	26
5.	6-3	" " " " $^{80}Se_2$	28
6.	0-9	F_2,F_3-F_2,F_3 absorption band of $^{80}Se_2$	75
Chapter II.		^{128}TeO	
7.	0-7	0^+-0^+ band	110
8.	0-7	1-1 band	111
Appendix A.		XeO	
9.	0-6	band	139

CHAPTER I

THE $B^3\Sigma_u^- - X^3\Sigma_g^-$ MAIN SYSTEM OF Se_2

Introduction

The change in properties down a group is most clearly seen in the homonuclear members where there is no dissymmetry caused by a difference in mass or electronegativity. The spectra of O_2 and S_2 have been extensively studied and firm conclusions reached about the nature of many of the electronic states and their relative energies, the transition probabilities, the interactions between states of similar energies, the dissociation energies and internuclear distances.

Similar studies of Se_2 have been much less conclusive, partly because of the elevated temperatures necessary for its observation but more especially because the spectrum is normally complicated by the presence of numerous isotopic species.

Many attempts have been made on the vibrational analysis of the main B-X system which is red-degraded and extends from 3270 - 6700 Å. During the 1930s the bands in this region were assigned to various systems[1-8]. In 1934, Olsson[9] made the first study of the isotopic shifts and this work was essentially confirmed by Nevin[10] in 1935. In 1938 Olsson[11] gave the following equation for the origins of the few emission bands (assigned as 8-6, 9-7, 10-4, 10-5, 10-6) of $^{80}Se_2$ that he measured with high resolution in the u-v region near 3900 Å:

$$\nu = 26083 + 271.1(v'+\tfrac{1}{2}) - 2.19(v'+\tfrac{1}{2})^2 - 391.9(v''+\tfrac{1}{2}) + 1.04(v''+\tfrac{1}{2})^2 .$$

The agreement between calculated and observed isotopic shifts for $^{80,80}Se_2$ and $^{80,78}Se_2$ was not satisfactory but he found that any change

in the upper state numbering gave worse agreement for the band-heads measured by Nevin. The rotational analysis showed single P and R branches, lines with odd values of J" being absent; from this he concluded that the bands arose from the transition $^1\Sigma_u^+ - {}^1\Sigma_g^+$. In 1939 Rosen[12] summarised his work on the absorption, emission and resonance spectra of Se_2 and found that the bands between 2800 Å and 5200 Å constituted a single system, in agreement with the conclusions of Asundi and Parti[7], the band-heads being given by

$$\nu = 26035 + 281.11(v'+\tfrac{1}{2}) - 2.65(v'+\tfrac{1}{2})^2 - 391.77(v''+\tfrac{1}{2}) + 1.06(v''+\tfrac{1}{2})^2 - 0.002(v''+\tfrac{1}{2})^3 .$$

However in 1937, Bhatnager, Lessheim and Khanna[17] found that the vapour of selenium was paramagnetic, although they did not know how much Se_2 was present. In similar work in 1964 Massen, Weijts and Poulis[68] studied the temperature dependence of the magnetic susceptibilities of the liquid and saturated vapour of selenium; they found that the Se_2 component of the vapour was almost entirely paramagnetic. This indicates that the ground state is $^3\Sigma_g^-$. Rosen[12], Asundi and Parti[7] and Leelavathi and Rao[15] also suggested that the main system of Se_2 must be $^3\Sigma - {}^3\Sigma$ by analogy with O_2 and S_2.

In 1951 Davis and Jenkins[14] used highly separated isotopes of selenium to reinvestigate under high resolution the emission bands in the u-v region; in 1954 Davis[13] gave a full account of the work, in which he came to the same conclusions as Olsson concerning the

singlet nature of the transition and found that vibrational perturbations in the upper state affected the isotopic shifts. He suggested that a reinvestigation of the whole of the main system was needed to elucidate the problems of vibrational analysis and electronic transition.

In 1963 the author[16] studied, with very high dispersion, some emission bands, in the red as well as in the u-v region, of the separated isotopic species $^{78}Se_2$ and $^{80}Se_2$ and showed that the main system arises from the transition $^3\Sigma_u^- - {}^3\Sigma_g^-$. However, the value of the case-b spin-splitting constant λ'' was found to be so large that the $^3\Sigma_g^-$ state was split into two widely separated components, F_1 and F_2,F_3, which could be treated independently, although their rotational and vibrational constants appeared to be similar. Despite the measurement, at the same time, of many emission band-heads of both isotopes, the agreement of the observed and calculated isotopic shifts was poor, and it was concluded that it would be necessary to study the absorption spectrum, again using separated isotopes, in order to get a reference point for the vibrational numbering, i.e. $v'=0$ at the red end and $v''=0$ at the u-v end of the main system. The results of that study, and of the analysis of some more emission bands, are given here.

Experimental

The emission bands previously studied by the author were of the isotopic species $^{80}Se_2$ and $^{78}Se_2$ and, for comparison, 96% separated samples of the same isotopes were obtained from A.E.R.E., Harwell, for the absorption work. Because of the availability of only milligram amounts of the isotopes, a small quartz absorption tube with windows sealed on by the manufacturers was used. In order to avoid recirculation problems this was sealed off under vacuum after the addition of about 1/4 milligram of selenium isotope. This quantity was found by preliminary tests with natural selenium to be sufficient for absorption studies and the same tubes were used at irregular intervals over a period of one year with no deterioration.

The tubes were 22 cm. long, diameter 1 cm., with side-arms about 12 cm. long. To prevent the condensation of material on the windows a heating system was devised which kept the windows hot and at the same time allowed the main-tube and side-arm temperatures to be varied independently. Three pieces of quartz tubing, of internal diameter just sufficient to enclose the absorption tube as sleeves, were wound with resistance wire and thoroughly lagged so that they could act as ovens up to the melting point of the quartz. Two of these 'ovens' were controlled by a Variac and they were capable of heating the main part of the absorption tube evenly to at least 900°C. The third 'oven' was separately controlled and this enabled the side-arm temperature to

be varied over a wide range. The 'ovens' were each 15 cm. long and thus the absorption tube was completely surrounded.

Preliminary photographs were taken on a Hilger E1 prism spectrograph to find the best temperature for clean spectra. It was found that quite low temperatures were sufficient and usually a main-tube temperature of about 400°C and a side-arm temperature of 250°C were used. But for bands at the red end of the system, from high ground state vibrational levels, temperatures of 800°C and 500°C were used. The main-tube temperature, which controlled the complexity of the spectrum, was kept as low as possible to prevent overlapping by unwanted bands arising from high ground state vibrational levels.

Photographs were taken in a third order of a 6.65 metre grating spectrograph, giving a reciprocal plate dispersion of about 0.3 Å/mm.. A 900W xenon lamp was used as a source of continuum, with which exposures of from 2 to 6 minutes on Ilford N.50 plates were sufficient. The plates were measured on a Zeiss Abbe comparator and the wavenumbers of the molecular lines interpolated, by the Oxford KDF9 computer, from measurements of standard iron arc lines.

The successful use of such a small absorption tube suggests that the method can be extended to other molecules of which only milligram quantities are available. The limitations are threefold: the aperture is cut-down thus slightly reducing the speed, the optimum amounts of the constituents must be found in preliminary experiments

and, unless the electronic transition is fully allowed, the short path-length may prevent efficient contrast being obtained. In the present case none of these points was found to be troublesome.

Rotational Analysis

The main features of the rotational analysis were revealed during the author's emission study, and it is necessary merely to recapitulate. Mulliken[47] and Herzberg[48] have shown that a $^3\Sigma$ state is described either by Hund's case-b or by case-c depending on the strength of the coupling of L and S with the internuclear axis. In case-b the electronic angular momentum Λ is zero for Σ states and the spin vector S is coupled to the angular momentum of rotation N. N and S give the resultant J, the total angular momentum, and the possible values of J for a $^3\Sigma$ state are thus N+1, N, N-1. These correspond to three energy states for each value of N and are designated by

F_1 where $J = N+1$

F_2 where $J = N$

F_3 where $J = N-1$

Kramers[18], Van Vleck[19], Hebb[20] and Kovács[21] have discussed the splitting of a $^3\Sigma$ state which is defined in terms of two parameters, λ and γ. The physical significance of these is as follows. The terms involving γ are due to the effect of rotation of the molecule. This produces directly a magnetic moment which interacts with the spin vector S, and also produces an L uncoupling mechanism; without rotation the precession of L for a Σ state is perpendicular to the internuclear axis but with rotation this precession becomes non-uniform and a resultant is formed along N which couples with S in the same way

as N. This uncoupling produces a component of angular momentum along the axis and is equivalent to promotion of the electrons from the Σ ($\Lambda=0$) state to a Π ($\Lambda=1$) state.

The terms involving λ arise from spin-spin interaction between the electrons which is equivalent to an interaction of S with the axis, and also arise from further L uncoupling; this is due to polarisation of the molecule by the electron spin moments, and again is equivalent to $\Sigma \rightarrow \Pi$ promotion.

The conclusion is reached that the size and sign of the constants λ and γ depend on the energy separation of Π states, which may be considered as perturbing states, from the $^3\Sigma^-$ state. The spin-spin and spin-orbit interactions for the $^3\Sigma$ and the Π states provide, in the first approximation, expressions of the same form, i.e. dependence on J. Thus the observed splittings are considered to be due to the sum of the two effects.

The original formula for the rotational levels of a $^3\Sigma$ state, given by Kramers, fails when B/λ is small; a more rigorous formula, given by Schlapp[22], is adequate for the present work but neglects centrifugal distortion terms:

$$F_1(N) = BN(N+1) + B(2N+3) - \lambda - (B^2(2N+3)^2 + \lambda^2 - 2B\lambda)^{\frac{1}{2}} + \gamma(N+1)$$

$$F_2(N) = BN(N+1)$$

$$F_3(N) = BN(N+1) - B(2N-1) - \lambda + (B^2(2N-1)^2 + \lambda^2 - 2B\lambda)^{\frac{1}{2}} - \gamma N$$

In the series O_2, SO, S_2 there is a rapid increase in the values of λ for the $^3\Sigma^-$ ground states (1.985[49], 5.276[42], 11.65[43] cm.$^{-1}$ respectively) but little change in the values of γ ($\pm$ about 0.01 cm.$^{-1}$). For the molecules in this series the lowest Π states lie above $^3\Sigma_g^-$ and the values of λ'' should therefore have the same sign; direct determination for O_2 and SO shows that λ'' is positive. Similar values for the upper $^3\Sigma^-$ states are less useful for comparison purposes because of the presence of extensive perturbations. The analysis by Barrow and Deutsch[23] of the $^3\Sigma^- - {}^3\Sigma^-$ system of SeO provided the key to the situation in Se_2. It was found that λ'' was so large (86.4 cm.$^{-1}$) that an adequate approximation to the Schlapp formula was possible by assuming that $\lambda^2 - 2\Lambda B \gg 4B^2N^2$. Then the square roots in the expressions for F_1 and F_3 may be expanded to give $C^{\frac{1}{2}} + B^2(2N+3)^2/2C^{\frac{1}{2}}$ and $C^{\frac{1}{2}} + B^2(2N-1)^2/2C^{\frac{1}{2}}$ respectively where $C = \lambda^2 - 2\Lambda B$. The combination differences are then given by

$$\Delta_2F_1(J) = (4B - 8B^2/C^{\frac{1}{2}})(J+\tfrac{1}{2}) + 2\gamma$$

$$\Delta_2F_2(J) = 4B(J+\tfrac{1}{2})$$

$$\Delta_2F_3(J) = (4B + 8B^2/C^{\frac{1}{2}})(J+\tfrac{1}{2}) - 2\gamma$$

Thus the combination differences are linear in $(J+\frac{1}{2})$ and the difference in the effective B values $(B \pm 2B^2/C^{\frac{1}{2}})$ for F_1 and F_3 enable the value of λ to be derived.

In addition, if γ is negligible, the Schlapp equations approximate to

$$F_1(J) = BJ(J+1) + B - 2\lambda$$

$$F_2(J) = BJ(J+1)$$

$$F_3(J) = BJ(J+1) + B$$

showing that the F_1 levels lie approximately 2λ below the adjacent F_2 and F_3 levels. The F_1-F_1 sub-band is therefore separated from the F_2,F_3-F_2,F_3 sub-bands by $2\lambda''-2\lambda'$.

For Se_2, ^{78}Se and ^{80}Se both have nuclear spin quantum numbers of zero and follow Bose-Einstein statistics, so that only the symmetrical rotational levels occur. In a $^3\Sigma_g^-$ state the odd numbered (N) levels are symmetric, and in a $^3\Sigma_u^-$ state the even numbered (N) levels are symmetric. However the levels have been shown to be determined by J, so that for the F_1 component of $^3\Sigma_g^-$, only $J''(=N+1)$ which are even can exist

F_2 " " " " $J''(=N)$ " " odd " "

F_3 " " " " $J''(=N-1)$ " " even " "

Since $B''(Se_2)$ is much smaller than $B''(SeO)$ the above approximation should hold for Se_2 if λ'' is about the same. Analysis by the author of some bands at the red end of the emission spectrum revealed widely separated triplet structure of the type described above. An approximate value for λ'' of 150 cm^{-1} was derived. The selection rule $\Delta J = \pm 1$ applies and only P and R branches are seen. In appearance the F_1-F_1 sub-bands are like $^1\Sigma$-$^1\Sigma$ bands, in which levels with odd J" are missing.

The bands analysed by Olsson were reinvestigated and shown to be these F_1-F_1 components. The F_2-F_2 and F_3-F_3 sub-bands have identical origins and very similar B values, but the absence of levels with even and odd J" respectively gives them the appearance of a single staggered band. The absence of F_2,F_3- F_2,F_3 transitions in the u-v region is discussed later.

The F_1-F_1 Sub-bands

The absorption study was begun at the u-v end of the system and extended towards the red. At the start the intention was merely to fix the vibrational numbering but the rotational analysis indicated so many points of interest that it became clear that it would be necessary to study at least one band for each upper state level, and preferably two for confirmation of the analysis. The F_1-F_1 bands appeared strongly throughout the absorption spectrum at the temperatures used but the F_2,F_3- F_2,F_3 bands only occurred at the red end.

In this section are presented the details found in F_1-F_1 bands from v'=21 to v'=0 for the two isotopes $^{78}Se_2$ and $^{80}Se_2$. The ground state levels were found to be always regular so that individual treatment is unnecessary. Additional evidence from previous emission work is included so that each level is discussed as completely as possible.

v'=21 to v'=16

These levels appear, by transitions from v"=0, at the u-v limit of the spectrum of both isotopes and the following observations apply for both species. There are no rotational perturbations in the range J=0 to J$\sim$60, but for each level the line width increases with J to such an extent that measurement of lines with J>60 was very inaccurate (see Plate 1). The diffuseness also increases with v' so that the

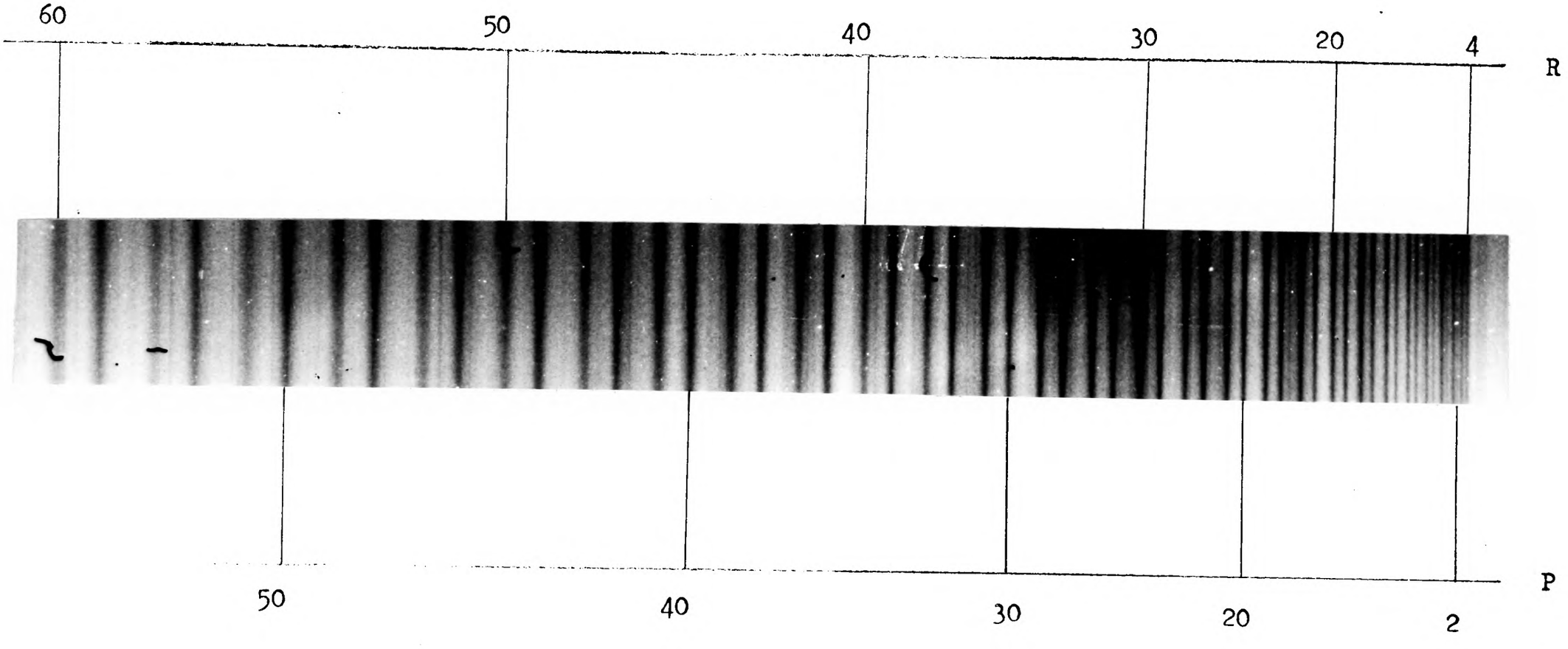

Plate 1. 16-0 F_1-F_1 Band of $^{78}Se_2$ showing diffuseness increasing with J, in absorption.

level v'=21 is the last analysed. However, inspection of low-dispersion plates of the area indicates an absorption maximum at a wavelength expected for the head of the 22-0 band. On the high dispersion plate this region appears to be completely diffuse. At 400° there is no absorption continuum after the 22-0 band; with increasing temperature a continuum appears causing total absorption in this region.

The rotational constant B_0'' was evaluated by averaging over all the bands and comparison with the values found in the emission work for v"=4, 5, 6, indicated a large discrepancy. Since the value of α'' was reliable and the short wavelength absorption bands must have v"=0, it was concluded that the vibrational numbering of the emission bands was wrong. In fact it was clear that the emission bands had values of v" too large by 3. In order to retain a sensible vibrational analysis it was necessary to decrease the v' numbering of the emission bands by 4. For example, the band identified by Rosen[12] and by Olsson[11] as the 10-6 band is correctly the 6-3 band. This large numbering change produced immediate agreement for the observed and calculated isotopic shifts of all the emission bands measured by the author.

Finally, one of the benefits of using separated isotopes is well demonstrated by the comparison between these bands and those discussed very recently by Herman[24] who used similar dispersion but natural

selenium. The diffuseness of the lines as well as the isotopic complexity of his spectrum make detailed analysis impossible.

v'=15

While bands with $v' > 15$ appeared to have sharp lines at low J values, comparison with those for $v'=15$ revealed that really they are still diffuse. The difference is so striking that it must mean that all levels with $v' > 15$, of both isotopes, are predissociated.

The analysis of bands with $v' \leqslant 15$ was complicated by numerous perturbations. As proved generally to be the case, there is insufficient overlap of the perturbed branches for much information about the perturbing state to be derived. For example, crossing points on a plot of $\Delta_2 F'/(J+\frac{1}{2})$ against $(J+\frac{1}{2})^2$ were seldom observed. This is a plot of "effective B'" and can give an estimate of the B value of the perturbing state (B_p), since at the crossing point $B^e = \frac{1}{2}(B'+B_p)$. The shape of the plot can, however, indicate whether B_p is larger or smaller than B'. Some B_p values were obtained in the author's emission study and each was smaller than B'_v; from the absorption work it has been confirmed that $B'_v > B_p$, for all v'. The absence of alternate levels makes it difficult to specify at which J' value a perturbation occurs; in the present work the figure quoted is that intermediate between the last observed (odd J') line and the first missing (odd J') line.

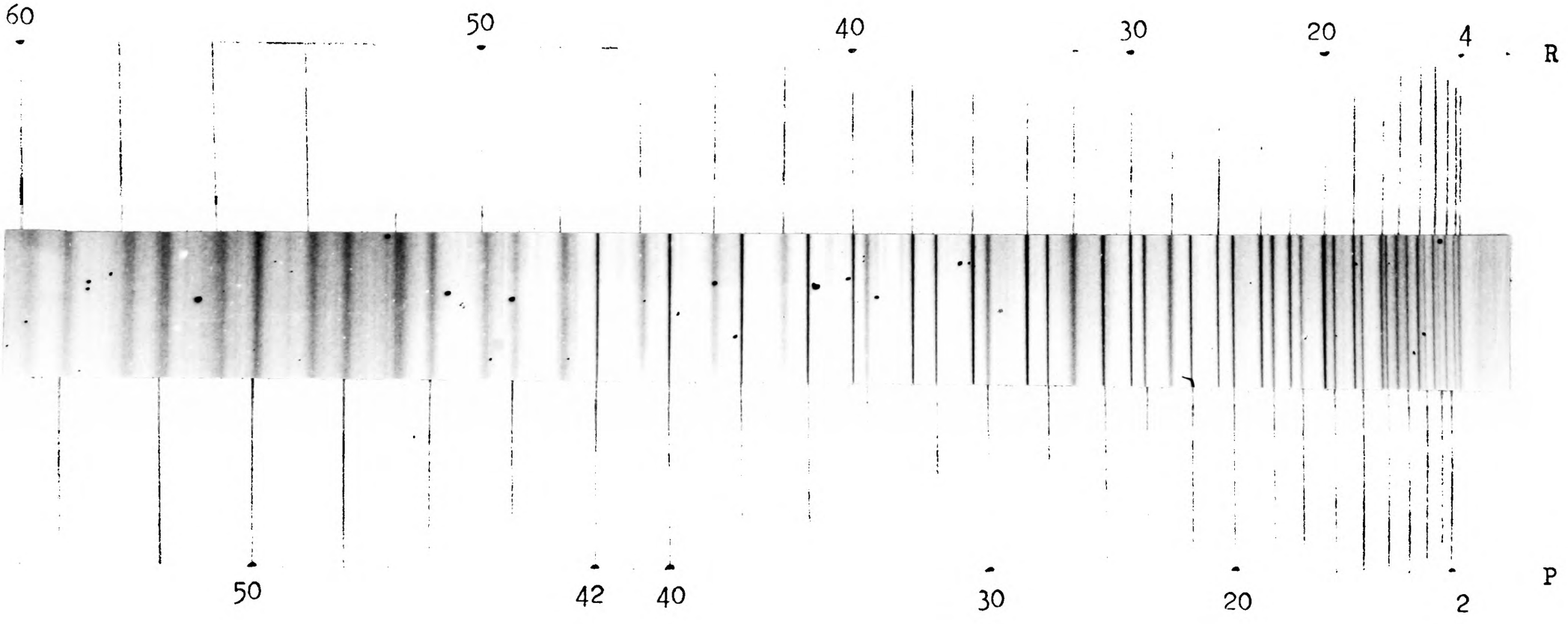

Plate 2. 15-0 F_1-F_1 Band of $^{78}Se_2$ showing predissociation at J'=42, in absorption.

The 15-0 band of each isotope has been analysed. For $^{78}Se_2$ there are four perturbations, at J' = 16, 24, 30 and 34, and at each the lines become increasingly displaced and diffuse; these "diffuse perturbations" are discussed later. However, there is a much more marked increase in diffuseness after the R(40) and P(42) lines (here, as is conventional, the numbers refer to J") which is not accompanied by any displacement. This indicates a predissociation at J'=42. After this point the lines are diffuse, becoming more so with increasing J, and beyond J'=70 no analysis was possible. No further perturbations occur in this diffuse region. The band is illustrated in Plate 2.

For $^{80}Se_2$ a similar situation occurs; there are diffuse perturbations at J' = 8, 22, 34 and 46. The presence of the perturbation at J'=8 means that the values given for the band origin ν_0 and B' are uncertain since no unperturbed region has been analysed. There is a sharp cut-off with no line displacement, assigned as a predissociation, at J'=50, and no analysis at greater J values was possible because of the diffuseness of the lines.

v'=14

The 14-0 band of each isotope has been analysed. For $^{78}Se_2$ diffuse perturbations occur at J' = 24, 36, 40, 46, 56 and 64. There is a predissociation at J'=72. Likewise, for $^{80}Se_2$, diffuse perturbations

occur at J' = 20, 34, 48, 54, 58 and 66; there is a predissociation at J'=78.

v'=13

The 13-0 and 13-1 bands of each isotope have been analysed. For $^{78}Se_2$ there is additional evidence from some emission bands not previously analysed. These appear on plates supplied by Dr. B. Meyer (then at the University of California, Berkeley) in 1962, and have been recently analysed because of their interesting rotational structure. As will be shown later, the emission bands from levels v' = 4, 5 and 6 show predissociations at decreasing J values and the limiting curve of dissociation indicates that bands with v' > 6 should not occur. Inspection of the region to shorter wavelengths, however, shows that several bands arising from v'=13, 12 and 11 do occur in emission, although they are weak. Analysis was only possible for $^{78}Se_2$ because the similar region for $^{80}Se_2$ was overlapped by impurity bands.

The 13-3, 13-4, 13-5 and 13-6 bands of $^{78}Se_2$ have been analysed. The R and P branches of each are blended and the structure is very short. There is a marked intensity drop four lines before the blended branch completely ceases, with no apparent line displacement, equivalent to a cut-off after R(22), P(24). This is interpreted as a predissociation at J'=24. Inspection of the absorption bands indicates

that R(26) and P(28) are the first diffuse lines - revealed by a marked increase in intensity - in agreement with the usual observation that diffuseness in absorption is a less sensitive test than cut-off in emission for predissociation. The diffuseness increases thereafter and reaches a maximum at J'=36 where there is a perturbation. It is concluded that there is a predissociation at J'=24 and probably a diffuse perturbation at J'=36. There is a perturbation at J'=54 and the lines are then diffuse until a diffuse perturbation at J'=66. There is a cut-off with no apparent line displacement at J'=88 in which the lines become diffuse before disappearing; this is assigned as a diffuse perturbation.

For $^{80}Se_2$ the first diffuse lines are at J'=34 which is assigned as a predissociation. There are diffuse perturbations at J'=42 and 58 and a perturbation at J'=72 which is not diffuse. There is a sharp cut-off at J'=96 which is assigned as a predissociation.

v'=12

For $^{78}Se_2$, the 12-4 and 12-6 emission bands have been analysed as well as the 12-0 and 12-1 absorption bands. The emission bands are headless since only lines for $43 \leq J' \leq 57$ occur. In absorption there is an area of diffuseness whose maximum is at about J'=34, but no perturbation is marked. There is a diffuse perturbation at J'=64,

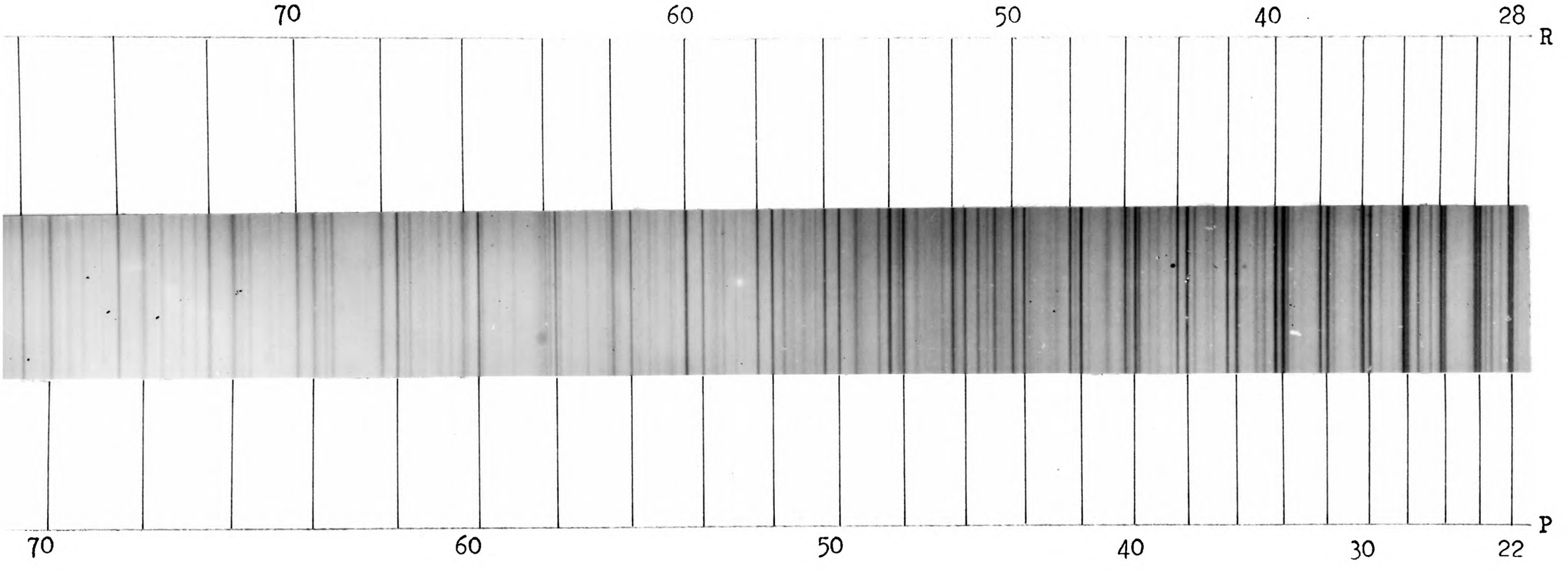

Plate 3. 12-0 Band of $^{78}Se_2$ showing the diffuse perturbations at J'=34 and 64.

and a perturbation at J'=80 which is not diffuse. The absence of lines in emission and the diffuseness in absorption are clearly related. It is suggested that there are perturbations at J'=34 and 64 but that the perturbing state is itself predissociated by a third unstable state. These are accidental predissociations which arise if direct radiationless transfer to the unstable state is not possible. First suggested by Ittmann[25], this type of predissociation is discussed by Herzberg[48]. The effect in emission is that some lines have reduced or zero intensity and in absorption they become diffuse; they may not be perturbed. The emission cut-off is again more sensitive than the absorption diffuseness and for v'=12 it occurs about 8 rotational levels from the centre of the perturbation. Some supporting evidence has already been provided in v' = 13, 14 and 15; the presence of diffuse perturbations (? accidental predissociations) in these levels would be expected if the perturbing state is predissociated above a certain lower lying level. No other explanation for the close recurrence of absorption diffuseness in many bands is readily found.

For $^{80}Se_2$, the 12-0 and 12-1 absorption bands have been analysed but not for $J' < 45$. There is a diffuse perturbation at J'=44 so that with increasing J', from 45, the lines become less perturbed and less diffuse. At J'=68 and 80 the lines become diffuse again but are not perturbed. The values given for ν_0 and B' are uncertain in levels such as this where no unperturbed region has been analysed. The diffuse perturbations in the 12-0 band of $^{78}Se_2$ are illustrated in Plate 3.

v'=11

For $^{78}Se_2$, the 11-2, 11-3 and 11-4 emission bands and the 11-0 and 11-1 absorption bands have been analysed. The emission bands all have blended R and P branches and are short, but no common cut-off is observed, J'=27 being the highest seen. The absorption bands become very diffuse at J'=51 and no further lines are observed until J'=63, this being interpreted as a diffuse perturbation at J'~58. There is a second diffuse perturbation at J'=80.

For $^{80}Se_2$, the 11-0 and 11-1 bands have been analysed. There are diffuse perturbations at J'=54 and 78.

v'=10

The 10-0 and 10-1 bands of each isotope have been analysed. For $^{78}Se_2$ there is a diffuse perturbation at J'=70 and possibly also at J'=114.

For $^{80}Se_2$ there is a diffuse perturbation at J'=38, no lines being analysed below J'=37. There is a diffuse perturbation at J'~74, no lines being seen between J'=67 and 79.

v'=9

The 9-1 and 9-2 bands of each isotope have been analysed. They

are diffuse throughout and no common cut-off point was found for either isotope.

v'=8

The 8-0 and 8-1 bands of each isotope have been analysed. For $^{78}Se_2$ there is a diffuse perturbation at J'=68. For $^{80}Se_2$ there is a progressive increase in diffuseness from J' ≈ 39, so that for J' > 55 no lines could be analysed; no perturbation was observed.

v'=7

The 7-1 band of each isotope has been analysed. For $^{78}Se_2$ there is a diffuse perturbation at J'=64. For $^{80}Se_2$ there is a decrease in diffuseness with increasing J' from the origin and a diffuse perturbation at J'=72.

Although emission bands with v' = 13, 12 and 11 have already been described, the author found no trace of levels $7 \leqslant v' \leqslant 10$ on the same plates. These have been reported in emission before however. Rosen[12] found that v'=7 was present but weak; v'=8 appeared strongly in emission and resonance spectra; v'=9 was very weak; $v' \geqslant 10$ did not appear. Olsson[11] found no trace of $v' \geqslant 7$. To check these observations, Davis[13] searched for v'=7 and 8 on heavily exposed

plates using separated isotopes and high dispersion. He found and analysed very weak 7-2 and 7-3 bands but only for one species, $^{77}Se_2$; he found no bands from v'=8.

The evidence of the high dispersion work using separated isotopes must be accepted in preference to Rosen's low dispersion studies using natural selenium. He gave no rotational analysis so that his identifications cannot be checked. It may be concluded that bands from v'=7 do exist but are extremely weak and bands from $8 \leq v' \leq 10$ do not appear.

v'=6

There is evidence from emission and absorption bands for each isotope. For $^{78}Se_2$ previous emission studies were made by Davis (6-1 and 6-2 bands) and the author (6-2 band). Davis found a predissociation at J'=46, no lines after R(44), P(46) being reported, for both bands, but inspection of his published print reveals weak lines after this. The author found that there was indeed a sharp drop in intensity at J'=46 but that the branches continued after this, the intensity rising again to a normal value at about R(58),P(60) and then dropping slowly so that no lines after R(62), P(64) were seen. No perturbations were observed.

Some medium dispersion plates, also supplied by Dr. Meyer, of

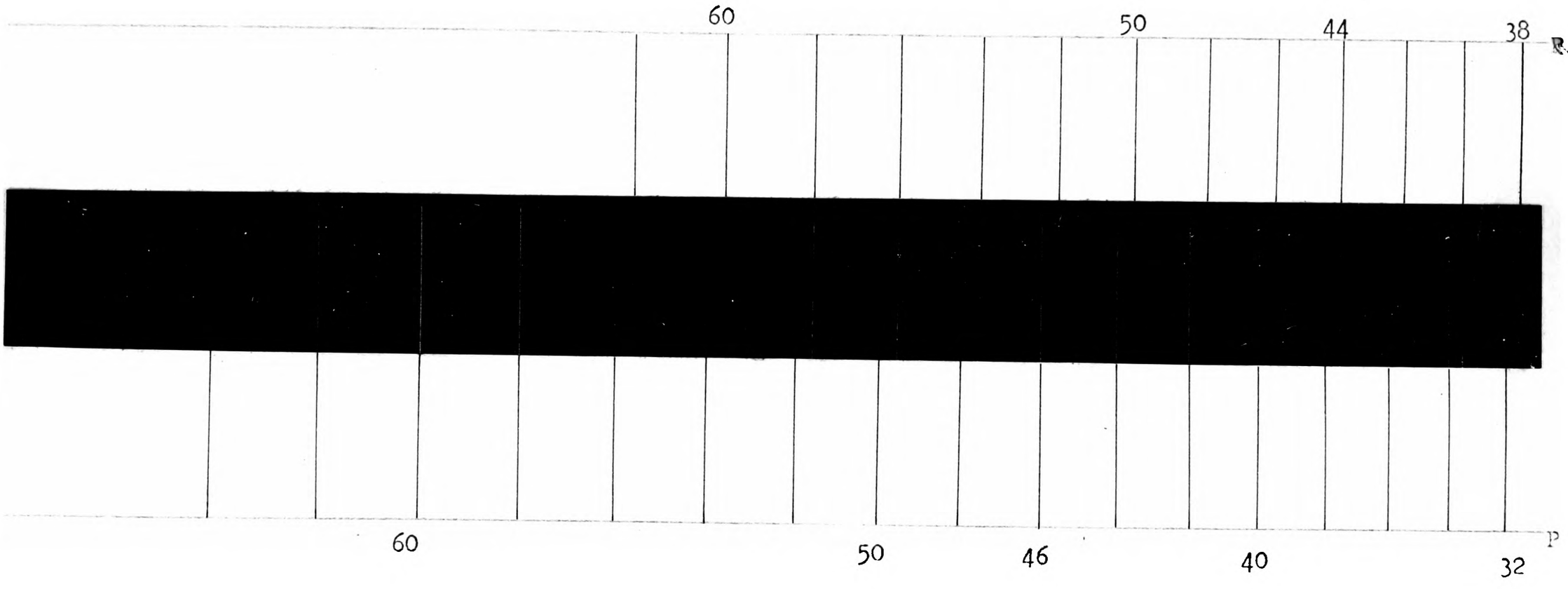

Plate 4. 6-2 F_1-F_1 band of $^{78}Se_2$ showing weak predissociation at J'=46, in emission.

the 6-1, 6-2 and 6-3 bands have been analysed to investigate the predissociation. In each band there is a predissociation at J'=46 but some weak lines always occur at higher values of J. The 6-3 absorption band has also been analysed and this shows no increase in diffuseness at J'=46. The R(48) and P(50) lines appeared somewhat stronger than normal and this may reflect a slight broadening but the effect is small. The lines continue, unperturbed, until at least R(66). It is concluded that there is a weak predissociation at J'=46.

In addition Davis reported a weakening of a single R and P line in each band involving v'=6 for the isotopic species $^{77}Se_2$, $^{78}Se_2$ and $^{80}Se_2$. In $^{78}Se_2$ the weak lines were R(36) and P(38) and the same lines are found to be abnormally weak in the emission bands studied here, but no effect is noticeable in the absorption band. The predissociation at J'=46 and the weak lines following it are shown in Plate 4.

For $^{80}Se_2$, previous emission studies were made by Olsson (6-1, 6-2 and 6-3 bands), Davis (6-1 and 6-2) and the author (6-3 and 6-31). All agreed that there is a sharp cut-off due to a predissociation at J'=50. The R(40) and P(42) lines were found by Davis to be abnormally weak, but the author found that although weak they are also split into two. Inspection of an enlargement of the 6-3 absorption band shows that the lines are noticeably diffuse at J'=56 and the diffuseness reaches a maximum at J'=66. The R(40) and P(42) lines appear to be split somewhat but overlapping branches from another band make

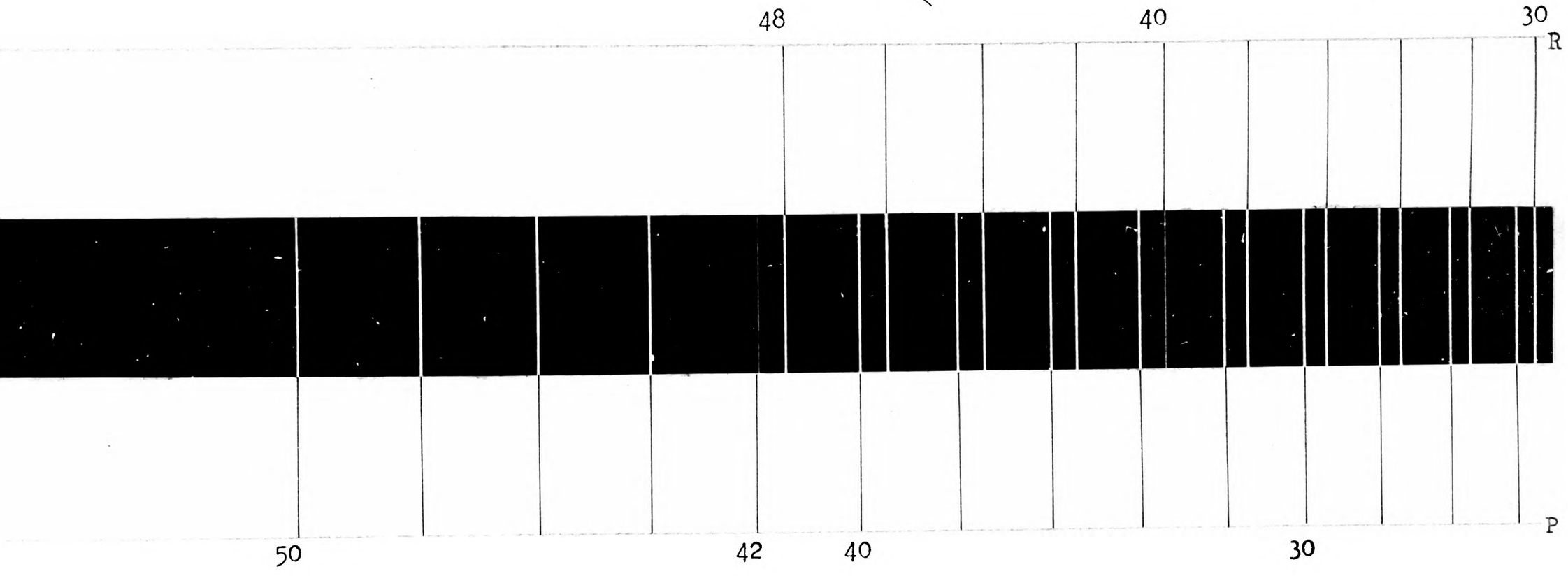

Plate 5. 6-3 F_1-F_1 Band of $^{80}Se_2$ showing predissociation at J'=50 and splitting for J'=41, in emission.

definite statements about this or about any intensity change impossible. Davis suggested that the instances of weakening of single R and P lines in v'=6 are due to accidental predissociations. This is certainly possible but the effects are much less obvious than in the higher lying levels where the absorption diffuseness and perturbations extend over several lines. The predissociation at J'=50 and the splitting at J'=41 are shown in Plate 5.

v'=5

For $^{78}Se_2$ there is evidence from emission and absorption bands. Davis analysed the 5-1 and 5-2 bands as far as J'=66 and suggested that a predissociation or perturbation occurred then but overlapping prevented further analysis.

The 5-2 band has been analysed in absorption and emission. The absorption analysis indicates a perturbation, with no diffuseness, at J'=70. The analysis has been extended to J'=94, no diffuseness being observed, nor a further perturbation, and lines are observed to at least J'=106. In emission some weak lines appear after the perturbation which have been assigned by comparison with the absorption branches. Only the R(74) line is found but P lines are found up to P(78). The emission band is very free from overlapping and it was thought that further lines would be apparent if present. It is

suggested that there is a predissociation at about J'=78.

For $^{80}Se_2$, previous emission studies were made by Olsson (5-4 band), Davis (5-1 and 5-2 bands) and the author (5-2, 5-4, 5-30 and 5-31 bands). Olsson and Davis analysed as far as J'=66 and 64 respectively and suggested that there was a perturbation. The author analysed through the perturbation and found that the branches could be extended only to J'=82. These plates have been closely restudied to determine whether this is due to a predissociation. The 5-30 band, in particular, is free from overlapping and the R(82) and P(84) lines are clearly absent; there is no perturbation and it is concluded that there is a predissociation at J'=82.

Inspection of absorption bands with v'=5 shows that the perturbation at J'=66 occurs with no diffuseness.

v'=4

For $^{78}Se_2$ no emission bands were studied and therefore the 4-3 absorption band has been analysed to see whether it is perturbed or predissociated. There are two perturbations, at J'=60 and 74, and no diffuse lines are seen throughout the band.

For $^{80}Se_2$ previous emission studies were made by Olsson (4-3 band) and the author (4-3, 4-29 and 4-30 bands). Olsson reported a perturbation at J'=54; this was confirmed by the author who also found a smaller perturbation at J'=40 and extended the analysis to

J'=106. These bands have again been closely restudied and are not overlapped, so that the structure is very clear; the cut-off is sharp and it is concluded that there is a predissociation at J'=106. Inspection of absorption bands with v'=4 shows that the perturbations occur without diffuseness.

v'=3

The 3-4 band of each isotope has been analysed. For $^{78}Se_2$ there is a perturbation at J'=34 and normal structure thereafter until at least J'=90. For $^{80}Se_2$ there is a perturbation at J'=18 below which no branches could be analysed; the structure thereafter is normal until at least J'=92.

v'=2

The 2-5 band of each isotope has been analysed; the structure of each is normal until at least J'=90.

v'=1

The 1-8 band of each isotope has been analysed. For $^{78}Se_2$ there is a perturbation at J'=76, no further structure being analysed. For

$^{80}Se_2$ there is a perturbation at J'=68 and the structure thereafter is normal until at least J'=94.

v'=0

The 0-7 band of each isotope has been analysed. For $^{78}Se_2$ there is a perturbation at J'=28 below which no branches could be analysed. There is a second perturbation at J'=68 and the structure thereafter is normal until at least J'=96.

For $^{80}Se_2$ there is a perturbation at J'=22 below which no branches could be analysed. There is a perturbation at J'=66 and possibly another at J'=90, where the lines are very weak.

Determination of Rotational Constants

The values of the ground state constants were determined, over the whole range of J" in the band, by a least squares method on the Oxford KDF9 computer. The values for the emission bands were re-calculated in the same way, having been done previously by a centre of gravity method, with a significant increase in accuracy. They enable good estimates of γ_e'' to be given. The values are given in Tables 1 and 2, with derived constants; the error estimate given throughout this work is one standard error (65% probability). The brackets signify a value for which D is clearly wrong: this usually occurs when all lines are blended so that there is a consistent error in B. The standard error quoted therefore sometimes refers more to the fitting process than to the derived B value. For comparison purposes, Kratzer D ($=4B^3/\omega^2$) is found to be 2×10^{-8} $cm.^{-1}$ for the upper and lower states of each isotope.

Since the upper state is perturbed, the constants were found where possible from ΔB and ΔD values in unperturbed regions. For some bands, e.g. v'=10 and 12 for $^{80}Se_2$, estimates are given by taking the branches which are most regular in the perturbed region. This can give very poor results. Since alternate levels are missing the constants were determined, using an Oxford statistical programme, by multiple linear regression on the line given by

$$R_J + P_J = 2\nu_0 + 2B' + 2(B'-B'')J(J+1) - 2(D'-D'')J^2(J+1)^2.$$

A test plot of B'_v against $(v'+\frac{1}{2})$ revealed that, for each isotope, there is a marked change of slope for $v' > 15$; values above this could not be sensibly fitted to the expression

$$B'_v = B'_e - \alpha'_e(v'+\tfrac{1}{2}) + \gamma'_e(v'+\tfrac{1}{2})^2 .$$

In addition the B'_v values in the region $9 < v' < 16$ show so much scatter, because of the numerous perturbations at low J values, that little regularity is apparent. The constants B'_e and α'_e, for each isotope, were therefore evaluated for the region $0 \leq v' \leq 8$ over which the γ'_e term was found to be insignificant.

Using the derived constants, the B'_v values were calculated and compared with those observed; a plot of B'_v(observed-calculated) x 10^5 against v', for each isotope, is given in Fig. 1. The scatter is much enlarged, but the deviation for $v' > 15$ is clear, these values being also probably more reliable because of the absence of rotational perturbations. The values of the upper state rotational constants are given in Tables 3 and 4.

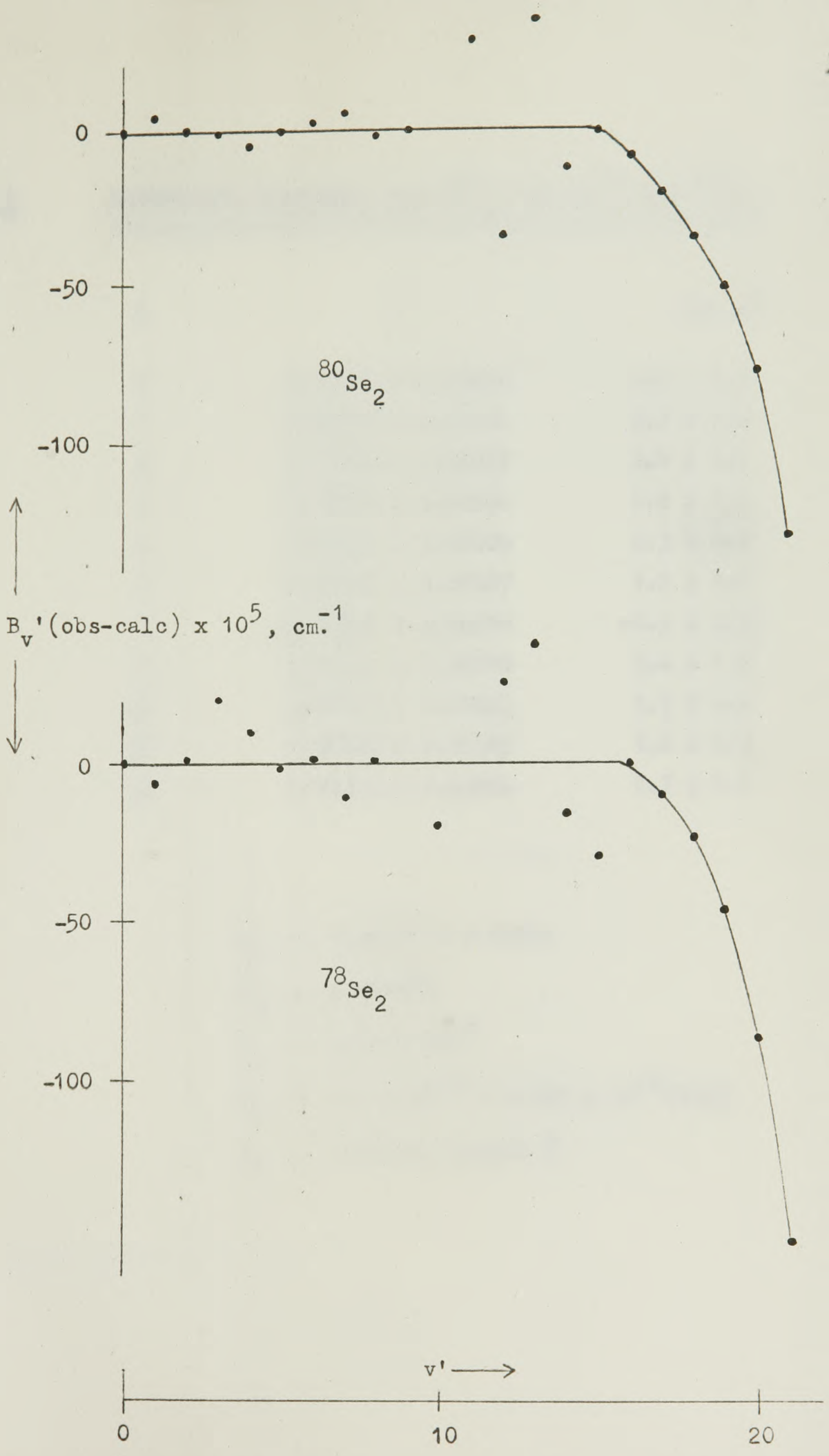

Fig. 1 Plot of B_v'(obs-calc) x 10^5, $cm.^{-1}$ against v'; F_1 component

TABLE 1 Rotational Constants for $X^3\Sigma_g^-$, in $cm.^{-1}$, for $^{80}Se_2$ F_1

v	B	$D_x 10^8$
0	0.08976 ± 0.00006	2.0 + 1.3
1	0.08950 ± 0.00004	2.7 ± 1.0
2	0.08920 ± 0.00007	2.8 ± 1.2
3	0.08890 ± 0.00004	2.2 ± 0.5
4	0.08859 ± 0.00005	2.3 ± 0.8
5	0.08825 ± 0.00007	1.9 ± 1.0
7	(0.08731 ± 0.00010	-0.5 ± 1.2)
8	0.08744 ± 0.00010	2.4 ± 1.5
29	0.08089 ± 0.00005	1.7 ± 0.6
30	0.08059 ± 0.00005	1.6 ± 0.5
31	0.08026 ± 0.00004	1.7 ± 0.6

$B_e = 0.08992 \pm 0.00001$

$\alpha_e = 0.000288$

$\gamma_e = -6.1 \times 10^{-7}$

$D_v = 2.4 \times 10^{-8} - 0.023 \times 10^{-8}(v+\frac{1}{2})$

$r_e = 2.1659 \pm 0.0001$ Å

TABLE 2 Rotational Constants for $X^3\Sigma_g^-$, in $cm.^{-1}$, for $^{78}Se_2$ F_1

v	B	D x 10^6
0	0.09206 ± 0.00004	2.0 ± 0.6
1	0.09170 ± 0.00004	1.8 ± 0.6
2	0.09145 ± 0.00007	2.4 ± 1.9
3	0.09115 ± 0.00009	2.0 ± 1.5
4	(0.09008 ± 0.00013	-8.1 ± 2.1)
5	0.09054 ± 0.00009	2.4 ± 1.5
6	(0.09034 ± 0.00049	20.3 ±88.7)
7	0.08979 ± 0.00009	1.2 ± 1.1
8	0.08959 ± 0.00010	0.6 ± 1.9

$$B_e = 0.09219 \pm 0.00002$$

$$\alpha_e = 0.000299$$

$$\gamma_e = -6 \times 10^{-7}$$

$$D = (1.8 \pm 0.2) \times 10^{-8}$$

$$r_e = 2.1663 \pm 0.0002 \text{ Å}$$

cf. values calculated from $^{80}Se_2$

$$B_e = 0.09223$$

$$\alpha_e = 0.000299$$

TABLE 3 Rotational Constants for $B^3\Sigma_u^-$, in $cm.^{-1}$, for $^{80}Se_2$ F_1

v	B
0	0.07032 ± 0.00005
1	0.07000 ± 0.00010
2	0.06962 ± 0.00007
3	0.06925 ± 0.00005
4	0.06887 ± 0.00005
5	0.06857 ± 0.00005
6	0.06826 ± 0.00005
7	0.06794 ± 0.00004
8	0.06752 ± 0.00004
9	0.06719 ± 0.00004
10	0.06774 ± 0.00006
11	0.06678 ± 0.00005
12	0.06583 ± 0.00019
13	0.06615 ± 0.00005
14	0.06536 ± 0.00007
15	0.06460 ± 0.00011
16	0.06471 ± 0.00006
17	0.06424 ± 0.00006
18	0.06376 ± 0.00006
19	0.06325 ± 0.00006
20	0.06265 ± 0.00006
21	0.06178 ± 0.00006

$B_e = 0.07048 \pm 0.00002$

$\alpha_e = 0.000345$

$D = 4 \times 10^{-8}$

$r_e = 2.4464 \pm 0.0003$ Å

TABLE 4 Rotational Constants for $B^3\Sigma_u^-$, in $cm.^{-1}$, for $^{78}Se_2$ F_1

v	B
0	0.07241 ± 0.00028
1	0.07167 ± 0.00010
2	0.07138 ± 0.00009
3	0.07120 ± 0.00009
4	0.07075 ± 0.00009
5	0.07026 ± 0.00005
6	0.06993 ± 0.00005
7	0.06945 ± 0.00007
8	0.06920 ± 0.00004
9	0.06862 ± 0.00004
10	0.06930 ± 0.00004
11	0.06837 ± 0.00004
12	0.06834 ± 0.00004
13	0.06776 ± 0.00004
14	0.06686 ± 0.00004
15	0.06636 ± 0.00007
16	0.06629 ± 0.00004
17	0.06583 ± 0.00004
18	0.06533 ± 0.00004
19	0.06473 ± 0.00004
20	0.06397 ± 0.00004
21	0.06297 ± 0.00009

		cf. calc. from $^{80}Se_2$
B_e	= 0.07228	0.07229
α_e	= 0.000363	0.000358
D	= 5×10^{-8}	
r_e	= 2.4465 Å	

Vibrational Analysis

The early attempts on the vibrational analysis of the main system of Se_2 have already been mentioned; the complexity caused by the use of natural selenium may be exemplified as follows. Natural selenium has isotopes in the following abundances: 74, 0.87%; 76, 9.02%; 77, 7.58%; 78, 23.52%; 80, 49.82%; 82, 9.19%. These give rise to molecules of which the following are the most abundant:

78-82	4.32%
80-80	24.82%
78-80	23.44%
77-80	7.55%
78-78	5.53%
76-80	8.99%

The relative wavelengths of the band heads depend on the reduced masses and the molecules given above form four groups centred on molecules of the type $^{80}Se_2$, $^{79}Se_2$, $^{78\frac{1}{2}}Se_2$, $^{78}Se_2$. These have the following abundances and intensity ratios:

	abundance %	ratio
80	29	4
79	23	3
78½	8	1
78	15	2

While some of the early workers were aware of this complicating factor, others were apparently not, so that their analyses are very unreliable. In addition, the author's emission study has shown that the main system consists of two overlapping sub-systems with very similar vibrational constants.

It is not fruitful, for these reasons, to give detailed comparison with the early analyses, since there is agreement in some regions and disagreement in others. As an example may be taken the vibrational analysis of Rosen[12], which is the most comprehensive of the early work and, in fact, covers most of the F_1-F_1 sub-system. As a result of the analysis of the absorption bands described shortly, it has been shown that: for the progressions from v'=0 and 1, Rosen's analysis is correct; for the progressions from v"=0 and 1, the numbering of the upper state is too low by 1; for intermediate bands, v" is too high by 3 and v' too high by 4.

Before giving the results of the absorption study, three points arising from the author's emission study may be made.

(1) The region λλ 5950-5450 Å has been described by Rosen and Montfort[3] as consisting of "fluctuation bands". This is the region covered in the emission work and there are no fluctuations of intensity when using separated isotopes. However, both sub-systems are strongly present and medium-dispersion plates appear extremely complex, with observed isotopic shifts, between the band heads due to $^{78}Se_2$ and $^{80}Se_2$, of about 100 $cm.^{-1}$. Using natural selenium the complexity would be at least four time greater which accounts for the early observations.

(2) A study of medium-dispersion plates of the region λλ 3890-6040 Å, in which no bands were rotationally analysed, revealed very many bands

of which most were assigned to the F_1 and some to the F_2,F_3 sub-systems. The distinguishing features are not apparent even at such a dispersion (0.6 Å/mm. at about 4000 Å and 1.2 Å/mm. at about 5000 Å) when the overlapping is great. However, so many bands are present that some unassigned bands must be F_2,F_3 at least in the region down to 4000 Å. Below this all the bands are rotationally analysed as F_1 and it is suggested that the F_2,F_3 bands are predissociated.

(3) In the region rotationally analysed at about 6000 Å, the band overlapping is less and it is suggested that earlier workers, using natural selenium and low dispersion (>5 Å/mm.) identified the F_2,F_3 bands as new systems, e.g. the system reported as recently as 1955 by Leelavathi and Rao[15] in the region λλ 5900-6800 Å. Using separated isotopes, this region is found to contain only $^3\Sigma_u^- - {}^3\Sigma_g^-$ bands, when the spectrum is excited in a microwave discharge; this method usually produces spectra very similar to those from the high-frequency discharge previously used.

The $^1\Sigma_1$-$^1\Sigma_1$ Sub-bands

The evidence from the B''_0 value of the absorption bands at the extreme u-v end of the system was the first indication that the v" numbering of the emission bands was wrong. Vibrational constants had already been derived for the few v' levels studied and it was assumed that these were roughly correct. The ground state constants had been accurately derived over a range of 30 in v" and both sets agreed rather well with earlier work. To maintain these values and to reduce v" by 3 required a reduction of 4 in v'. Then test calculation of the isotopic shifts for the emission bands gave excellent agreement with observation, implying that at least the new v" constants were correct. However, numerous vibrational perturbations were reported by almost all the previous workers and the values for the upper state constants must be considered unreliable until it has been shown that the levels used to derive them are not perturbed in this way.

Vibrational perturbations are said to occur if a whole band deviates from the regular course of a band progression, and can arise as follows: the strength of a perturbation depends on the energy difference between the unperturbed levels and on the magnitude of the matrix element W_{12} given by

$$W_{12} = \int \psi_1^* W \psi_2 dr .$$

W_{12} contains two factors, one an electronic-rotation factor and the

other a Franck-Condon factor. The latter depends on the relative positions and forms of the potential energy curves and if this term is large there can be a perturbation between the two states even if the energy resonance is not very sharp. In such a case the energy separation ΔE may be about the same for all values of J. The result will be a shift of all the rotational levels and the slight dependence of ΔE on J will be revealed by a small change in the rotational constant B of the perturbed state. However, as Herzberg[48] has observed, many instances of vibrational perturbations have, on close study, been shown to arise from rotational perturbations at low J values. This produces a shift of the band head and thus the appearance of a vibrational perturbation; it may be concluded that vibrational perturbations are not fundamentally different from rotational perturbations.

For Se_2 all the bands have been rotationally analysed and thus the band origins are known and also the B' values. It should therefore be possible to decide firstly whether the reported vibrational perturbations do exist, and if so, what type they are. The best way to determine the upper state constants is by means of the term values $T'_{v,e}$ for the upper state with respect to the bottom of the potential curve of the lower state. These are given by

$$T'_{v,e} = \nu_{00} + G''_v .$$

Accurate ground state constants for $^{80}Se_2$ were found by using the author's emission results for the 5-1, 5-2, 5-3, 5-4, 5-30 and 5-31 bands.

The origins of these bands were fitted to the polynomial

$$T'_{5,e} = \nu_{00} + \omega''_e(v''+\tfrac{1}{2}) - x_e\omega''_e(v''+\tfrac{1}{2})^2 + y_e\omega''_e(v''+\tfrac{1}{2})^3$$

Using these values of the ground state constants, the term values for all the upper state levels of $^{80}Se_2$ were calculated from the band origins.

For $^{78}Se_2$ no information was available at high v" levels and so the ground state constants were not derived independently, but by using the relationships $\omega_e{}^i = \rho\omega_e$, $x_e\omega_e{}^i = \rho^2 x_e\omega_e$, $y_e\omega_e{}^i = \rho^3 y_e\omega_e$ where ρ is derived in the usual way from $^{78}\mu_A = 38.97116$ and $^{80}\mu_A = 39.97103$. These values are taken from Townes and Schawlow[49]. The calculated values of $\Delta G''$ were checked by comparison with those observed. Thus, using these constants, the term values for all the upper state levels of $^{78}Se_2$ were calculated from the band origins.

Sufficient data were now available to fit the observed $T'_{v,e}$ values for each isotope to the polynomial

$$T'_{v,e} = T_{ee} + \omega'_e(v'+\tfrac{1}{2}) - x_e\omega'_e(v'+\tfrac{1}{2})^2 + y_e\omega'_e(v'+\tfrac{1}{2})^3$$

by a least squares method. However, a test plot of $T'_{v,e}$ against $(v'+\frac{1}{2})$ for each isotope revealed a marked change in the slope for $v' > 13$ and attempts to fit all the term values to the above expression failed.

Therefore for each isotope term values for $v' > 13$ were omitted from the calculation; for $^{80}Se_2$ those for $v'=10$ and 12 were also omitted because no analysis was available in an unperturbed region.

Using the derived constants, the term values were calculated and a plot of $T'_{v,e}$(observed-calculated) against v' for each isotope is given in Fig. 2. The excellent agreement shows that there are no vibrational perturbations in the levels for $v' < 14$; the special cases of v'=10 and 12 have already been mentioned. Values of the band origins are given in Tables 5 and 6. Values of the derived vibrational constants are given in Table 7. The agreement between the observed and calculated upper state constants for $^{78}Se_2$ is seen to be excellent.

The isotopic shifts were also calculated and are compared with the observed values in Table 8 for the absorption bands and in Table 9 for the emission bands. It should be recalled that the band origins are measured from different photographic plates,usually with different iron arc comparison spectra for the two isotopes; this produces larger errors in the isotopic shifts than those obtained by direct comparison on the same plate. Nevertheless there is excellent agreement throughout the whole of the upper state levels, exceptfor $v' > 14$, and a large range of the ground state levels, which confirms the vibrational analysis.

It is now interesting to consider why the upper state levels with $v' > 13$ show such marked deviations, for each isotope, in values of $T'_{v,e}$, these being reflected in the similar deviations in the isotopic shifts, and in the B'_v values. It is suggested that the

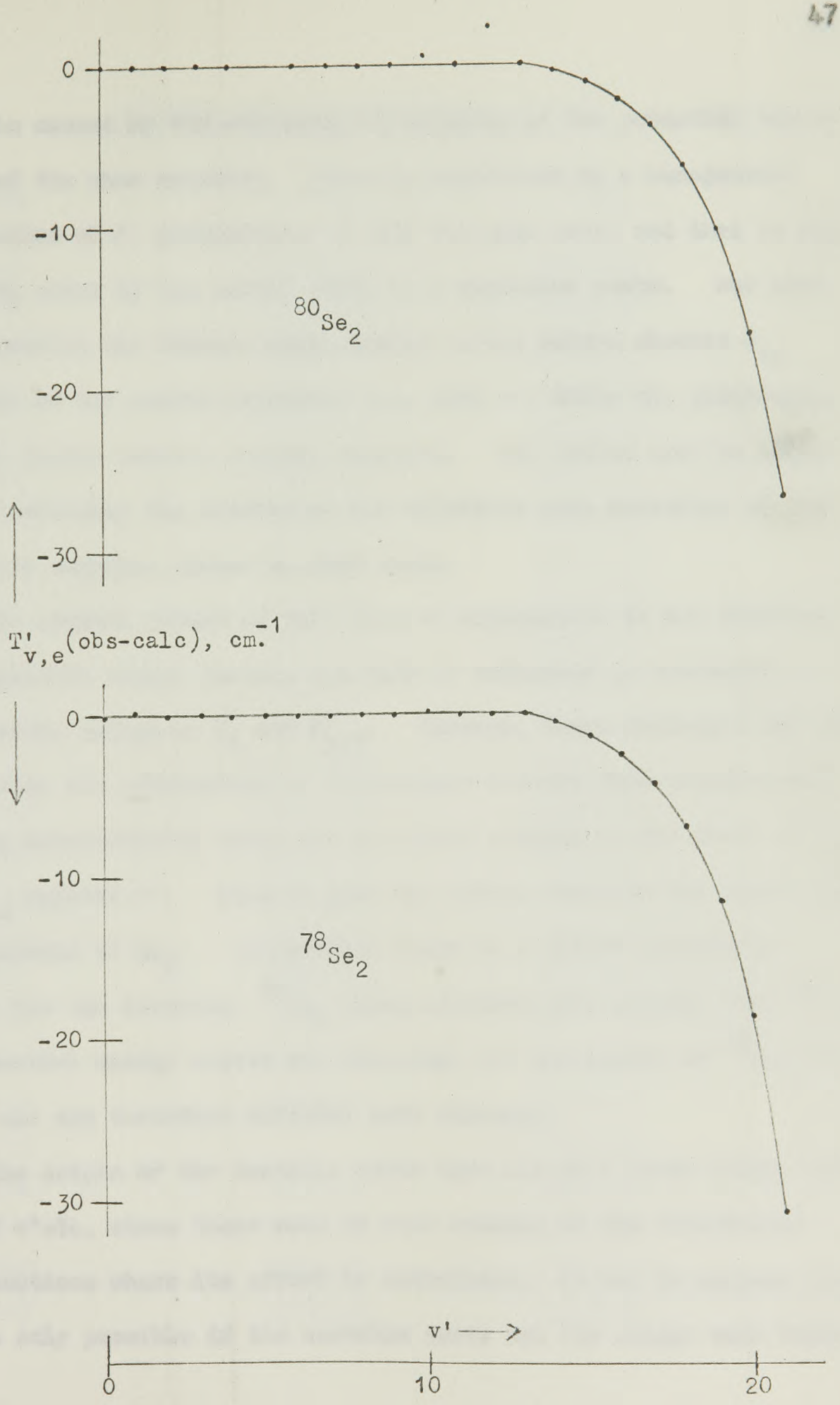

Fig. 2 Plot of $T'_{v,e}$(obs-calc), cm.$^{-1}$ against v'; F_1 component.

effect is caused by the avoidance of crossing of two potential energy curves of the same symmetry. This is equivalent to a homogeneous (independent of J) perturbation at J=0 for each band, and that is only likely to occur if the second state is a repulsive state. For such an interaction the Franck-Condon factor in the matrix element W_{12} increases as the curves approach, i.e. with v', while the electronic rotation factor remains roughly constant. The latter must be large because initially the overlap of the vibration wave functions of the stable and unstable states is very small.

The overall effect of this type of interaction is the formation of a potential energy maximum and this is reflected in decreases in the expected values of B'_v and $T'_{v,e}$. However, these decreases can only appear when the interaction is significant and are thus revealed not by large anharmonicity terms but by marked changes in the slope of B'_v and $T'_{v,e}$ against v'. This is just the effect shown in the upper state F_1 components of Se_2. In addition there is a slight difference between the two isotopes, $^{78}Se_2$ being affected more sharply than $^{80}Se_2$; the potential energy curves are identical but the levels of $^{78}Se_2$ lie higher and are therefore affected more strongly.

The origin of the unstable state must lie at a lower energy than that of v'=14, since there must be some overlap of the vibrational wave-functions where its effect is noticeable; it may be assumed that this is only possible if the unstable curve has its origin well below v'=14.

TABLE 5 Origins of Absorption Bands, in $cm.^{-1}$ $^1F_1$-$^1F_1$

Band	$^{80}Se_2$	$^{78}Se_2$
21-0	30532.27	30579.08
20-0	30346.08	30392.95
19-0	30153.28	30199.13
18-0	29955.52	30000.03
17-0	29753.69	29796.40
16-0	29548.24	29589.20
15-0	29339.93	29378.63
14-0	29128.30	29165.21
13-0	28914.21	28948.67
12-0	28699.54	28729.41
11-0	28477.65	28507.57
10-0	28256.21	28283.33
8-0	27804.70	27826.97
13-1	28530.79	28560.38
12-1	28315.71	28341.11
11-1	28094.26	28119.26
10-1	27872.91	27895.09
9-1	27647.98	27667.93
8-1	27421.27	27438.65
7-1	27192.26	27206.99
9-2	27266.49	27281.72
4-3		25727.57
3-4	25115.53	25104.47
2-5	24499.78	24481.23
1-8	23142.59	23107.40
0-7	23267.98	23233.85

TABLE 6 — Origins of Emission Bands, in $cm.^{-1}$ — F_1-F_1

Band	$^{80}Se_2$	$^{78}Se_2$
5-1	26727.45 *	26736.67 *
5-2	26346.12 *	26350.38
6-1	26960.99 *	26973.00
6-2	26579.54 *	26586.58
6-3	26200.12 *	26202.46
4-3	25730.80 *	
5-4	25588.94 *	
5-3	25966.64 *	
11-2		27733.08
11-3		27348.85
11-4		26966.67
13-3		27789.91
13-4		27407.63
13-5		27027.45
13-6		26649.15
5-31	16147.99 *	
5-30	16471.19 *	
4-29	16560.73 *	
6-31	16381.47 *	

* These results are taken from the author's emission study.

TABLE 7 Vibrational Constants, in cm.$^{-1}$ $^1\Sigma_g^+$ components

		$^{80}Se_2$	$^{78}Se_2$ obs.	$^{78}Se_2$ calc.
$B^3\Sigma_u^-$	ν_{ee}	25980.36	25980.25	
	ω_e	246.291	249.436	249.430
	$x_e\omega_e$	1.016	1.035	1.042
	$y_e\omega_e$	-5.49×10^{-3}	-6.27×10^{-3}	-5.7×10^{-3}
$X^3\Sigma_g^-$	ω_e	385.3028		390.2143
	$x_e\omega_e$	0.96363		0.98835
	$y_e\omega_e$	-8.184×10^{-4}		-8.501×10^{-4}

TABLE 8 Vibrational Isotope Effect: Values in $cm.^{-1}$ of $\Delta\nu$, $^{80}Se_2 - {}^{78}Se_2$ F_1-F_1

Band	Δν obs	Δν calc	obs-calc
0-7	34.13	33.88	0.25
1-8	35.19	35.29	-0.10
2-5	18.55	18.56	-0.01
3-4	11.06	10.94	0.12
4-3	3.23	3.30	-0.07
7-1	-14.76	-14.68	-0.08
8-1	-17.38	-17.37	-0.01
8-0	-22.27	-22.23	-0.04
9-1	-19.95	-19.98	0.03
9-2	-15.23	-15.17	-0.06
10-1	-22.18	-22.53	pert.
10-0	-27.12	-27.39	pert.
11-1	-25.00	-25.02	0.02
11-0	-29.92	-29.88	-0.04
12-1	-25.40	-27.44	pert.
12-0	-29.87	-32.30	pert.
13-1	-29.59	-29.80	0.21
13-0	-34.46	-34.66	0.20
14-0	-36.91	-36.94	0.03
15-0	-38.70	-39.16	0.46
16-0	-40.96	-41.29	0.33
17-0	-42.71	-43.37	0.66
18-0	-44.51	-45.36	0.85
19-0	-45.85	-47.28	1.43
20-0	-46.87	-49.13	2.26
21-0	-46.81	-50.89	4.08

TABLE 9 Vibrational Isotope Effect: Values in $cm.^{-1}$ of $\Delta\nu$, $^{80}Se_2 - {}^{78}Se_2$ * F_1-F_1

Band	Δν obs from head	Δν obs from ν_0	Δν calc
5-1		-9.22	-9.13
6-1	-11.89	-12.01	-11.94
6-2	-7.13	-7.04	-7.13
5-2	-4.34	-4.26	-4.32
6-3	-2.36	-2.34	-2.37
5-4	5.04		5.16
4-4	7.91		8.02
4-5	14.05		12.67
4-26	98.40		98.62
5-27	99.63		99.27
6-28	100.36		99.92
4-27	100.98		102.13
5-28	103.44		102.73
3-24	94.78		94.36
5-26	96.36		95.76
4-25	95.73		95.05
4-24	91.32		91.44
3-23	91.20		90.70
2-21	87.00		86.15
2-20	82.04		82.34
1-19	81.67		81.49
1-18	79.14		77.55
1-17	73.83		73.56

* These results are taken from the author's emission study.

The Potential Energy Curves

The vibrational perturbations for $v' > 13$ have been ascribed to the formation of a potential maximum in the F_1 component of $B^3\Sigma_u^-$. It was decided to test this by calculating the shape of the potential curve by the method given by Richards and Barrow[26]. This is a direct calculation from spectroscopic data and depends on numerical integration of the Klein equations[27].

$$f(U) = \frac{1}{2\pi(2\mu)^{\frac{1}{2}}} \int_0^{I'} \frac{dI}{(U-E(I,K))^{\frac{1}{2}}}$$

$$g(U) = \frac{1}{2\pi(2\mu)^{\frac{1}{2}}} \int_0^{I'} \frac{(\partial E/\partial K)dI}{(U-E(I,K))^{\frac{1}{2}}}$$

where $f = \frac{1}{2}(r_{max} - r_{min})$ $\qquad g = \frac{1}{2}(1/r_{min} - 1/r_{max})$

$I = h(v+\frac{1}{2})$ $\qquad K = (h^2/8\pi^2\mu)J(J+1)$

and U is the energy for which turning points are required.

With the energies in wave numbers and changing the variable, the first equation becomes

$$f_n = \left(\frac{h}{8\pi^2\mu c}\right)^{\frac{1}{2}} \int_0^{n} \frac{dx}{(U_n - U_x)^{\frac{1}{2}}}$$

where U_n is the level for which turning points are required, U_x are the other lower vibrational energy levels (both measured from the minimum of the curve) and $x = v+\frac{1}{2}$.

The second equation is similar but involves $(\partial E/\partial K)$; this was shown to be equal to $1/hcr_v^2$, so that

$$\varepsilon_n = \left(\frac{h}{8\pi^2\mu c}\right)^{\frac{1}{2}} \int_0^n \frac{dx}{r_v^2 (U_n - U_x)^{\frac{1}{2}}}$$

The method then consists in evaluating the integrals numerically by division into three parts.

Thus
$$f_n = \left(\frac{h}{8\pi^2\mu c}\right)^{\frac{1}{2}} \left[\int_0^{\frac{1}{2}} \frac{dx}{(U_n - U_x)^{\frac{1}{2}}} + \int_{\frac{1}{2}}^{n-4} \frac{dx}{(U_n - U_x)^{\frac{1}{2}}} + \int_{n-4}^{n} \frac{dx}{(U_n - U_x)^{\frac{1}{2}}} \right]$$

$$= \text{constant } (I_1 + I_2 + I_3)$$

and
$$\varepsilon_n = \left(\frac{h}{8\pi^2\mu c}\right)^{\frac{1}{2}} \left[\int_0^{\frac{1}{2}} \frac{dx}{r_v^2 (U_n - U_x)^{\frac{1}{2}}} + \int_{\frac{1}{2}}^{n-4} \frac{dx}{r_v^2 (U_n - U_x)^{\frac{1}{2}}} + \int_{n-4}^{n} \frac{dx}{(r_v^4 (U_n - U_x))^{\frac{1}{2}}} \right]$$

$$= \text{constant } (I_1' + I_2' + I_3')$$

I_1 and I_1' are both small and are integrated by the trapezium rule. I_2 and I_2' are evaluated by Simpson's rule. For I_3 there remain only 4 values of $(U_n - U_x)$ one of which is exactly equal to zero. These are fitted by least squares to $(ay + by^2)$ and the integration performed analytically.

Thus $$I_3 = \int_0^4 \frac{dy}{(ay+by^2)^{\frac{1}{2}}} = \left[b^{-\frac{1}{2}} \cosh^{-1}\left(\frac{2by}{a} + 1\right)\right]_0^4$$

For I_3' there are four values of $r_v^4(U_n - U_x)$ one of which is again zero. These may be fitted to any expression which represents the data and which can be integrated; for example $cz - dz^2$ was used by Richards and Barrow for O_2 and H_2.

Then $$I_3' = \left[d^{-\frac{1}{2}} \sin^{-1}\left(\frac{2dz}{e} - 1\right)\right]_0^4$$

r_{max} and r_{min} are obtained from f_n and g_n.

Because this method should be of general application but is extremely tedious to carry out it was decided to do the calculations by computer. An algol programme has been written so that the ΔG values from 0 to n-1 and the B values from 0 to n are the required data. The calculations for H_2 and O_2 were found to be satisfactory but for Se_2 the programme failed. Investigation showed that the expression $cz - dz^2$ is not generally applicable for fitting $r_v^4(U_n - U_x)$; d can be positive or negative and for Se_2 it is negative. The programme was modified to allow for either possibility.

The data for the F_1 component of the upper state of Se_2 were taken from the observed values where these were known to be accurate. For the ground state the data were calculated using the derived constants. No extrapolated values were used in either case. The method is not

accurate for small values of n so the programme derives r_{max} and r_{min} for $n \geqslant 8$. The Morse curve may be used to derive the potential curve for lower vibrational levels. The resulting curves are given in Figs. 3 and 4. The calculations for $^{78}Se_2$ and $^{80}Se_2$ were done separately and the agreement is seen to be excellent, a smooth potential curve being given for the upper state. The Morse curve for the ground state was calculated using the value for the dissociation energy which is derived later; that for the upper state used the theoretical dissociation energy and not that of the potential maximum. The agreement between the Klein curve and the Morse curve is not good for high vibrational levels but the differences are about the same for each state. It must be concluded that the Morse curve is not a good approximation for Se_2.

In the upper state there is a clear deviation from the linearly extrapolated curve at v' about 15, indicating that it is dissociating. In fact extrapolation of the last few vibrational intervals gave a value of about 31,800 $cm.^{-1}$ for the dissociation limit, i.e. the potential maximum. The accurate calculation of the potential curves for Se_2 has not produced any new results but they do support qualitatively the conclusions previously drawn from the analysis. The computer programme is given in Appendix C.

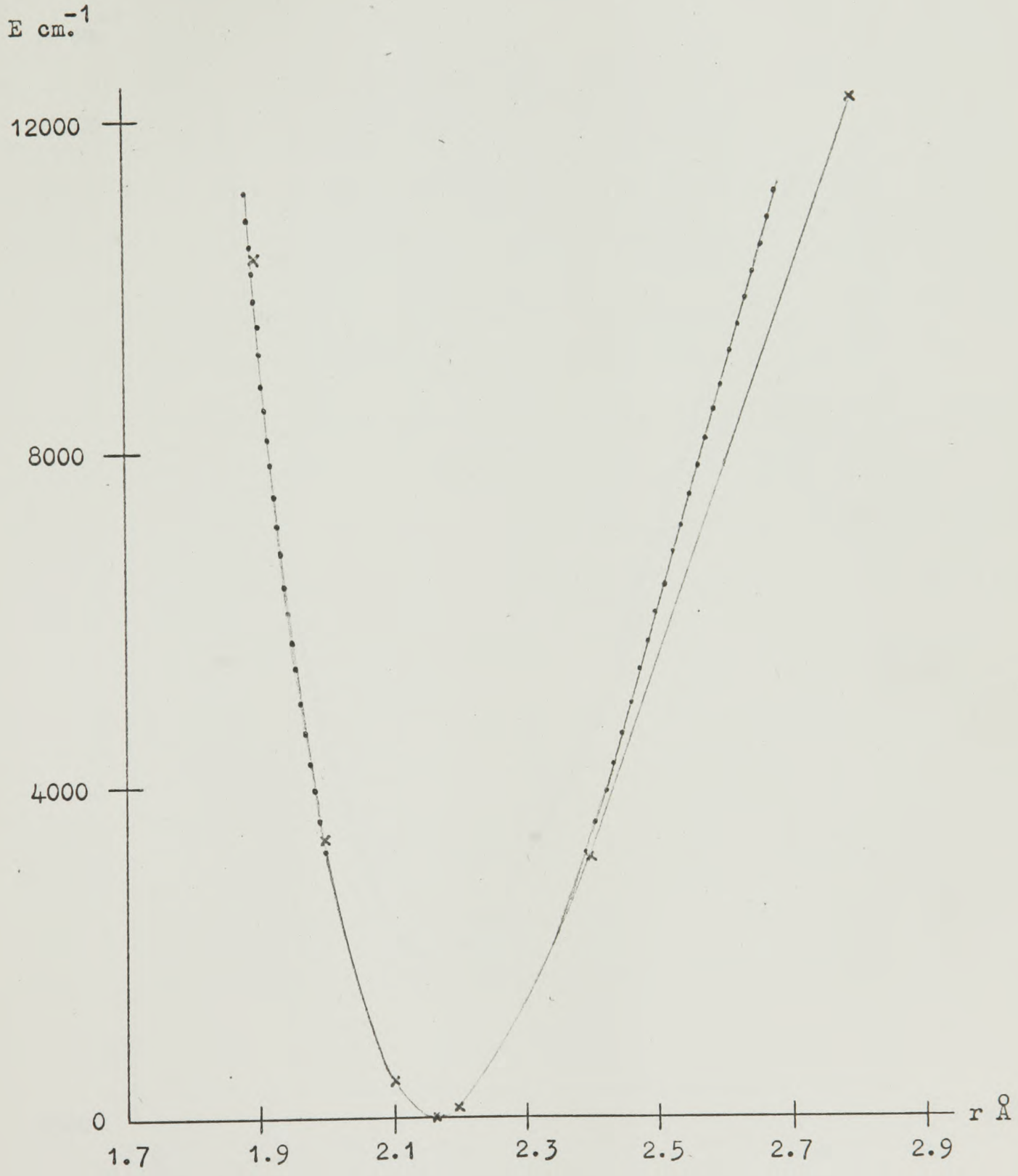

Fig. 3. Klein Curve (...) and Morse Curve (xxx) for the ground state $^3\Sigma_g^-$ of $^{80}Se_2$ F_1 component

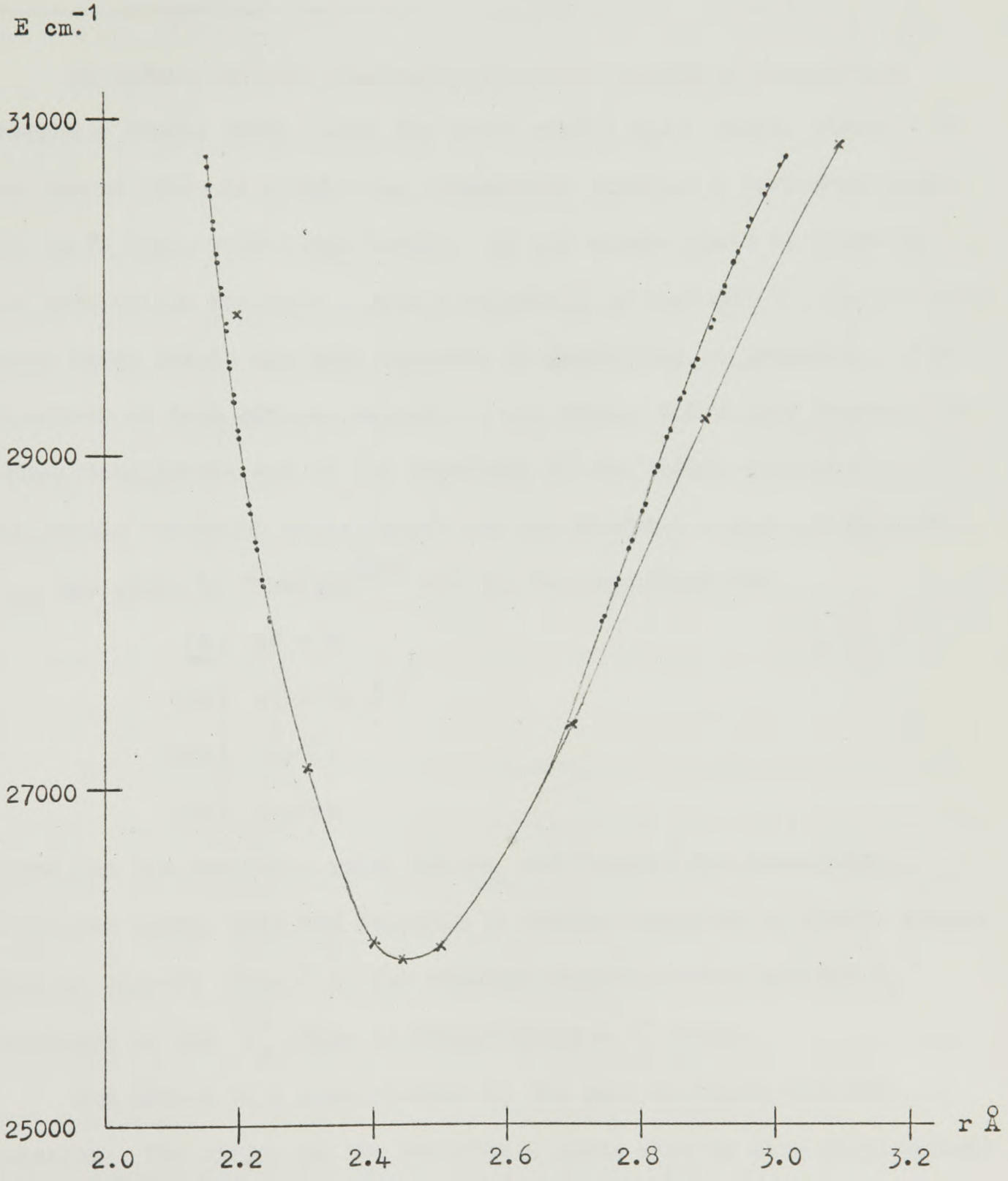

Fig. 4. Klein Curve (...) and Morse Curve (xxx) for the upper state $^3\Sigma_u^-$ of $^{78}Se_2$ and $^{80}Se_2$ F_1 component

Perturbations and Predissociations in $B^3\Sigma_u^-$ (F_1 component)

Perturbations and predissociations are caused by interaction between a stable state (here the upper state) and a second state. If the second state is stable the interaction produces a perturbation of the upper state rotational levels; if the second state is unstable the interaction produces a predissociation, so that all the higher lying upper state levels are made unstable by radiationless transfer. The magnitude of both effects depends on the energy difference between the interacting levels and on the magnitude of the matrix element W_{12}. The Kronig selection rules, which are the conditions for non-vanishing W_{12}, are given by Herzberg[48] and may be summarised as:

(i) $\Delta J = 0$

(ii) $\Delta\Omega = 0, \pm 1$

(iii) $+ \not\leftrightarrow -$

(iv) $s \not\leftrightarrow a$

These are the selection rules for Se_2 and involve the assumption, discussed later, that the molecule is better described by Hund's case-c than by case-b; then Ω is the relevant quantum number and the F_1 component of the $^3\Sigma_u^-$ state is described as a 0_u^+ state.

The effect of a perturbation is the same in absorption and emission; the mixing of the two states gives rise to line displacement and the appearance of extra lines, but the total intensity of lines involving a given J' is not altered. The mixing in a predissociation

produces diffuse upper state levels whose life-times depend on the probability of the radiationless transfer. By the Uncertainty Principle, (half width of a line) x (lifetime) = $h/2\pi$; for a fully allowed transition the lifetime is about 10^{-8} secs, giving a half width of about 10^{-3} $cm.^{-1}$. However, the broadening due to thermal motions produces lines whose Doppler width is 10^{-1} to 10^{-2} $cm.^{-1}$. Thus, if the predissociated state is the upper state, in absorption it is not possible to detect the broadening of a line due to a predissociation until that broadening is about 100 x Doppler width. In emission, however, there is very little occupation of the diffuse levels, and so the intensity of lines from these levels drops by a large factor; this in practice gives a sharp cut-off of the emission branches and it is thus much better to observe a predissociation in emission than in absorption.

But although the total line intensity at a perturbation does not change, the intensity in a branch usually drops (as extra lines appear) and this may be noticeable before the line displacement is measureable. In such a case, especially when there is much band overlapping, it may be difficult to decide whether the intensity drop is due to a perturbation or a predissociation. The only difference then lies in the appearance of the plot of " effective B' " against $(J+\frac{1}{2})^2$, which should remain linear for a predissociation. This method has been carefully applied in all the perturbations and predissociations identified here.

No analysis of any perturbation has been found during this work, the absorption bands being usually overlapped, but it has been frequently possible to pick up the branches at higher J values. The perturbations occur when terms of the perturbing state (comprising rotational and vibrational energies) intersect those of the upper state at a common J value. A plot of the upper state terms, for all the values of v', against J(J+1) was made and the points of perturbations marked in an attempt to find some regularity. However none was found, probably because the B'_v values are so small that a perturbation in, say, v'=x at a value of J < 50, may be expected to appear in v'=x-1 at J > 100, where the weakness of the branches precludes analysis.

The distribution of the perturbations is very significant, however. There are perturbations in every v' level from 0 to 15 which shows that the potential energy curve for the perturbing state extends to a lower energy than that of $^3\Sigma_u^-$. Also the perturbations increase in number with increasing v' until they stop at v'=15; this is attributed to the closing up of the vibrational levels of the perturbing state as it approaches its dissociation energy. This dissociation limit for the perturbing state cannot be found from the plot but it may be derived by a study of the predissociations in the upper state.

The predissociations in v'=13, 14 and 15 have been described; they occur at decreasing J values for increasing v'. Mulliken[28] has indicated the possible types of predissociation and of these only

two have the observed J-dependence, namely c^+ and b^+. Both types involve intersection of a second state B at the right hand limb of the upper state potential curve A, but in c^+ the intersection occurs above the asymptote of B, while in b^+ the intersection occurs below that asymptote. For heavy molecules like Se_2, where B' is very small, the differences in J-dependence between these two types of predissociation are slight. However the conclusions which can be drawn from each are quite different.

c^+

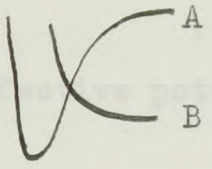

Above the intersection all levels of A are predissociated and to find the dependence on J it is necessary to consider the "effective potential curves" for each state, i.e. those which include rotation, in the manner first described by Oldenburg[29]. The effective potential energy $U_J(r)$ is given by

$$U_J(r) = U_0(r) + \frac{h}{8\pi^2 c\mu r^2} \cdot J(J+1)$$

This produces a set of potential energy curves, differing in their J values, for each state, which intersect at the same "critical" value, r_c, independent of J. These $\Delta J=0$ intersections coincide with actual levels of A only for particular values of J, the "critical", J_c, values,

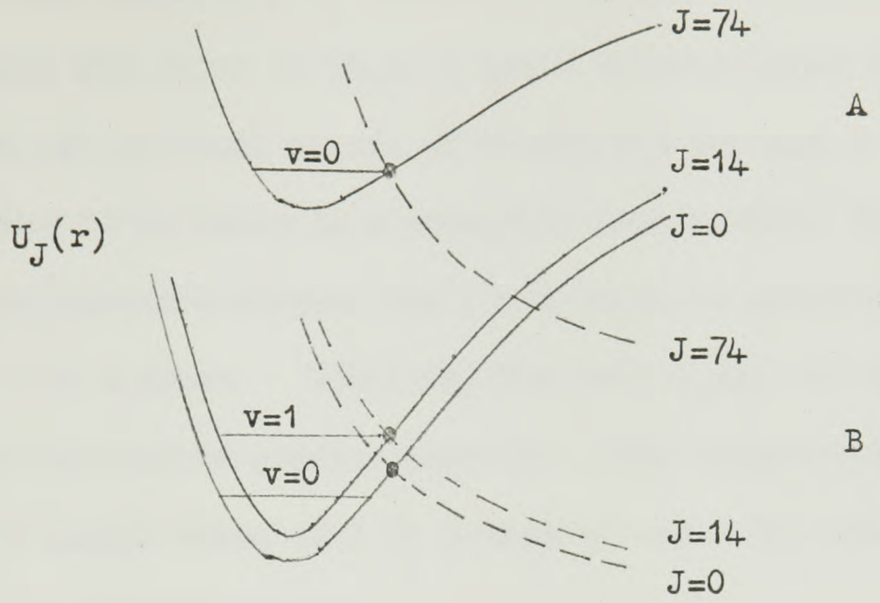

Fig. 5. Effective potential curves for stable A and unstable B, case C^+

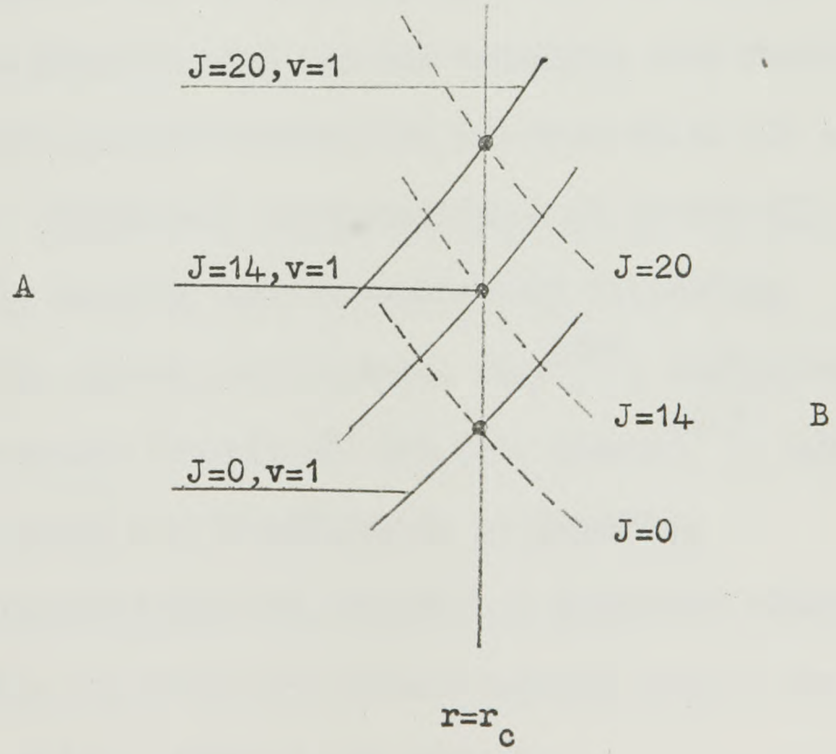

Fig. 6. Enlargement of Fig. 5 showing the intersections for v=1 of A

and in general there is a J_c value for several values of v. A few intersections are shown in Figs. 5 and 6 (adapted from Mulliken[28]) where there are critical values of J only for v=0 and 1. For v=1, J_c=14 and for $J < 14$ there is a potential hump between the actual level of A and the unstable state; for $J \geqslant 14$ there is no potential hump and the levels are diffuse. Similarly for v=0, J_c=74 and thus for $J \geqslant 74$ there is no barrier to predissociation. The diagrams show that for smaller v a larger value of J is needed to reach the limit and thus the higher energy that limit has.

The probability of predissociation at each intersection depends on a Franck-Condon factor and an electronic-rotation factor. The latter usually has a dependence on the J value. The Franck-Condon factor is proportional to the overlap integral of, for example, the v=1 vibrational wave function of A and the continuum wave function of B; this reaches a maximum somewhat above J=14 and then falls off slowly at higher J values. Below J=14 predissociation is classically forbidden but may theoretically occur by quantum-mechanical tunnelling. The tunnelling probability depends on the mass, Rice[30], differences being observed for example between AlH and AlD, Olsson[11], but for Se_2 the mass is too large for tunnelling to be feasible.

Thus, if predissociations are observed in different vibrational levels, the difference in their term values depends only on the rotational energy $B_c J(J+1)$ where B_c is given by

$$B_c = h/8\pi^2 c\mu r_c^2$$

A plot of (term values of predissociation) against J(J+1), for Mulliken's case c^+, will therefore give a straight line of slope B_c. This slope can also be calculated since r_c is about equal to r_{max} of the upper state at that value of v'. Thus a good estimate can be obtained if the shape of the potential curve is known. For the upper state of Se_2 a value of $r_c \doteq 2.85$ Å is derived for v' = 13, 14 and 15 (Fig. 4). This gives $B_c \doteq 0.05$ which should be compared with $B' \doteq 0.07$.

The term value obtained by extrapolating the plot to J=0 is that for the intersection of the two rotationless potential curves. Since this represents a potential maximum, it is not useful for determining the limit of the unstable state; it only sets a maximum value for it.

b^+

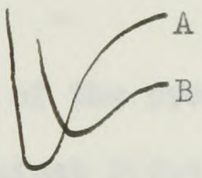

For Mulliken's case b^+ the critical J values and the predissociation probability are exactly the same as for c^+ but here the energy at J_c for some v lies below the asymptote of B. No predissociation can occur until that asymptote is reached; these intersections therefore give rise, by the same selection rules, to perturbations.

With rotation both curves have potential maxima of increasing height at large internuclear distances. These maxima occur at smaller values of r, the r^* values, for increasing values of J. Predissociation

of A will occur sharply when the energy is equal to that of the potential maximum of B, assuming again that no tunnelling occurs. A plot of (term value of predissociation) against J(J+1) will therefore give a curve whose slope is smaller than for case c^+ since r^* is greater than r_c, and the slope will decrease with decreasing J as r^* again becomes larger. In the extreme case of J=0 the slope is zero, representing $r^* = \infty$. This limiting curve of predissociation is very similar to the "limiting curve of dissociation" discussed by Schmid and Gerö[31]. Extrapolation of the observed curve to J=0 gives an accurate estimate of the limit of the dissociating state B. Below the predissociations A is perturbed by B, and above the predissociations all the levels of A are diffuse.

A plot of the predissociations in v' = 13, 14 and 15 for $^{78}Se_2$ and $^{80}Se_2$ against J(J+1) is shown in the upper half of Fig. 7. All the points fall on to a curve of very small slope, which increases rather slightly with J. The observation that the predissociations for both isotopes fall on the same curve supports the assumption that tunnelling does not occur; without it the two isotopes will have the same predissociation behaviour. The J dependence of the slope is small because of the large size of μ in the conversion factor from r^* to B^*. The slope at $J \sim 70$ was estimated to be about 0.006, i.e. about 10 times smaller than B' or B_c (calculated for case c^+). This is equivalent to a value for r^* of about 8 Å, far larger than r_{max} for

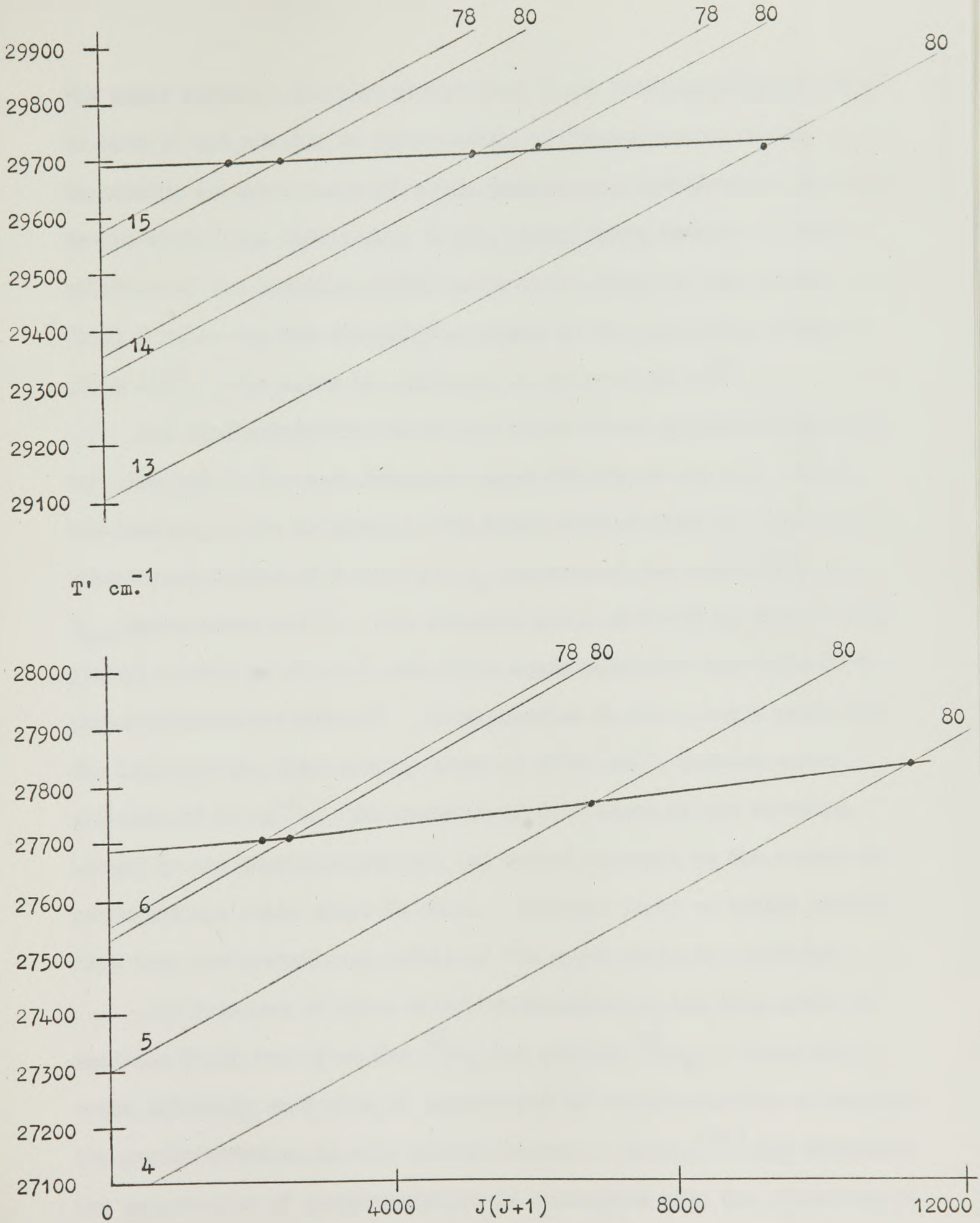

Fig. 7 Plots of term values against J(J+1) and limiting curves of predissociation for the upper state F_1 component

the upper state. It is concluded that these predissociations belong to case b^+ and are due to dissociation of the perturbing state. Supporting evidence comes from the perturbation distribution previously described and the diffuseness in all higher lying levels. Extrapolation of the limiting curve, so that the slope is zero at J=0, gives a value for the dissociation limit of the perturbing state of 29690 $cm.^{-1}$. The error is estimated to be about 20 $cm.^{-1}$.

The predissociations in v' = 4, 5 and 6 were plotted in the same way, the points for both isotopes again falling on the same curve. The limiting curve is shown in the lower half of Fig. 7. For these vibrational levels B' $\doteq$ 0.07 and B_c (calculated for case c^+) $\doteq$ 0.06, r_{max} being about 2.7 Å. The observed slope at J ~ 70 is about 0.009, giving a value of r* ~ 7 Å, and it is again concluded that this is a predissociation of type b^+. Extrapolation to J=0 gives a value for the limit of the dissociating state of 27700 $cm.^{-1}$, with an error estimate of 20 $cm.^{-1}$. The presence of this state is not revealed except by the predissociations; no marked increase in the number of perturbations below these is seen. Possibly it is so weakly stable that very few vibrational levels of the upper state are affected.

The presence of lines after predissociation has been noted in emission bands from v'=6 for $^{78}Se_2$ but not for $^{80}Se_2$. These can arise either by some kind of suppression of predissociation or because the predissociation is only weakly allowed. Olsson[11] has discussed the suppression of predissociation in connection with the structure of

AlH which is predissociated at different values of J depending on the excitation conditions. Mörikofer[32] found no predissociation in the aureole of an arc between Al electrodes in a low pressure of H_2, while there is predissociation in the core of the arc at the same pressure. Bengtsson-Knave and Rydberg[33], however, found that the predissociation depended on the pressure of H_2, no break off being seen at a high pressure. An explanation was first given by Farkas[34] who suggested that thermal equilibrium was being maintained so that the population of the upper levels depended only on the Boltzmann factor. Olsson[11] however suggested another mechanism which is more likely to occur commonly since thermal equilibrium in discharges is probably rare: the de-activating collisions, which remove excitation energy before radiation occurs, affect the predissociated (diffuse) levels much less than the sharp levels since the former have a much shorter lifetime. These collisions increase with pressure; thus the breaking-off may be apparently suppressed because of the greater quenching of the sharp levels. The exposure time should, however, show some increase in this region.

If the predissociation is only weakly allowed, the effect of an increase in pressure may be to relax the selection rules which are derived for the undisturbed molecule. This gives rise to "induced predissociation". Mersberg and Mundie[35] found such a pressure effect in the predissociation after J'=0 of the 4280 Å band of CuH, where the

probability is low because the predissociation is spin-forbidden ($^1\Sigma$-$^3\Sigma$). The predissociation was only marked at very low pressures, because at high pressure the stable J'=0 level was induced predissociated giving a weak, instead of an abnormally strong, P_1 line.

For Se_2, excited by a microwave discharge, the variations in temperature and pressure between different discharge tubes could be large. Since the emission experimental work was not done at the same time or place as the analysis no experimental details were available. But if there is thermal equilibrium or a large number of de-activating collisions, then the predissociated levels are either diffuse or the rotational structure should be weaker in the predissociated bands. It is found that the lines in v'=6 are sharp after the cut-off and no decrease in intensity of the bands occurs. It is concluded that the different behaviour of the two isotopes is due to a difference in their pressures and that the predissociation must be only weakly allowed.

Finally the "diffuse perturbations" must be discussed. These occur throughout the region $7 \leq v' \leq 15$. It has already been suggested that these are accidental predissociations involving a third unstable state as well as the perturbing state. The dissociation limit in v'=6 provides supporting evidence for this third state. There are rather few proven cases of accidental predissociation. Schmid and Gerö[36] reported intensity drops in the v'=0 and 1 bands of the γ system of NO where these interact with the predissociated levels of the upper state of the β-system. Kovacs and Budo[37] also studied these

bands and gave a theoretical explanation for the drop in line intensity in emission. This was based, however, on the absence of perturbations at the interactions with lower levels of the upper state of the β-system, which they assumed to be due to a small matrix element of interaction between the two stable states. If perturbations were present then, by their arguments, line displacement should accompany the drop in intensity in emission or the increase in diffuseness in absorption. Their observations are not supported by more recent work however. Herzberg, Lagerqvist and Miescher[38] give the potential curves for the low lying excited states of NO. The γ-bands correspond to the transition $A^2\Sigma^+ - X^2\Pi$ and the perturbing β-bands to $B^2\Pi - X^2\Pi$. But these curves do not overlap below $v'=4$ in $A^2\Sigma^+$ so that no interaction can occur in $v'=0$ or 1. In addition the lowest-lying dissociation limit, which could give rise to the desired unstable third state, occurs above $v'=3$ in $A^2\Sigma^+$. The complexity of the spectrum in the region of the γ-bands is so great that the observations of accidental predissociations must be rejected. However, the theoretical arguments of Kovacs and Budo are valid.

Reliable examples of accidental predissociations have been found in N_2 by Frackowiak[39] and in HBr by Barrow and Stamper[40]. In Band [26] of HBr, observed in absorption, the R(3), P(5) and the R(6), P(8) lines are split into two components and are much more intense than neighbouring lines. The intensity increase is an optical effect arising from the increased diffuseness. The upper state $^1\Pi$ is

perturbed at these intersections by $^3\Sigma^-$ and it is possible that the accidental predissociation occurs by interaction of $^3\Sigma^-$ with another triplet state, which cannot interact directly with $^1\Pi$. The predissociation is observed only in a single rotational level at each intersection, because the B values are so large, ~ 8.2 $cm.^{-1}$, that the energy separation between the perturbing states passes through the minimum very rapidly.

A situation very similar to that described in Se_2 appears in S_2. du Parcq[41] found that in the 0-0 band of the $C^3\Sigma_u^- - X^3\Sigma_g^-$ system, the F_3 component of the upper state has diffuse levels in absorption over a J range of about 14. The diffuseness is so strong at the centre that the lines could not be measured but there appeared to be a perturbation.

For Se_2 it is concluded that all the diffuse perturbations observed in absorption are accidental predissociations, the limit of the unstable state lying below v'=7 of $^3\Sigma_u^-(F_1)$. If the single weak rotational level observed in emission bands with v'=6 is also due to an accidental predissociation, then the limit lies below v'=6 of $^3\Sigma_u^-(F_1)$.

F_2, F_3 Analysis

The absorption spectrum of the F_1 components is quite heavily overlapped even when separated isotopes are used. For easier analysis the temperature was kept as low as possible throughout the range of $v' = 2$ to 21. But for $v' < 2$ the Franck-Condon parabola is such that $v'' \sim 7$ must be populated for absorption studies and correspondingly higher temperatures were used. In the region of the 0-8, 0-9 and 0-10 F_1 bands some extra bands have been observed at these temperatures (400° and 800° in side-arm and main tube respectively). These bands have four branches and analysis confirms that they are the F_2, F_3 components. The intensities are much lower than for the F_1 component (see Plate 6).

1. Rotational Analysis

The analysis was straightforward; the F_2 branches are numbered by even values of J and the F_3 branches by odd values of J. The relative numbering in each band is fixed by observation of a perturbation which occurs at about the same J value in F_2 and F_3; B'_v is again found to be greater than B_p. The absolute numbering is fixed by comparison of the ground state combination differences of the F_3 components with those of the F_1 component, which are rather similar. Both F_2 and F_3 numberings were checked by observing the linearity of a

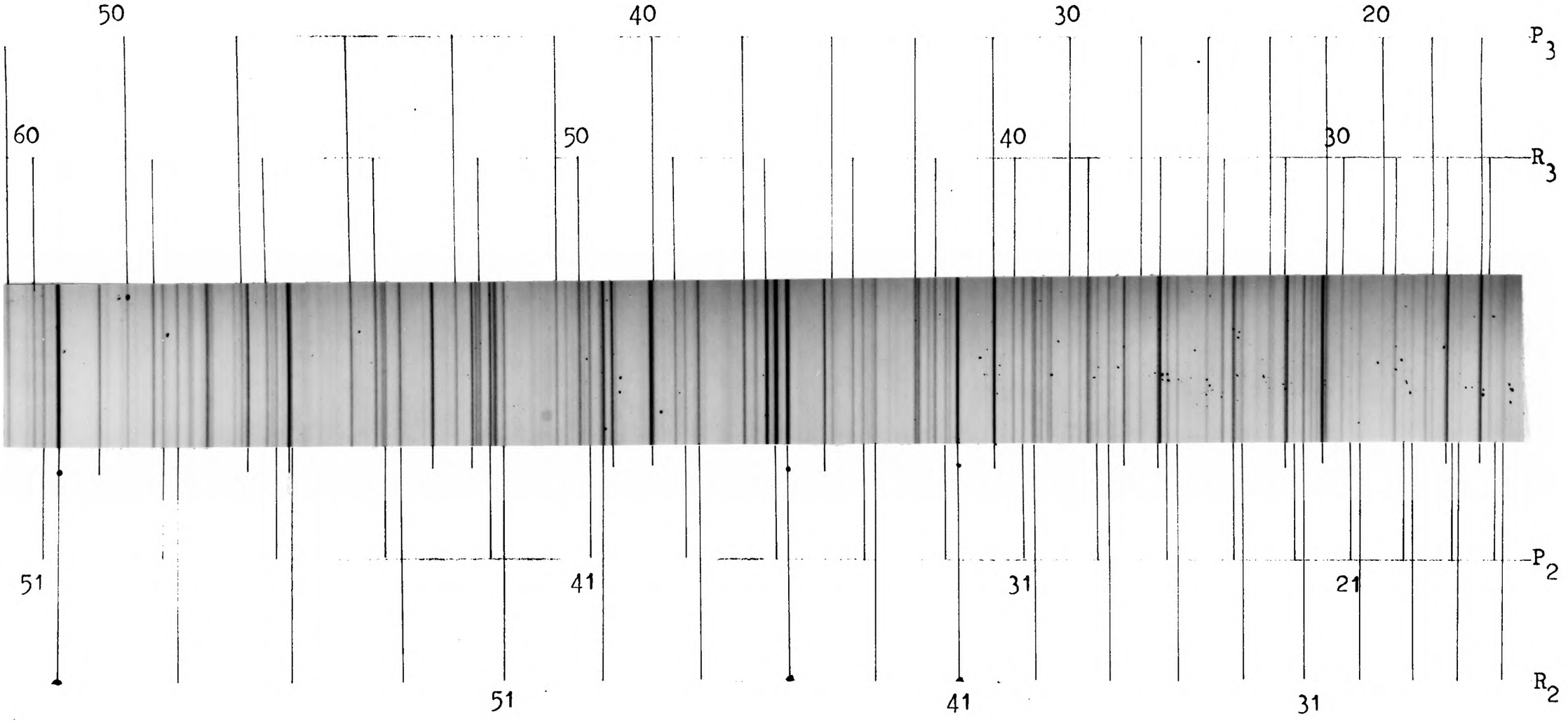

Plate 6. 0-9 F_2,F_3-F_2,F_3 Band of $^{80}Se_2$, overlapped by stronger 0-10 F_1-F_1 Band, in absorption.

plot of $\Delta_2 F''/(J+\frac{1}{2})$ against $(J+\frac{1}{2})^2$. The rotational constants were determined in the usual way and values are given in Tables 10 and 11, together with those from the previous emission work.

v'=5

The strong 5-28 and 5-29 bands of $^{80}Se_2$ were previously analysed but a perturbation at $J' \sim 12$ prevented the determination of B_5' and the band origins. The approximate values of ν_0 were found to be 16620 and 16290 $cm.^{-1}$ respectively. A perturbation was noted at $J' \sim 70$; this region has been re-analysed because of the sharp cut-off in the perturbed region. Two lines of each branch occur strongly beyond the perturbation but no structure appears, with similar intensity, thereafter. The new analysis indicates a predissociation at J'=73 and 72 for the F_2 and F_3 components respectively. A search was then made for bands from v'=6; the Franck-Condon parabola is such that the 6-29 and 6-30 bands, at 16518 and 16190 $cm.^{-1}$ respectively, should occur strongly. Neither of these bands has been found and it is concluded that v'=6 is predissociated. This explains the absence of F_2,F_3 bands in the u-v region below about 4000 Å, where the 6-2 and 6-1 bands should also occur strongly.

v'=4

The 4-28 band of $^{80}Se_2$ was previously analysed. There are

TABLE 10 Rotational Constants, in $cm.^{-1}$, F_2, F_3 components $B^3\Sigma_u^-$

	v	$B(F_2)$	$B(F_3)$
$^{80}Se_2$			
	0	0.07041 ± 0.00006	0.07085 ± 0.00007
	1	0.06980 ± 0.00007	0.07019 ± 0.00007
	3	0.06887 ± 0.00009	0.06918 ± 0.00011
	4	0.06809 ± 0.00010	0.06846 ± 0.00010

$$\alpha(F_2) = \alpha(F_3) = 0.000553$$

$$B_e(F_2) = 0.07067 \qquad B_e(F_3) = 0.07105$$

$$B_e(\text{m.v.}) = 0.07086$$

$$r_e(\text{m.v.}) = 2.4398 \text{ Å}$$

$^{78}Se_2$			
	0	0.07219 ± 0.00006	0.07260 ± 0.00007
	1	0.07153 ± 0.00006	0.07193 ± 0.00008

$$\alpha(F_2) = \alpha(F_3) = 0.000574 \quad \text{calc. from } ^{80}Se_2$$

$$B_e(F_2) = 0.07244 \qquad B_e(F_3) = 0.07284$$

$$B_e(\text{m.v.}) = 0.07264 \quad \text{cf. calc. } 0.07268$$

$$r_e(\text{m.v.}) = 2.4405 \text{ Å}$$

$$D(^{78}Se_2) = D(^{80}Se_2) = 2 \times 10^{-8}$$

TABLE 11 Rotational Constants, in cm^{-1}, F_2, F_3 components $X^3\Sigma_g^-$

	v	$B(F_2)$	$B(F_3)$
$^{80}Se_2$			
	8	0.08758 ± 0.00008	0.08762 ± 0.00007
	9	0.08736 ± 0.00006	0.08737 ± 0.00007
	27	0.08193 ± 0.00009	0.08193 ± 0.00012
	28	0.08167 ± 0.00010	0.08158 ± 0.00004
	29	0.08141 ± 0.00007	0.08140 ± 0.00011

$$\alpha(F_2) = \alpha(F_3) = 0.000297$$

$$B_e(F_2) = B_e(F_3) = 0.09012$$

$$r_e = 2.1635 \text{ Å}$$

$^{78}Se_2$			
	8	0.08993 ± 0.00006	0.08996 ± 0.00010
	9	0.08943 ± 0.00007	0.08954 ± 0.00007

$$\alpha(F_2) = \alpha(F_3) = 0.000309 \quad \text{calc. from } ^{80}Se_2$$

$$B_e(F_2) = B_e(F_3) = 0.09250 \quad \text{cf. calc. } 0.09243$$

$$r_e = 2.1626 \text{ Å}$$

$$D(^{78}Se_2) = D(^{80}Se_2) = 2 \times 10^{-8}$$

perturbations at J' ~ 70 and 86, and no analysis at higher J values was achieved.

v'=3

The 3-27 and 3-28 bands of $^{80}Se_2$ were previously analysed. There are perturbations at J' ~ 40 and 72. Insufficient analysis of the F_2 component of the 3-28 band at J' < 40 was found for determination of B' and ν_0.

v'=1

The 1-8 and 1-9 absorption bands have been analysed. There is a perturbation at J' ~ 78 for each isotope.

v'=0

The 0-9 absorption band has been analysed; there is a perturbation at J' ~ 74 for $^{80}Se_2$ and J' ~ 82 for $^{78}Se_2$.

2. Vibrational Analysis

The band origins of the F_2 and F_3 components are found to be identical so that both fit into the same vibrational scheme. An attempt was made to find the vibrational numbering of the F_2,F_3

components by comparison of the B''_v values with those of the F_1 component. This was unsuccessful because the values have too much scatter and regularity is not apparent over such a small range of v". However, it did give some idea of the numbering of the emission bands of $^{80}Se_2$ which all have high values of v". The absorption bands occur in the region of the F_1 (0-9) band and the Franck-Condon parabolae must be very similar for the two components. Using the isotopic shifts calculated from F_1 vibrational constants, the numbering of the F_2,F_3 absorption bands was tentatively assigned, although the agreement was not very good. The difference (F_1 origin - F_2,F_3 origin) of the absorption bands was found to be about 450 $cm.^{-1}$ using this numbering.

For TeO (see Chapter II) the ground state vibrational constant ω''_e of the 1 component is slightly larger than that of the 0^+ component, and in S_2[43] and SeO[23] the spin-splitting constant λ'' increases with v". These both suggest that the separation of the F_1 and F_2,F_3 components increases slightly with v". The same situation is expected to occur in Se_2, so that the (F_1 - F_2,F_3) difference for each band should be slightly larger at high v" values. Using this as a guide, the emission F_2,F_3 bands were given a vibrational numbering, which in fact differed from that deduced from the B''_v values by one. The vibrational constants were derived for each of these two possible numberings of the emission bands and for one only were the values at all comparable with the F_1 constants, but for that the agreement was

very close. This is the numbering adopted; band origins and derived vibrational constants are given in Table 12.

The term values $T'_{v,e}$, relative to the bottom of the F_2,F_3 ground state potential curve, were calculated using the derived constants. Values for each isotope are compared with those from (ν_0 observed + G''_v) in Table 13. The observed value for v'=1 of $^{78}Se_2$ is anomalous. It is suggested that there is an undetected rotational perturbation at a low J value which makes the ν_0 values for v'=1 uncertain. This is supported by the failure to analyse this level of $^{78}Se_2$ to the low J values found elsewhere. The isotope effect is also shown in Table 13; there is good agreement for v'=0 but not for v'=1 bands as expected.

The vibrational analysis thus depends on three considerations:

(i) reasonable agreement between the B''_v values for all the components;

(ii) close agreement of the vibrational constants for F_1 and F_2,F_3 but $\omega''_e(F_2,F_3)$ slightly larger than $\omega''_e(F_1)$;

(iii) reasonable agreement between calculated and observed isotopic shifts.

All these factors are only satisfied for the numbering given. The derived value of $\nu_e(F_2,F_3)$ is smaller than $\nu_e(F_1)$ by 434.51 $cm.^{-1}$, which is equal to $2\lambda'' - 2\lambda'$.

TABLE 12 Band Origins and Vibrational Constants, in $cm.^{-1}$, F_2, F_3 components

Band	$^{80}Se_2$		$^{78}Se_2$	
	F_2	F_3	F_2	F_3
0-9	22080.59	22080.59	22037.61	22037.61
1-9	22324.57	22324.56	22284.98	22284.94
1-8	22694.38	22694.37	22659.39	22659.33
3-27	16478.72	16478.74		
3-28		16146.12		
4-28	16382.86	16382.74		

Derived constants for $^{80}Se_2$

$\nu_{ee} = 25545.85$ $\quad\quad$ $\omega''_e = 386.43$

$\omega'_e = 246.42$ $\quad\quad$ $x_e\omega''_e = 0.9058$

$x_e\omega'_e = 1.225$ $\quad\quad$ $y_e\omega''_e = -13.13 \times 10^{-4}$

TABLE 13 Vibrational Term Values and Isotope Effect, in $cm.^{-1}$, $^2F_2, ^2F_3$ components

Values of $T'_{v,e}$

v	$^{80}Se_2$ obs.	$^{80}Se_2$ calc.	$^{78}Se_2$ obs.	$^{78}Se_2$ calc.
0	25668.80	25668.75	25670.48	25670.31
1	25912.78	25912.72	25917.88	25917.36
3	26393.25	26393.31		
4	26629.86	26629.93		

Values of $\Delta\nu(^{80}Se_2 - ^{78}Se_2)$, in $cm.^{-1}$

Band	obs.	calc.
0-9	42.98	43.10
1-9	39.61	40.02
1-8	35.02	35.52

Triplet Splitting

The relationship $B(F_3) - B(F_2) = B(F_2) - B(F_1) = 2B^2/(\lambda^2-2\lambda B)^{\frac{1}{2}}$ for case-b (large λ) was found to hold for SeO[23]. A value of $\lambda'' \sim 150$ cm.$^{-1}$ was previously derived for Se_2 by a centre of gravity method from the differences $B_v(F_3) - B_v(F_2)$ for v" = 28, 29 and 30. Recalculation using least squares techniques has shown, however, that there is no significant difference in the B values for these levels nor for v"=8 and 9 found in absorption. Furthermore the completion of a vibrational analysis for the $F_2,F_3 - F_2,F_3$ transition enables direct comparison to be made with $B_v(F_1)$, the values of which for all v" are much lower than for $B_v(F_2,F_3)$. Thus the case-b (large λ) relationship does not hold for the ground state of Se_2 and it is better described by case-c.

A $^3\Sigma_g^-$ state in case-c gives rise to 0_g^+ and 1_g states whose rotational energies depend on the quantum number J. The correlation is $F_2(J) \rightarrow 1^-$ and $F_3(J) \rightarrow 1^+$ (see Fig. 10 but neglect levels with - symmetry). The Λ-doubling in the 1_g state is presumably caused mainly by interaction with the 0_g^+ state (lying below at a distance which may be called 2λ) so that the order of the levels is expected to be $F_3(J) > F_2(J)$. The negligible difference between $B(F_2)$ and $B(F_3)$ suggests that the Λ-doubling is small. However, recently Åslund[94] in Stockholm has developed a method for the determination of rotational term values which gives rotational constants more precise by about a

factor of 10 than from combination differences. A computer programme has been written in Oxford by Gissane[95] and Dr. W.G. Richards and used to derive very accurate B values for v"=9 of the F_2 and F_3 component of $^{80}Se_2$. Thus by a conventional least squares method on combination differences

$$B(F_2) = .08736 \pm .00006 \quad cm.^{-1}$$

$$B(F_3) = .08737 \pm .00007$$

By a least squares method on term values

$$B(F_2) = .087385 \pm .000009 \quad cm.^{-1}$$

$$B(F_3) = .087401 \pm .000008$$

The difference (0.000016 ± 0.000008) may be found still more accurately by direct determination of the slope of $F_3(J) - F_2(J)$ against J(J+1), giving 0.000021 ± .000002. This is thus the Λ-doubling constant q for the 1_g state. In case-b (large λ) this is correlated with $2B^2/(\lambda^2-2\lambda B)^{\frac{1}{2}}$, i.e. with $2B^2/\lambda$ when λ is large. In case-c, if the Λ-doubling is due only to the lower 0^+_g state, then the case of "pure precession" suggested by Van Vleck[19] may occur; q is then given by $q = 2B^2L(L+1)/\nu(\Pi,\Sigma)$, where $\nu(\Pi,\Sigma)$ is here the $1\text{-}0^+$ separation 2A". If L=1, $q = 2B^2/\lambda$.

The result is the same in each case, perhaps because both have the same assumption - that the F_3-$F_2(1)$ splitting is due only to the lower $F_1(0^+)$ component. The only case-c molecule which has been analysed and which can be used to test the result for the configuration

$\ldots\pi^2$ is BiH. Heimer[37] gives $q = 0.020$ and $B = 5.141$ cm.$^{-1}$ for the 1 state. This gives a 0^+-1 separation in the $^3\Sigma^-$ ground state of 5290 cm.$^{-1}$ which compares quite well with the directly determined value of 4916.9 cm.$^{-1}$.

For Se_2, substitution of the most accurate values of q and B gives $\lambda'' = 727$ cm.$^{-1}$. This result need not be accepted however because (i) the case-b (large λ) relationships do not hold for all three components of $^3\Sigma_g^-$; (ii) the simplification implied by "pure precession" may not be justified; (iii) the value given to L in case-c is not certain for two electrons each with l=1. This is the only method, however, for obtaining an estimate of the $F_2, F_3 - F_1$ separation from the B values.

For the upper state, comparison of the B_e values shows that $B_e(F_3) - B_e(F_2)$ is about twice as large as $B_e(F_2) - B_e(F_1)$. This may indicate that the upper state has more case-b character than the ground state, but has limited significance in the determination of the sign or value of λ'. The F_1, F_2 and F_3 nomenclature has been retained because of the doubt that Se_2 is fully in case-c.

The States of Se_2

If Se_2 is described by Hund's case-c, then the F_1-F_1 transition of $B^3\Sigma_u^- - X^3\Sigma_g^-$, which has been so extensively studied, becomes $B0_u^+ - X0_u^+$. The selection rules therefore permit interactions with 1_u and 0_u^+ states only. The vibrational perturbations for $v' > 13$ have been assigned as homogeneous perturbations, i.e. with $\Delta\Omega=0$, so that the unstable state causing the potential maximum must be 0_u^+. The perturbing state, which dissociates at 29690 $cm.^{-1}$, causes no such marked change in the potential curve of $B0_u^+$ which suggests that it cannot also be 0_u^+. No direct inference from the perturbations has been made but the perturbing state does interact strongly with $B0_u^+$, and therefore it is assigned as a 1_u state. In addition the diffuseness of the lines in bands above 29690 $cm.^{-1}$, i.e. with $v' > 15$, increases with J; the predissociation is thus heterogeneous, which confirms the 1_u assignment. The accidental predissociations only occur in $B0_u^+$ via the perturbing 1_u state and so the third unstable state could be a 2_u state.

However, it is unlikely that the transition from case-b to case-c is complete in Se_2 so that the transition retains some of the character of $^3\Sigma_u^- - {}^3\Sigma_g^-$. The lowest lying electron configurations of Se_2 and the resultant case-b states are:

$....(\sigma_g\ 4p)^2\ (\pi_u\ 4p)^4\ (\pi^*_g\ 4p)^2$ .... $^1\Sigma^+_g,\ ^3\Sigma^-_g,\ ^1\Delta_g$

$....(\sigma_g\ 4p)^2\ (\pi_u\ 4p)^3\ (\pi^*_g\ 4p)^3$ .... $^1\Sigma^+_u,\ ^1\Sigma^-_u,\ ^1\Delta_u,\ ^3\Sigma^+_u,\ ^3\Sigma^-_u,\ ^3\Delta_u$.

By Hund's rules, the $^3\Delta_u$ is the lowest lying stable state from the first excited configuration, i.e. below the upper state $^3\Sigma^-_u$. In S_2 the perturbing state is assigned by Ketteringham[44] as $^3\Pi_u$, which in Se_2 can come from the configuration

$....(\sigma_g\ 4p)^2\ (\pi_u\ 4p)^4\ (\pi^*_g\ 4p)\ (\sigma^*_u\ 4p)$ .... $^3\Pi_u,\ ^1\Pi_u$.

The $^1\Pi_u$ state will, by Hund's rules, lie higher than $^3\Pi_u$. If the analogy with S_2 is close, then in Se_2 the perturbing state is also $^3\Pi_u$ which in case-c gives a 1_u state in agreement with observation.

Further specification of the states is difficult because there are so many 0^+_u, 1_u and 2_u states in Se_2 if it is near case-c, and the case-b to case-c transition may be different for each.

The Dissociation Energy

Two methods have been previously used to study the dissociation energy of Se_2: (1) equilibrium studies; (2) u-v spectroscopy by (a) band convergence studies and (b) predissociation studies.

(1) The equilibrium studies were done by Nernst and van Wartenburg; their values for the degree of dissociation of Se_2 were used by Goldfinger, Jeunehomme and Rosen[45] in 1936 to obtain an approximate value for the dissociation energy of either 60 or 70 k.cals. The value depended on the statistical weight of the ground state, and since this is now known to be 3, at least at high temperatures, the derived value is 60 k.cals.

(2) The band convergence and predissociation studies require accurate vibrational analyses and knowledge of the electronic transition. The previous analyses have been shown to be wrong on both counts so that their conclusions are unreliable; however the points of difference must be discussed.

(a) Linear (Birge-Sponer) extrapolation of the ground state vibrational levels of Rosen[12] gives the value of D''_e = 104 k.cals. In the other Group VI molecules, O_2 and S_2, this method gives values which are about 25% too high; application of this rough correction gives D''_e = 83 k.cals. The upper state converges more rapidly and graphical extrapolation by Olsson[11] gave D''_e = 23 k.cals. To get a value of D''_e

from this the ν_e for the transition and the excitation energy of the upper state atomic products must be known. While the value taken for ν_e is roughly correct, Olsson correlated the atomic product as $^3P + {}^1D$, thus violating the Wigner-Witmer rules, since he believed the upper state to be a $^1\Sigma_u^+$ state.

(b) Rosen[12] reported predissociations in v'=6 to 10 at decreasing values of J and deduced a limit at 29500 cm.$^{-1}$. The absence of these predissociations in the recent high dispersion emission work has already been discussed. Rosen also studied the intense absorption predissociations for v' > 22 and deduced a limit at 30865 cm.$^{-1}$. The absorption maximum was studied by Asundi and Parti[7] who gave a limit at 31557 cm.$^{-1}$. Nevin[10] suggested that there was an induced predissociation with a limit at 30535 cm.$^{-1}$. Several other observations have also been made[72-77]. In 1963 Herman and Herman[24] restudied the last few absorption bands with high dispersion but using natural selenium; their conclusions about the crossing of the potential curves were indefinite.

Olsson[11] and Davis and Jenkins[14] correctly assigned the cut-off in the emission bands with v'=6 as a predissociation, and this was used to give an upper limit to D_e'' of 28670 cm.$^{-1}$ but the vibrational numbering of the v'=6 bands was incorrect - being assigned for example as 10-6 instead of 6-3. The incorrect assignment of v' does not affect the dissociation limit but that for v" does, since the value

given is a term value relative to the bottom of the potential curve of the ground state. This is derived from (wavenumber of last observed line) + G''_v + F''_J. The value for G''_v was thus taken as G''_6 instead of the correct value G''_3. This correction lowers the value given by about 1100 $cm.^{-1}$. In addition the observation of only one predissociation cannot provide information about the stability of the state causing it.

Using the results from these methods, Gaydon[66] concluded that a value of 65 k.cals. was probably correct. Using the same information, Détry[67] recently deduced a value of 74 ± 3 k.cals. Both these conclusions must be rejected because the upper state converges to a potential maximum and the increase in diffuseness arises from a quite different interaction with a perturbing state. Also there is the failure to differentiate between the various isotopic species, and the non-recognition of the triplet nature of the transition.

The dissociation energy may be derived, however, by using the results of the present analysis of the $^3\Sigma_u^- - {}^3\Sigma_g^-$ transition. It has been shown that λ'' is large and positive. The F_1 component therefore lies below the F_2, F_3 component of $^3\Sigma_g^-$ so that in the case-c limit the 0_g^+ component lies below the 1_g component. The potential curves for these components are then independent but they may be quite similar.

The dissociation limits of the two states which predissociate

BO_u^+ have been found to lie at 29690 ± 20 $cm.^{-1}$ and 27700 ± 20 $cm.^{-1}$ respectively. The energy difference between these limits, 1990 $cm.^{-1}$, should agree with the difference between some atomic terms of Se. Moore[69] gives the low-lying terms for Se in $cm.^{-1}$ as

$$^3P_2 - 0$$

$$^3P_1 - 1989.5$$

$$^3P_0 - 2534.3$$

$$^1D - 9576.1$$

The interval $^3P_1 - {}^3P_2$ therefore corresponds exactly to the observed origin difference; this surely confirms that the state predissociating BO_u^+ at 27700 $cm.^{-1}$, but not otherwise observed, is stable. The atomic configurations for these two states are therefore either

(I)	$^3P_1 + {}^3P_2$	or (II)	$^3P_1 + {}^3P_1$	or (III)	$^3P_1 + {}^3P_0$
	$^3P_2 + {}^3P_2$		$^3P_2 + {}^3P_1$		$^3P_2 + {}^3P_0$
giving	$D_e'' = 27700$ $cm.^{-1}$		25710 $cm.^{-1}$		25166 $cm.^{-1}$

The terms of Se are so evenly spaced that differentiation between these three is not obvious. A Birge-Sponer extrapolation of the upper state cannot be used and that for the ground state is too inaccurate. Looking at non-spectroscopic evidence the value from the equilibrium study is also too inaccurate. However, during the course of this

work some mass-spectroscopic studies were carried out by Detry[67] who found D_0^0 (Se_2) = 74 ± 3 k.cals. He also indicated that a similar study by Jeunehomme[70] gave 77.2 ± 5 k.cals. These results were pointed out in a personal communication from Professor J. Drowart in 1965 who derived from these and other studies by Colin, a mean value of D_0'' (Se_2) = 75 ± 2 k.cal. All these workers used double Knudsen cells, of the type described by Porter[71], containing ZnSe or In_2Se_3. The equilibrium $Se_2(g) \leftrightarrow 2Se(g)$ was studied and application of standard 2nd and 3rd law techniques gave the value for D_0^0 (Se_2) equal to 26238 ± 700 $cm.^{-1}$, equivalent to D_e'' (Se_2) = 26430 ± 700 $cm.^{-1}$. Of the spectroscopic values the only one to fall within the quoted range is (II), 25710 $cm.^{-1}$. The values of (III), 25166 $cm.^{-1}$, and (I), 27700 $cm.^{-1}$, would both require errors of about ± 3.5 k.cal. in the mass spectroscopic value. Although this is larger than the quoted error it cannot be ruled out as a possibility. Thus, although the mass-spectroscopic value may be sufficiently good for most thermodynamic purposes, it is not known precisely enough for the spectroscopic atomic products to be defined.

A purely spectroscopic argument can, however, be given by studying the possible states arising from the atomic products. Hund's case-c is a good approximation at large internuclear distances where the field is weak, so that the J values of the atomic products may be correlated with the Ω values of the molecular states. The correlations

are given in Fig. 8. Now a 0_u^+ state has been found to cause the vibrational perturbations for $v' > 13$ and the origin has been shown to lie below $v'=14$, i.e. below the predissociation at 29690 $cm.^{-1}$. For (I) this means that the 0_u^+ state comes from atomic products lower than $^3P_2 + {}^3P_1$. The only lower products are $^3P_2 + {}^3P_2$ and these do not give rise to a 0_u^+ state (Fig. 8). This eliminates (I) from further consideration, but the same argument cannot be used to differentiate between (II) and (III). It may be noted, however, that the highest lying products which can give a 0_u^+ state are $^3P_2 + {}^3P_0$ and in both (II) and (III) these lie well below 29690 $cm.^{-1}$. This confirms that only a repulsive 0_u^+ state can perturb $B0_u^+$ above $v'=13$.

The atomic products and their energies for (II) and (III) are shown in Fig. 9. The arguments for accepting (III) as correct follow:

(a) For (III) the 1+1 products at 29145 $cm.^{-1}$ can give rise to a 1_u state which could interact with $B0_u^+$. This interaction is found in the predissociation at a low J value in $v'=13$ for each isotope at an energy of about 29180 $cm.^{-1}$. Such a convincing explanation for this predissociation cannot be found for (II).

(b) The observation of accidental predissociation for each isotope in emission in $v'=6$, but below the 27700 $cm.^{-1}$ predissociation, is easily explained for (III) by the presence of the 2+1 limit at 27155 $cm.^{-1}$ which could give rise to an unstable 2_u state. For (II) the unstable 2_u state would have to come from 2+2 which has

$^3P_0 + {}^3P_0$ (5068.6) 0_g^+

$^3P_1 + {}^3P_0$ (4523.8) 1_u, 1_g, 0_u^-, 0_g^-

$^3P_1 + {}^3P_1$ (3979.0) 2_g, 1_u, 1_g, 0_g^+, 0_g^+, 0_u^-

$^3P_2 + {}^3P_0$ (2534.3) 2_u, 2_g, 1_u, 1_g, 0_u^+, 0_g^+

$^3P_2 + {}^3P_1$ (1989.5) 3_u, 3_g, 2_u, 2_g, 2_u, 2_g, 1_u, 1_g, 1_u, 1_g, 1_u, 1_g, 0_u^+, 0_g^+, 0_u^-, 0_g^-, 0_u^-, 0_g^-

$^3P_2 + {}^3P_2$ (0) 4_g, 3_u, 3_g, 2_u, 2_g, 2_g, 1_u, 1_g, 1_u, 1_g, 0_g^+, 0_g^+, 0_g^+, 0_u^-, 0_u^-

Fig. 8 Correlation of atomic J with molecular Ω for Se_2, with energies in $cm.^{-1}$

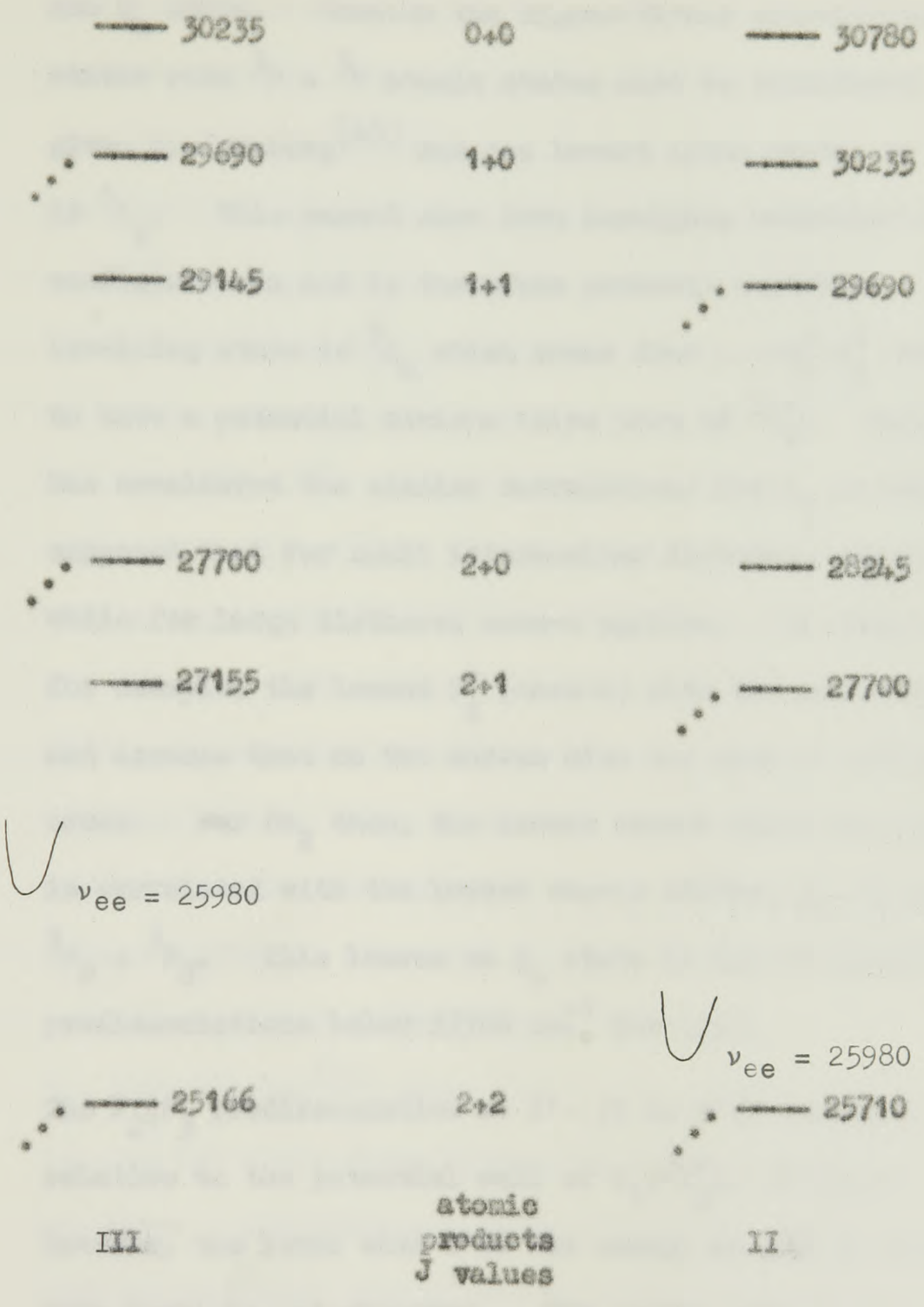

Fig. 9 J values for the $^3P + {}^3P$ atomic products and their energies in $cm.^{-1}$ for the possible configurations II and III, with stable states marked by ...

one 2_u state. However the Wigner-Witmer correlation of molecular states with $^3P + {}^3P$ atomic states must be considered. This is given by Herzberg[48] and the lowest lying state, by Hund's rules, is $^5\Delta_g$. This cannot come from low-lying molecular orbital configurations and is therefore probably unstable. The next low-lying state is $^3\Delta_u$ which comes from $....\pi_u^3\,\pi_g^3$ and is expected to have a potential minimum below that of $^3\Sigma_u^-$. Mulliken[90] has considered the similar correlations for I_2 in which it is supposed that for small internuclear distances case-b applies while for large distances case-c applies. He then correlates, for example, the lowest 0_g^+ (case-c) with the lowest 0_g^+ (case-b) and assumes that no two curves with the same Ω and symmetry can cross. For Se_2 then, the lowest case-b state of u-symmetry, $^3\Delta_u$, is correlated with the lowest case-c states, 3_u, 2_u and 1_u, from $^3P_2 + {}^3P_2$. This leaves no 2_u state in 2+2 to provide accidental predissociations below 27700 $cm.^{-1}$ for (II).

(c) The F_2,F_3 predissociation at $J' \sim 72$ in $v'=5$ occurs at a term value, relative to the potential well of $F_1(^3\Sigma_g^-)$, of 27201 + 2A". However, the level with $v'=6$ has energy at $J=0$ of 27096 + 2A" and this level is not observed. The energy difference, 105 $cm.^{-1}$ over a $J(J+1)$ range of about 5000 gives an effective slope of predissociation greater than 0.02, far larger than that of the limiting curve of predissociation at 27700 $cm.^{-1}$. The two

predissociations are therefore not the same, that for F_2,F_3 probably arising from interaction with an unstable state, i.e. case c^+ of predissociation. It seems reasonable to correlate this with the ^2_u unstable state already postulated at 27155 cm.$^{-1}$ in (III). This enables limits to be set on the size of $2\lambda''$, since v'=5 of the F_2,F_3 component appears with an energy at J=0 of 26864 + $2\lambda''$ and v'=6 does not appear at 27096 + $2\lambda''$. Thus $59 < 2\lambda'' < 291$ cm.$^{-1}$. Since $2\lambda'' - 2\lambda' = 434.51$ cm.$^{-1}$; this gives $-376 < 2\lambda' < -144$ cm.$^{-1}$. If the origin of the unstable ^2_u state were assigned to 27700 cm.$^{-1}$ in (II), then the limits set on $2\lambda''$ are $604 < 2\lambda'' < 836$, giving $169 < 2\lambda' < 401$ cm.$^{-1}$. Neither range for $2\lambda''$ agrees with that estimated from the B values (1454 cm.$^{-1}$); addition of this value gives predissociation at about 28650 cm.$^{-1}$, far removed from the energies of any atomic products, and hence rather unlikely. The sign of λ' in related molecules could be used as a guide for differentiation between (II) and (III) - for S_2, Ketteringham[44] found that λ' is smaller than λ'' and negative but for TeO it is shown later that λ' is probably large and positive. No values are available for SO or SeO. Thus, it can only be concluded that λ'' for Se_2 is roughly 100 or 350 cm.$^{-1}$, and if (III) is accepted as correct, λ'' is about 100 cm.$^{-1}$.

Individually the arguments are not conclusive but together they indicate that only (III) fits all the spectroscopic observations.

Indeed for (III) molecular states are found, where interactions with $B^3\Sigma_u^-$ are allowed, for all the $^3P + {}^3P$ products above $^3P_2 + {}^3P_2$.

The derived value for $D_e''(Se_2)$ is thus 25166 ± 20 cm.$^{-1}$; that for $D_0^0(Se_2)$ is 24974 ± 20 cm.$^{-1}$, equivalent to 71.39 ± 0.03 k.cal./mole. If the energy of $^3P_2 + {}^3P_2$ is 25166 cm.$^{-1}$ then that of $^3P_0 + {}^3P_0$ is 30235 cm.$^{-1}$. The upper state potential maximum has been extrapolated to 31800 cm.$^{-1}$ so that correlation of BO_u^+ with $^3P + {}^3P$ products is not possible. If the case-b analogue, $^3\Sigma_u^-$, is considered, the Wigner-Witmer rules also give no correlation with $^3P + {}^3P$. The lowest possible correlation is with $^3P_2 + {}^1D$ which is found for the $^3\Sigma_u^-$ upper states of O_2 and S_2 and may be confirmed for Se_2 as follows. Birge-Sponer extrapolation (using $\omega_e^2/4x_e\omega_e$) of the ground state levels gives a limit at 38500 cm.$^{-1}$ for D_e''. Comparison with $D_e''(Se_2)$ shows that this is too high by a factor of 1.53. A similar extrapolation for the upper state levels, in the region below the vibrational perturbations, gives a limit at 12977 cm.$^{-1}$ for D_e'. If this limit is correlated with $^3P_2 + {}^1D$, then D_e' is given by

$D_e' = D_e'' + \Delta - T_{ee}$ where Δ is $^1D - {}^3P_2$ difference,

i.e. $D_e'(Se_2) = 25166 + 9576 - 25980 = 8762$ cm.$^{-1}$. Comparison with the extrapolated value shows it to be too high by a factor of 1.48. The close similarity between the upper and lower state ratios confirms the correlation with $^3P_2 + {}^1D$.

Discussion

The use of two separated isotopes in this work, despite the doubling of analysis and experimentation, has been essential - providing clarification of the spectrum, confirmation of the new vibrational analysis, and confirmation of the two limiting curves of predissociation which, because of the high reduced mass, extend over rather few vibrational levels. The smooth potential curve found for the upper state of both isotopes (Fig. 4) is a fine demonstration of the Klein method, and this clearly applies in a region of vibrational perturbations - the right hand side showing the perturbation but the left hand side remaining regular.

The transition from case-b to case-c in the molecules of the oxygen group has been extended by this analysis. The $0_g^+ - 1_g$ separation, $2\Lambda''$, of the ground state cannot be definitely estimated by comparison of the rotational constants as was possible in case-b (large λ). If this separation was found (e.g. by observation of a transition from a 0_u^+ state to both 0_g^+ and 1_g components of $X^3\Sigma_g^-$), one of the two possible values for the dissociation energy of the lower 0_g^+ component could be eliminated immediately. As it is, the accumulated spectroscopic evidence suggests very strongly that $D_0^0(Se_2) = 71.39 \pm 0.03$ k.cal./mole. This extremely precise value may be used in the determination of the bond energies of all selenium compounds and in

quantitative valency theory. At the same time it gives limits for $2A''$ which indicate that this is large and positive, as expected.

For future work the following may be suggested. A quantitative analysis of the perturbations in v'=4 and 5 of $^3\Sigma_u^-(F_1)$ is planned, although there seems little doubt that the interaction is with a less stable state of ^1_u character. The ground state has been almost completely analysed, and this provides a basis for the analysis of other systems, for example the u-v bands reported by Choong[92] and re-analysed by Migeotte[93]. Since these are apparently violet-degraded and involve the ground state, the latter's analysis, with $\omega_e' > \omega_e''$, is to be preferred. The system is probably analogous to $C^3\Sigma_u^- - X^3\Sigma_g^-$ in S_2, in which the state C is assigned as the first Rydberg state[78]. Also in S_2 strong $^1\Delta_u - {}^1\Delta_g$ bands appear just to the violet of the main system in emission[91]. No similar bands have been previously reported for Se_2 but close inspection of the diffuse absorption bands with v' > 15 (see Plate 1) shows that there is some very weak but sharp underlying structure. Further investigation of this region, preferably in emission, is therefore necessary. The numerous states recently found in S_2[78] and SeO[96] suggest also that investigation of the spectrum of Se_2 in the infra-red and far u-v is overdue.

Finally, it may be observed that the large triplet splitting, the rotational and vibrational perturbations, and the pressure-induced,

accidental and allowed predissociations in the main system of Se_2 provide strikingly clear examples of almost all the possible interactions between electronic states. The analysis of so many features in a single transition has been a source of great fascination to at least one spectroscopist.

CHAPTER II

THE $A^3\Sigma^- - X^3\Sigma^-$ MAIN SYSTEM OF TeO

Introduction

The spectrum of TeO was first reported by Choong[50] in 1938. Later observations were given by Haranath, Rao and Sivaramamurty[51] and by Purbrick[52]. There was little agreement about the vibrational analysis and no rotational analysis was reported. In 1964, Barrow and Hurst[53] gave a rotational analysis of one band at 31300 $cm.^{-1}$, photographed in absorption, using natural tellurium. The analysis indicated that, as expected, the main system was $^3\Sigma^- - {}^3\Sigma^-$ which in Hund's case-c would appear as separate 0^+-0^+ and 1-1 systems. The band at 31300 $cm.^{-1}$ showed the simple two-branch structure expected for a 0^+-0^+ transition.

The spectrum was complicated, however, by the presence of the different isotopic species of tellurium. It was decided to continue the investigation using isotopically pure TeO with a view to resolving the problems of vibrational analysis and electronic transition. In Group VI the $^3\Sigma^- - {}^3\Sigma^-$ main systems of O_2, SO, S_2, SeO and Se_2 have all been studied and it would be valuable to compare that of TeO with this series. In particular the detection of a 1-1 system in TeO would aid the study of the changing nature of a $^3\Sigma$ state as the nuclear charge increases. Because of the problems involved in the experimental work and the amount of analysis of the results required, the author studied the isotopic species ^{128}TeO and H.J. Hurst[54] studied ^{130}TeO at the same time.

Experimental

Naturally occurring tellurium contains isotopes of the following abundances: 126 - 19%, 128 - 32%, 130 - 34%. Separated isotopes of tellurium were available in elemental form but the high cost demanded the use of milligram quantities only. Samples of mass number 128 and 130 were obtained from A.E.R.E. Harwell with 96% separation.

For the preparation of TeO it was essential to avoid wasteful loss of the tellurium and so Te and O_2 were heated together in a sealed quartz tube. For absorption work the windows of the tube must be hot to prevent condensation, and attempts were made to photograph the spectrum using a sealed quartz tube inside an electric oven of greater length. However, at about 800°C, which seemed to be necessary for the reaction to occur, the windows were attacked and soon became opaque.

It was decided to excite the spectrum in emission using a microwave generator. This type of power supply is particularly favourable for small quantities of very pure materials because it requires no internal electrodes, which are a source of contamination, and because it can provide a very intense light source. The microwave generator was designed and built by P.W. Fry[55], but there were problems in the transmission of the power into the quartz discharge

tube. For the excitation of the PbO spectrum in a microwave discharge, Barrow, Deutsch and Travis[56] used a quartz tube placed as a continuation of the centre-pin of the coaxial supply, but this method is very wasteful of the available energy. In preference to this a tuned cavity working in the TM 011 mode, designed by Deutsche-Electronik in association with A.E.R.E. Harwell, was attached by a short length of coaxial tubing to the microwave generator. The cavity and the connecting waveguide were all tuned so that maximum power was delivered into a short region in the centre of the cavity. With a maximum output of 200 watts at a wavelength of 12.24 cm. this system produced a brilliant, stable discharge in the small quartz tubes placed inside the cavity. The tubes were made about 4 cm. long with an internal diameter of 2 mm. and viewed from the side through a slot cut in the walls of the cavity.

The TeO was made <u>in situ</u> by heating a trace of tellurium with oxygen at 5 mm. pressure in the presence of 5 mm. pressure of spectroscopically pure xenon. These conditions were found by trial and error to provide the brightest and most stable source. Thus xenon was found to be preferable to helium as an aid to the discharge over a long period, perhaps because white-hot quartz is not impermeable to the smaller helium atoms. The amount of tellurium was judged by eye and was estimated to be about 1/100 milligram. However, at no time was any tube found to last longer than 1/4 hour before the TeO

discharge disappeared to be replaced by that of Te_2 or atomic xenon. This was thought to be due to either an initial excess of Te or O_2, or to the generation of such an excess during the discharge - for example, by the reaction of oxygen with the hot quartz walls.

The 6.65 metre concave grating spectrograph at Oxford is of the Eagle type which is an astigmatic mounting. This makes the instrument relatively slow and indeed it was found that exposure times for the spectrum of TeO would have to be many times the average tube-life. Although it was possible to make several tubes it was decided to try and photograph the spectrum on some faster spectrographs. Dr. E.W.T. Richards of the Spectroscopy Division at A.E.R.E. Harwell kindly made available a 3 metre Baird and a 6 metre stigmatic grating spectrograph for this purpose. Some successful photographs were taken in the strongest region at the u-v end of the system on the Baird with exposures of about 1/4 hour on OaO plates. However, attempts to photograph in weaker regions or on the 6 metre instrument were unsuccessful because of repeated failures of the discharge tubes. The tube life could be lengthened somewhat by constant adjustment of its temperature by means of the microwave power, bunsen burner and compressed air.

It was notable that in the microwave excitation of the PbO spectrum the tubes lasted for several hours at least. The PbO was prepared, however, from $PbCl_2$ and O_2 and it was thought possible that

the presence of Cl_2 might lengthen the tube life. Since tellurium was not available as the chloride, chlorine gas at low pressure was added. This gave no improvement in tube life. The kinetics involved in discharge tubes are probably very complex and further refinement was thought to depend very much on chance - the high temperature necessary for the production of TeO might also be the cause of this difference in behaviour.

Finally, it was appreciated that the best chance for success lay in balancing the rate of failure with the rate of production of the tubes, which could only be done at Oxford. Therefore attempts were again made to photograph on the Oxford spectrograph but with one person controlling the discharge and another continually producing new tubes. In this way enough tubes could be made for successful photographs to be taken of the whole of the main system of TeO. This is limited at the u-v end (3300 Å) by a sharp cut-off due to predissociation above v'=9 and at the red end (about 5500 Å) by the bands due to Te_2 which could not be eliminated. The exposure times were between 4 and 6 hours on Kodak OaO plates in a third order of the Oxford 6.65 metre spectrograph which gave a reciprocal plate dispersion of about 0.5 Å/mm.. An iron arc spectrum was used as a standard and the wavenumbers in vacuum of the molecular lines were formed by interpolation in the usual way.

Rotational Analysis

Since in the $^3\Sigma^-$ ground state of SeO the constant λ'' of the case-b spin-splitting formulae is about 85 $cm.^{-1}$ and in Se_2 the transition to case-c is well developed, for TeO it might be expected that λ'' would be very large, several hundred $cm.^{-1}$, and the transition to case-c complete. In the limit of case-c, two separate systems are formed, 0^+-0^+ and 1-1. The analysis of the TeO spectrum shows that this is indeed the situation.

The 0^+-0^+ bands possess single R and P branches (see Plates 7 & 8) and the 1-1 bands show, at low values of J, single R and P branches which, at $J \sim 50$ and upwards, split into two, R_c, R_d and P_c, P_d. As defined by Herzberg[48], the subscripts c and d refer to the 1^+ and 1^- components respectively and the correlation of levels in the transition

$^3\Sigma^-$(case-b)$\rightarrow 0^+$, 1 (case-c) is

F_2 (N, J)$\rightarrow 1^-$ and F_3 (N+1, J)$\rightarrow 1^+$ (see Fig. 10)

The weakness, or absence, of Q branches and 0^+-1 transitions prevents direct determination of the Ω-doubling of the 1 state, but the order of the levels 1^+, 1^- may be inferred from the following considerations. In the ground state of S_2, $F_3(N+1)$ lies above $F_2(N)$ and in the ground states of SeO and Se_2, $B_v(F_3) > B_v(F_2)$. Also if, as in the case-c 0^+, 1 ground state of BiH[57], the major contribution to the splitting of the levels of the 1 state arises from interaction with the lower 0^+ state, then $F_J(1^+) > F_J(1^-)$. In the present case it was therefore assumed that $F_J(c) > F_J(d)$.

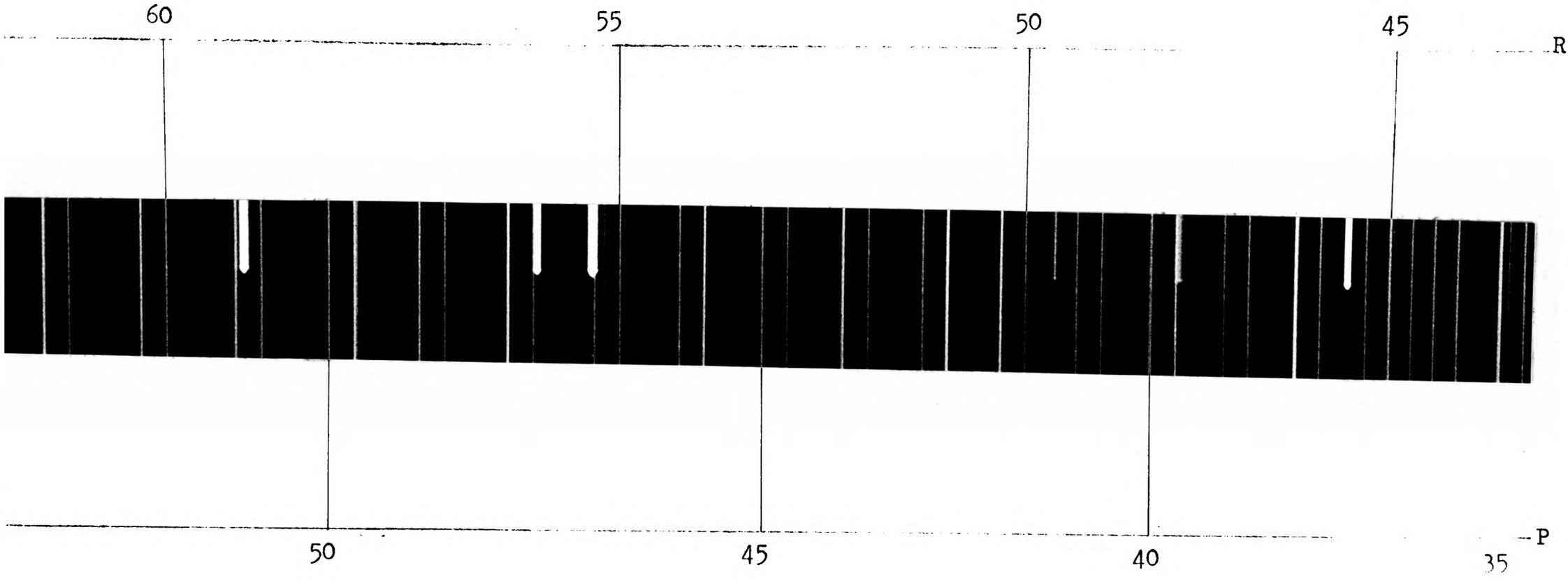

Plate 7. 0-7 (0^+-0^+) Band of ^{128}TeO.

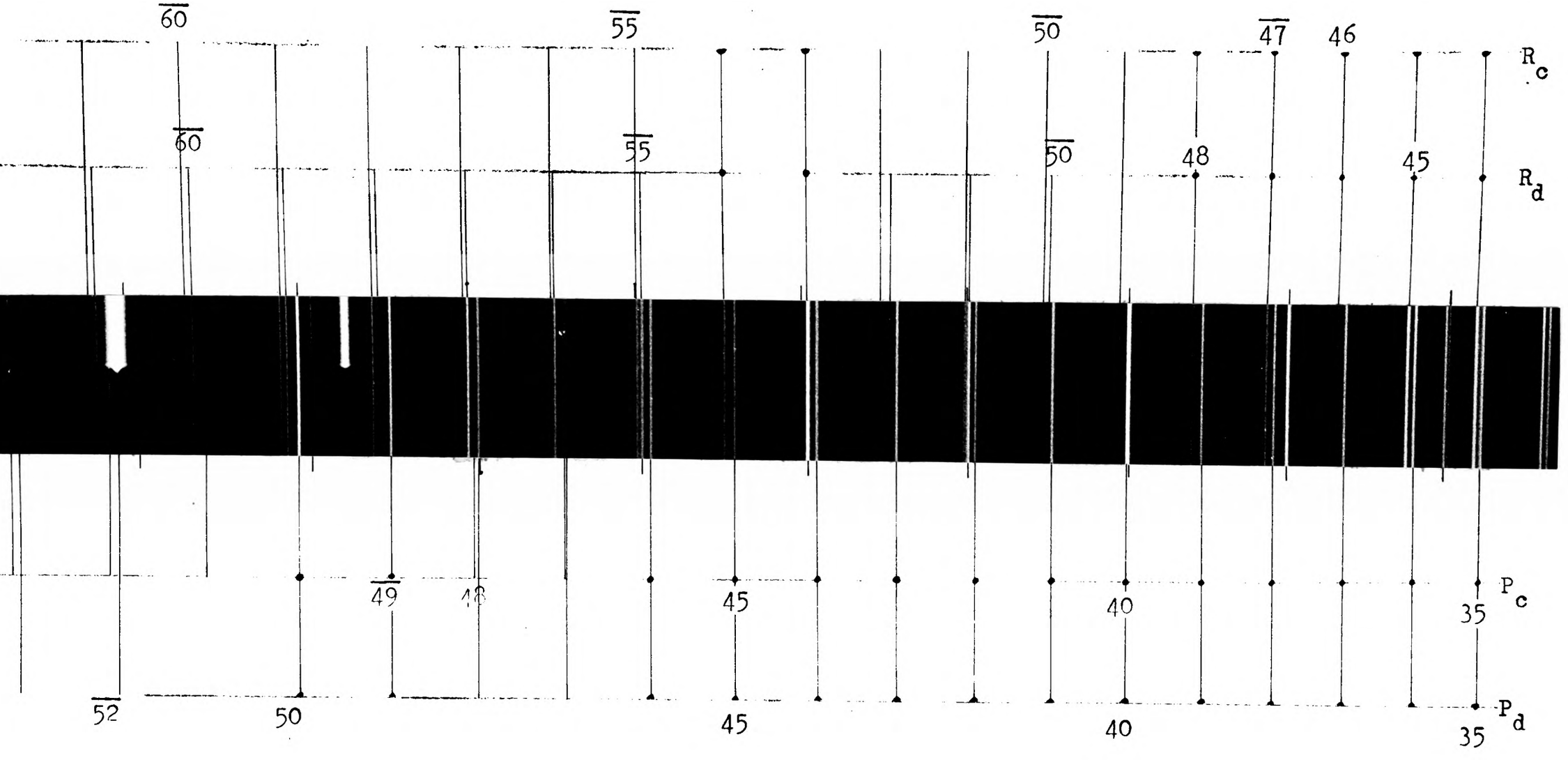

Plate 8. 0-7 (1-1) Band of ^{128}TeO overlapped by the (0^+-0^+) band.

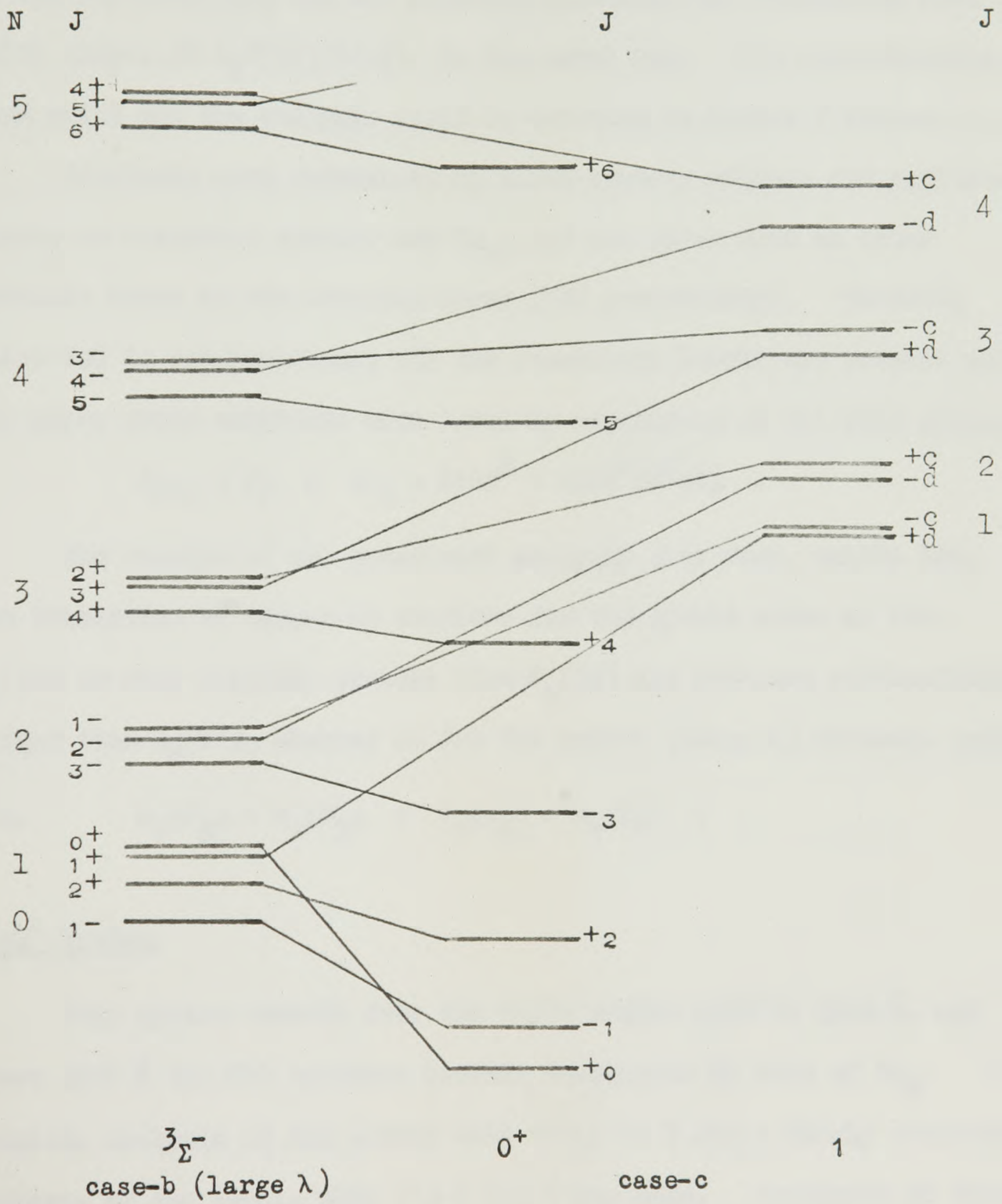

Fig. 10. Transition from case-b (large λ) to case-c.

The rotational analysis was straightforward, although the upper states are perturbed. The relative numbering followed from the analysis of the perturbations and the absolute numbering was determined from trial values of $\Delta_2 F''(J)/(J+\frac{1}{2})$ in the usual way. The perturbations were small and the analysis could be extended to higher J values.

Constants were determined by least squares methods for perturbed bands, as described earlier for Se_2, and are given with an error estimate which is one standard error (68% probability). However, since TeO is heteronuclear, all the rotational levels are present and the upper state constants were found by regression on the line given by

$$R_{J-1} + P_J = 2\nu_0 + 2\Delta BJ^2 - 2\Delta DJ^2(J^2+1) \quad .$$

The results of the rotational analysis show that, unlike SeO, the transition to case-c is complete for the ground state of TeO. $B_v(1c)$ is only slightly greater than $B_v(1d)$ and both are substantially larger than $B_v(0^+)$, whereas in SeO the case-b (large λ) criteria apply, i.e. $B_v(F_3) - B_v(F_2) = B_v(F_2) - B_v(F_1)$.

0^+-0^+ System

This system extends over the whole region 5500 to 3300 Å, and above 5500 Å the TeO spectrum becomes overlapped by that of Te_2. A complete analysis of the levels with v" = 4 to 7 and a fairly complete analysis of the levels with v' = 0 and 1 was made. Constants of the bands were determined as if each were an independent $^1\Sigma$-$^1\Sigma$ band; values are given in Table 14.

1-1 System

The long wavelength limit for the system is due to overlap by Te_2 but, in contrast to the 0^+-0^+ system, no bands are observed below about 3880 Å. A complete analysis of the levels with v" = 3 to 7 and with v' = 0 was made. Constants for the bands were determined as if each were an independent $^1\Pi-^1\Pi$ band; values are given in Table 15.

TABLE 14 Rotational Constants for AO^+ and XO^+, in $cm.^{-1}$, for ^{128}TeO

	v	B	D x 10^7	α x 10^3
AO^+	0	0.2735 ± 0.0001	4.18 ± 0.16	
	1	0.2680 ± 0.0002	3.6 ± 1.2	
		B_e = 0.2764 ± 0.0002		
		α_e = 5.5 x 10^{-3}		
		D = 4 x 10^{-7}		
		r_e = 2.071 Å		
XO^+	4	0.3454 ± 0.0001	2.88 ± 0.11	2.376 ± 0.007
	5	0.3428 ± 0.0003	2.78 ± 0.28	2.375 ± 0.001
	6	0.3406 ± 0.0001	2.88 ± 0.06	2.373 ± 0.001
	7	0.3382 ± 0.0001	2.87 ± 0.09	
		B_e = 0.3560 ± 0.0002		
		α_e = (2.375 ± 0.004) x 10^{-3}		
		D = (2.9 ± 0.2) x 10^{-7}		
		r_e = 1.825 Å		

These values may be compared with those derived for ^{130}TeO as follows:

$^{128}B''_e / {}^{130}B''_e$ = 1.00169 ρ^2 = 1.00172

$^{128}B'_e / {}^{130}B'_e$ = 1.00145 ρ^2 = 1.00172

$^{128}\alpha'' / {}^{130}\alpha''$ = 1.0021 ρ^3 = 1.0026

TABLE 15 Rotational Constants for A1 and X1, in $cm.^{-1}$, for ^{128}TeO

	v	B	D x 10^7	α x 10^3
A1	0c	0.2779 ± 0.0002	3.6 ± 0.4	
	0d	0.2775 ± 0.0002	3.9 ± 0.4	
X1	3c	0.3490 ± 0.0003	2.6 ± 0.5	
	3d	0.3484 ± 0.0003	2.3 ± 0.5	
	4c	0.3467 ± 0.0002	2.6 ± 0.4	
	4d	0.3462 ± 0.0002	2.7 ± 0.4	c 2.371 ± 0.003
				d 2.361 ± 0.003
	5c	0.3447 ± 0.0002	2.9 ± 0.3	
	5d	0.3443 ± 0.0001	3.1 ± 0.2	c 2.388 ± 0.002
				d 2.378 ± 0.002
	6c	0.3422 ± 0.0001	2.8 ± 0.2	
	6d	0.3418 ± 0.0003	3.1 ± 0.4	c 2.378 ± 0.003
				d 2.365 ± 0.003
	7c	0.3399 ± 0.0002	2.7 ± 0.4	
	7d	0.3399 ± 0.0002	3.8 ± 0.6	

$B_e^c = 0.3575 \pm 0.0003$ $\qquad \alpha_e^c = (2.379 \pm 0.003) \times 10^{-3}$

$B_e^d = 0.3572 \pm 0.0003$ $\qquad \alpha_e^d = (2.368 \pm 0.003) \times 10^{-3}$

$$D^c \sim D^d = (2.9 \pm 0.4) \times 10^{-7}$$

$$r_e = 1.821 \text{ Å}$$

These values may be compared with those derived for ^{130}TeO as follows:

$^{128}B_e'' / {}^{130}B_e'' = 1.0022$ $\qquad \rho^2 = 1.00172$

$^{128}\alpha_e'' / {}^{130}\alpha_e'' = 1.0047$ $\qquad \rho^3 = 1.0026$

Vibrational Analysis

Once the nature of the transitions was known, the failure of all the previous vibrational analyses became clear. The 0^+-0^+ and 1-1 systems have independent vibrational schemes in which the value of T_{00} for 0^+-0^+ is larger than that for 1-1 by 394.65 $cm.^{-1}$. These two systems comprise the A-X system of TeO. All other reported bands of TeO can be re-analysed as follows:

(1) The C-X system of Choong[50], λλ 2770-3060 Å, was restudied at a dispersion of about 3 Å/mm.. In absorption the strong bands are the diffuse v' = 10 to 15 bands of the $A0^+$-$X0^+$ system of TeO. In emission the strong bands reported by Choong are observed even when separated isotopes are used and yet they agree very well both in wavelength and rotational structure with the main system bands of SO. This is apparently a persistent impurity.

(2) The B-X system of Choong is largely the 0^+-0^+ component of the A-X system of TeO.

(3) The remaining bands, including those reported in the red region, are either part of the A-X system of TeO or part of the main system of Te_2. With isotopically pure samples the difference in rotational structure between TeO and Te_2 is marked, even at low dispersion.

The $A0^+$-$X0^+$ System

The v" numbering is fixed by the observation of an intense v"=0 progression at the u-v end of the absorption spectrum. The upper state is extensively perturbed and the derived constants have a limited validity. For ^{130}TeO, within the range $3 \leq v \leq 10$, Hurst found that the vibrational levels are quite well expressed by

$$\nu_{v,0} = 28122.46 + 410.71(v+\tfrac{1}{2}) - 5.772(v+\tfrac{1}{2})^2 \ .$$

However, large deviations are found for $v < 3$ and $v > 10$. The errors introduced by using these constants in the calculation of vibrational isotopic shifts for v' = 0 and 1 are found to be negligible. Values of the shifts, determined from band origins, are given in Table 16 and indicate that the original values of v' proposed by Choong should be increased by three.

The A1-X1 System

No bands of the 1-1 system have been identified in absorption. In emission the intensity distribution is similar to that of the 0^+-0^+ system and this indicates that the strongest bands form a v'=0 progression, bands with v'=1 also being observed. Bands with v'=2 may be present but there is no evidence for bands with $v' \geq 3$. It appears that the state A1 is predissociated at about v' = 2 or 3. The vibrational numbering is fixed by the comparison of observed and calculated isotopic shifts and values are given in Table 16.

TABLE 16 Vibrational Isotope Effect: Values in $cm.^{-1}$ of $\Delta\nu$ $^{130}TeO - {}^{128}TeO$

	Band	$\Delta\nu_{obs}$	$\Delta\nu_{calc}$ (i)	(ii)	(iii)
$A0^+-X0^+$	0-4	2.77	2.74	3.40	2.42
	0-5	3.26	3.35	4.02	3.03
	0-6	4.18	3.96	4.62	3.64
	0-7	4.81	4.54	5.21	4.22
	9-0	-2.02	-2.12	-1.44	-2.38
A1-X1	0-4	2.66	2.74	3.39	2.42
	0-5	3.37	3.36	4.01	3.04
	0-6	4.05	3.96	4.60	3.64
	0-7	4.73	4.55	5.18	4.23

(i) v', v" as given

(ii) v" increased by 1

(iii) v' increased by 1

TABLE 17 Band Origins and Vibrational Constants, in $cm.^{-1}$, ^{128}TeO

Band	0^+-0^+	1-1
0-4	24925.64	24527.05
0-5	24168.01	23768.33
0-6	23418.37	23017.59
0-7	22676.71	22274.93
1-4	25372.34	
1-5	24614.63	
1-6	23864.91	
9-0	31301.37	

0^+-0^+

$$\nu_{0-0} = 28036.48 \pm 0.06$$
$$G_v'' = 797.69(v+\tfrac{1}{2}) - 4.00(v+\tfrac{1}{2})^2$$
$$\Delta G'_{\frac{1}{2}} = 446.62$$

1-1

$$\nu_{0-0} = 27641.83 \pm 0.04$$
$$G_v'' = 798.70(v+\tfrac{1}{2}) - 4.00(v+\tfrac{1}{2})^2$$
$$\Delta G'_{\frac{1}{2}} \sim 458$$

Thus $\nu_{0-0}(0^+) - \nu_{0-0}(1) = 394.65$

Band origins and vibrational constants for the $A0^+$-$X0^+$ and A1-X1 systems are given in Table 17. The vibrational constants for the two components are very similar.

Perturbations

The perturbations in both $A0^+$ and A1 could not be quantitatively studied because of the lack of extra lines. For example, no crossing point on a plot of $\Delta_2F'/(J+\frac{1}{2})$ against $(J+\frac{1}{2})^2$ was observed for either state. As in the case of Se_2 already discussed, the shape of the plot is, however, informative, since it does indicate whether B_p is larger or smaller than B'.

In v'=0 of $A0^+$ two perturbations occur. The first is at $J'\sim 92$ and involves a perturbing state of lower B value than B_0'. The second occurs at $J'\sim 116$ and also appears to have $B_p < B_0'$, but the line intensities are here so low that no branches could be picked out at higher J values. For v'=1 a perturbation occurs at $J'\sim 87$ for which B_p appears to be greater than B_1', although the low intensities here again prevented analysis at higher J values. Although these statements can only be tentative until a full perturbation analysis is done, it appears that there are at least two states perturbing $A0^+$. No quantitative treatment of these perturbations was possible because it

requires both a fairly large perturbation and an analysis on each side of the critical J value. In the only case where such an analysis has been carried out the perturbation is small.

In v'=0 of the A1 state, perturbations occur at J'~ 50, 81 and 91 for the 1^- component and at J'~47, 54, 80 and 92 for the 1^+ component. The perturbations are fairly small and B_p in all cases is smaller than B'_0.

If these perturbations could be treated quantitatively, then the nature of the perturbing states, which must have Λ=0, 1 or 2, might be found. However, very many stable states of this type are expected from the combination of the normal atoms $Te(^3P)$ and $O(^3P)$ so that identification would not be very useful. Most of these states would be expected to have smaller B values than those of $A0^+$ or A1, so that the perturbation in $A0^+$ by a state of larger B value might merit further study. The $0^+(^1\Sigma^+)$ state arising from the ground state configuration ....π^2 is the state most likely to be responsible.

Dissociation Energy and 0^+-X1 Splitting

By linear extrapolation of the ground state levels and from the observation of a predissociation in $A0^+$ at about v'=9, Hurst found for ^{130}TeO that D_0^0 is about 90 k.cal.mole^{-1} or 31450 cm.$^{-1}$. An extrapolation of the levels $3 \leqslant v \leqslant 10$ in $A0^+$ was good enough to identify the dissociation products as $Te(^3P_0)$ and $O(^3P)$ and also supported this value.

For the $^3\Gamma^-$ ground states of O_2, SO, S_2, SeO and Se_2, λ has been shown to be positive, and when it is large the F_1 levels lie below the F_2,F_3 levels by roughly 2λ. By analogy with these, in case-c the 0^+ levels will lie below the 1 levels by an amount which can also be called 2λ. An attempt can be made to estimate the value of λ in the ground state of TeO as follows. The intensity distribution in the 1-1 system is anomalous since, although bands with v'=0 and 1 are strong in emission, no bands with $v' \geqslant 3$ have been seen. A few bands have been assigned to v'=2 but it may be assumed that there is a predissociation limit between v'= 2 and 3, that is at about 28700 cm.$^{-1}$ above v"=0 in X1. It is then assumed that this limit corresponds with that observed in $A0^+$ at 31450 cm.$^{-1}$, giving a value of $2\lambda" = 31450 - 28700 = 2750$ cm.$^{-1}$ Then $2\lambda' = 2750 - 395 = 2355$ cm.$^{-1}$. Thus values of $\lambda" \sim 1375$ and $\lambda' \sim 1178$ cm.$^{-1}$ are deduced. It should be noted that there are several assumptions in this argument, and that the constant λ is not that defined in the case-b spin-splitting equations.

Discussion

The increasing separation of the $F_1(0^-)$ and the $F_2,F_3(1)$ levels of the $^3\Sigma^-$ ground states of the series O_2, SO, S_2, SeO, Se_2, TeO is made apparent by the increase in the value of the case-b splitting constant λ''. As the nuclear charge increases the $\Pi - \Sigma$ separation decreases, producing a larger case-b splitting. This type of interaction might be larger for heteronuclear than for homonuclear molecules because the symmetry restriction prevents interaction, in the latter, of $^3\Sigma_g^-$ with the lowest lying Π state which is $^3\Pi_u$.

It has been shown, however, that the increasing $F_1 - F_2,F_3$ separation may also be described in terms of increasing case-c character. The difference between case-b (large λ) and case-c is revealed only in the relative difference in the component B values. The transition to case-c appears to be complete for TeO, by this criterion, so that the $\Pi - \Sigma$ interaction used to explain case-b splitting has been superceded by a $1 - 0^+$ interaction whose energy separation is relatively much smaller. The mutual repulsion produces Λ-doubling in the ground state which may be used to determine λ'' assuming "pure precession". Thus $q = 0.0003$ and $B = 0.3573$ cm.$^{-1}$, giving $\lambda'' = 851$ cm.$^{-1}$; compare $\lambda'' = 1375$ cm.$^{-1}$ estimated from the predissociations. The agreement, as in Se_2, is not good so that, while the values are of the same order, "pure precession" cannot apply.

This transition from case-b to case-c arises in two ways: firstly,

the coupling of L and S with the internuclear axis becomes weaker as the internuclear distance increases; thus the size of λ'' might show a dependence on the vibrational level v", and indeed λ'' increases with v" for S_2, SO and SeO and $\omega_e'' {}^3\Pi_{2,3}(1)$ is larger than $\omega_e'' {}^3\Pi_1(0^+)$ for Se_2 and TeO. Secondly, the coupling of l and s for an electron with those of other electrons becomes weaker with increasing nuclear charge as described by a transition from Russell-Saunders to j-j coupling. Mulliken[47] has defined case-c by "case-c exists whenever the atomic L,S couplings are strong compared with the effects of the departure of the molecule from atomic conditions". A comparison may therefore be made between the observed molecular splittings λ'' and the spin-orbit coupling constants a, for the atoms O....Te, in ....np^4, ^3P, which are given by $3a/2 \doteqdot {}^3P_0 - {}^3P_2$. Values, in $cm.^{-1}$, are as follows:

	λ''			a (ref. 69)
O_2	1.985	(ref. 49)	O	151
SO	5.276	(" 42)	S	382
S_2	11.65	(" 43)	Se	1690
SeO	86.4	(" 23)	Te	3138
Se_2	c. 100	(present work)		
TeO	c. 1375	(" ")		

It seems likely that this rapid increase in the spin-orbit coupling constants is the most significant case for increase in λ'', since all the other effects would be more gradual.

The problem raised by these results is that in case-c the selection rule $\Delta\Omega = 0, \pm 1$ would permit the appearance of the transitions $A0^+ - X1$ and $A1 - X0^+$ for TeO. The position of the bands would depend on the values of λ' and λ'' and, while those given are tentative, it is certain that they are of the right order. Close inspection of the spectrum indicates that these bands are absent or at most very weak. The non-appearance of "cross-transitions" has also been reported for the spectrum of NBr[58] and no satellite branches ($P_1 - P_3$ etc.) have been found in the main systems of SeO or Se_2. In this series the only molecule in which these transitions appear is S_2, where the strong upper state perturbations have been assigned to interaction with a $^3\Pi_u$ state[44], and it is suggested that this mixing of $^3\Pi_u$ and $^3\Sigma_u^-$ allows strong satellite branches to occur.

However the upper states of SeO, Se_2 and TeO are also perturbed, probably by $^3\Pi$-type states, and although these interactions appear weaker than in S_2 the transition to case-c should make the $0^+ - 1$ transitions fully allowed. A rather similar situation occurs in the spectra of Br_2 and I_2 in which the case-c character is fully developed. Mulliken[46] has given an explanation for the high intensity of the $^3\Pi_{0^+,u} - {}^1\Sigma_g^+ (0_g^+)$ transition compared with the low intensity of

$^3\Pi_{1,u} - {}^1\Sigma_g^+ (0_g^+)$ in terms of perturbations of $^3\Pi$ by several other states, some of which have ionic character. The ionic → non-ionic transitions are theoretically found to be extremely strong. The extension of this argument to Se_2 and TeO, where 0^+ and 1 components occur in both upper and lower states, is not clear. A more widely applicable explanation may be that, if Σ is defined at all, a selection rule of the type $\Delta\Sigma = 0$ is operating.

APPENDIX A

THE SPECTRUM OF XeO

Introduction

Bands attributed to XeO were first reported in 1946 by Kenty[79] and Herman[81]. A green glow was produced when small amounts of O_2, H_2O or CO_2 were added to xenon and excited by a high frequency discharge. The red-degraded band system extended from about 4900 Å to 5577 Å where the atomic oxygen $^1S_0 - {}^1D_2$ line appeared strongly. Herman gave a Deslandres scheme for the band heads measured at low dispersion. In 1950, Herman and Herman[80] reported further systems at about 2430, 2930 and 3080 Å. These were violet-degraded and since the oxygen was prepared from $KMnO_4$ it was suggested that they might be impurity bands. They also reported very weak green bands with Ar-Xe mixtures, but no bands were found with He-Xe.

Cooper[83] and Tolnas[82] gave further reports and in 1961 Cooper, Cobb and Tolnas[84] gave details of the XeO spectrum, and discussed the weaker KrO and ArO bands occurring in the same region. They suggested that metastable ($^3P_0$) inert gas atoms, with about 9.5 e.v., excited oxygen by collisions to the $^1S_0$ state in a process like

$$Xe(^3P_0) + O_2 \rightarrow Xe(^1S_0) + O(^1S_0) + O(^3P) .$$

The spectrum then arises from $XeO(^1S_0 + {}^1S_0) \rightarrow XeO(^1S_0 + {}^1D_2)$ giving a $^1\Sigma - {}^1\Sigma$ transition. A broad weak continuum was also seen at 8600-6500 Å which they associated with the $O(^1D_2) \rightarrow O(^3P)$ transitions at about 6300 Å. No vibrational analysis of the KrO or ArO green bands

was found but the bands of XeO were represented by

$$\nu = 20097 + 142v' - 9.9v'^2 + 0.1v'^3 - 360v'' + 12.0v''^2$$

No rotational analysis was obtained because of the measurement inaccuracy due to the large line widths (~ 1.5 cm.$^{-1}$). Extrapolation of the vibrational intervals gave $D_0' = 0.06$ e.v. and $D_0'' = 0.36$ e.v. The present work was initiated to find a rotational analysis of this unstable molecule and hence the internuclear distance for a single Xe-O band. Very many xenon compounds have been recently isolated, mainly with the very electronegative elements fluorine and oxygen; Cooper et al. found no spectrum with sulphur instead of oxygen, but a band of XeN has been reported by Herman and Herman[89]. The lowest atomic level of fluorine lies at 12.7 e.v. above the ground state and thus the spectrum of XeF cannot occur by a process like that of XeO; if it does appear it will be in the vacuum u-v region. Thus the most accessible spectrum is that of XeO.

Experimental

The previous workers found that the bands were best observed using an ozoniser-type discharge at a high frequency and with a high ratio of xenon to oxygen. As little as 10 parts per million gave the green discharge strongly. An ozoniser-type discharge tube was constructed, about 40 cm. long with external diameter 5 cm.. A central electrode, consisting of an air-cooled copper tube, was placed in a glass finger extending down the centre of the discharge tube. Copper foil, underlined with asbestos and air-cooled, was wrapped round the outside of the discharge tube as the second electrode. A 600W r/f generator was used as a power supply operating at 7 Mc/s. This was tuned by having a coil and variable condenser in parallel with the electrodes - the discharge tube acting as a condenser. With no oxygen the xenon discharge fills the tube and purple streamers appear. Addition of a trace of oxygen produces a green glow and bright green streamers. Previous workers used Xe pressures of about 75 cm.Hg. but to prevent pressure broadening the pressure was kept below 10 cm. although the intensity increases somewhat with pressure. So little oxygen is needed at this pressure of xenon that the following procedure was finally employed. About 2 mm. of O_2 were put into the evacuated tube and slowly pumped out until the pressure was just low enough to support a Tesla discharge. Addition of 5 cm. of spectroscopically pure xenon then gave a satisfactory ratio.

The XeO discharge is rather weak using the ozoniser-type discharge and attempts were made with other sources. A strong green glow (relative to the small power output) is given by a Tesla discharge but this is not necessarily due to XeO. A photograph of the ozoniser discharge near to the tube walls revealed that the bright glow that sometimes appears is due to the Swan bands of C_2. The Tesla discharge occurs near the walls and may be due to C_2 also. A large induction coil was tried to see if the high voltage was significant but only a very weak discharge was given. The excitation methods are limited by the need to have external electrodes to prevent contamination when such small concentrations are used. The r/f generator was also used with the tuning coil surrounding the discharge tube and no other electrodes. This gave only the strong CO spectrum. With two external electrodes wrapped at different points along the tube the XeO bands appeared only weakly.

The ozoniser-type discharge gave the brightest source of those tried and this was used to maximum effect by careful lens positioning. Because of the ring shape of the source, when viewed end-on, only about a quarter of the output can be focussed on to the spectrograph slit. Jacques[85] gives a 2-lens arrangement for maximum intensity gain with a long discharge tube but this contains several misprints; the correct solutions have been derived (see diagram overleaf). The lenses L_1 and L_2 (of focal lengths f_1 and f_2) are placed so that the front of the

discharge tube (of length d) is focussed on to the slit S, while the back is focussed on to the collimator C (of focal length g and half-aperture c).

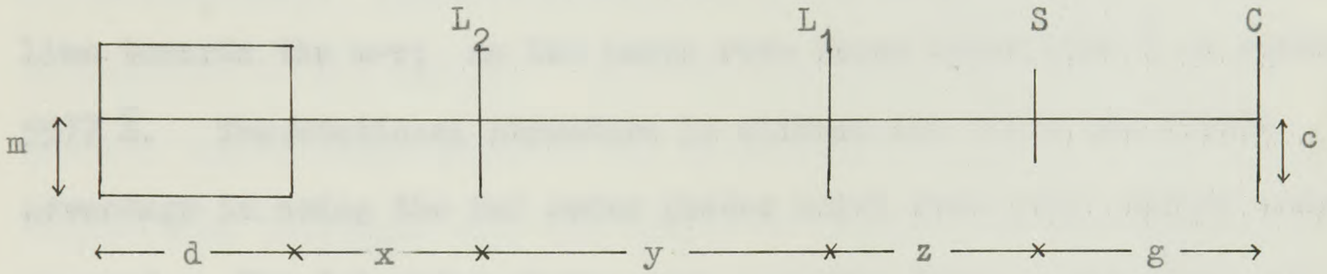

Two lens arrangement for use with a long discharge tube

The values of the distances x, y and z are given by

$$x = f_2 + \frac{c^2d^2}{(gm^2+c^2d)}\left(\frac{mgf_2}{f_1cd} - 1\right)$$

let $j = mf_2/(d + x - f_2)$

then $z = f_1 - g + f_1c/j$

and $y = xf_2/(x - f_2) - zf_1/(f_1 - z)$

Values of f_1 and f_2 are quickly found by trial and error.

Spectra were taken in the 1st and 2nd orders of a 6.65 metre spectrograph with a slit of 50 microns; exposure times of between 8 and 20 hours were required using the fastest available presensitised plates, Kodak 103aF. Each band is superimposed on a locally intense continuum, the overall intensity decreasing from the 5577 Å oxygen line towards the u-v; no XeO bands were found below 4900 Å or above 5577 Å. The rotational structure is diffuse and there was little advantage in using the 2nd order plates which were still rather under-exposed. The 1st order plates were measured twice, using high and low magnifications of the comparator, to get accurate estimates of the line centres. The reciprocal plate dispersion was 1.2 Å/mm., rather better than that of Cooper et al. (1.8 Å/mm.).

Analysis

The bands do not form heads under high dispersion although there are intensity maxima at low dispersion. Previous analyses applied to the violet edges of the bands where the line spacing is found to be considerable; indeed the value of ΔB is so small that the red-degradation is not marked. Thus the previous Deslandres schemes provide only a rough guide to the vibrational analysis; without good vibrational constants only the ratios of the various isotope shifts can be given. There are 5 main isotopes of xenon with the following natural abundances: 129 - 26%; 131 - 21%; 132 - 27%; 134 - 11%; 136 - 9%. The isotope spacing therefore has the ratios 2:1:2:2 between the species of increasing mass. So few rotational lines are found for each branch that there can be no significant rotational isotope effect.

A rotational analysis has not been achieved but the earlier conclusions are surely wrong. Cooper et al.[84] identified resolved structure as P lines and unresolved structure as R heads, so that for example the P branch of the 0-5 band overlapped the R head of the 0-6 band. They also reported that, for the P branch, the early lines are diffuse and with increasing J split into two (1 weak and 1 strong) which later again split into two. No reasons were given for the great differences in sharpness and wavelength of the P and R branches, and no isotope effect was found in any band.

A new analysis is proposed which is based on the isotope effect. Each band has three strong branches whose intensity and sharpness reach a maximum at the centre of the band. The spacing has a 2:1 ratio and these are assigned as isotope branches. The two close branches lie on the high frequency side of the third. However, no branch is continuous through the band; the discontinuity at the intensity maximum is due either to a perturbation or to the branch becoming diffuse and being overlapped by another sharp band. It is suggested that P and R branches lie symmetrically about the intensity maximum and are diffuse at both high and low J values. Thus R and P branches are sharp and intense for the same J values. There is no evidence, however, that R and P branches, in a given region, belong to the same band. Indeed the almost constant spacing of the low frequency branch is always larger than that of the high frequency branch. While this might be due to red-degradation, it is possible that the high frequency branch is a head-forming R branch and the low frequency branch is the P branch of an adjacent band.

The line spacing in the branches varies between 5 and 7 $cm.^{-1}$. The value of ΔB is clearly significant, for if $\Delta B=0$ estimates of $B'+B''$ obtained from the branch spacing lead to a ridiculously low value for r (~ 0.5 Å). A mean value of $\Delta B = -0.04$ $cm.^{-1}$ is derived by averaging over all the branches and this suggests that a sensible B value can only be obtained if $J \sim 80$ for the ten or so observed sharp lines in a branch. X-ray diffraction studies of xenon fluoride are reported by

Jortner, Wilson and Rice[88] to give an Xe-F distance of 2 Å; similar studies of XeO_3[87] give the Xe-O distance as 1.7 Å. If these are about correct for XeO then B is about 0.4 $cm.^{-1}$ which implies that the observed line-origin separation is about 300 $cm.^{-1}$ and confirms the problems of vibrational analysis.

A study of the vibrational isotope effect shows that there are two arrangements which satisfy the 2:1 ratio for the three strong branches, but only one when all five strong isotopes are considered. The distribution is given schematically below, with frequency increasing to the right.

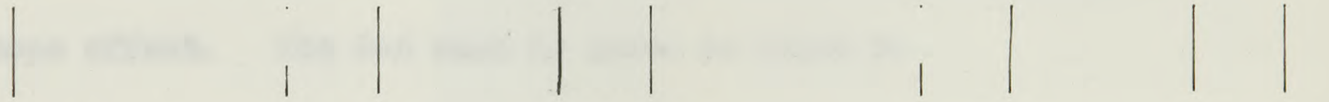

I.			129			134		131		136	132		129		134		131		132	136	129
II.	132		(134)		136 129		131	132		(134)		136 129				131	132				

II may thus be eliminated because the expected lines for ^{134}XeO do not appear. The isotope spacing is twice as large for I as it is for II. The average isotope shifts for I are given below; the vibrational numbering is that given by Cooper et al. and the shifts are of the type $\Delta\nu$, $^{131}XeO - {}^{129}XeO$, in $cm.^{-1}$.

Band	129	131	132	134	136
0-3		5.42	2.27		
1-4		5.05	2.47	4.95	5.05
0-5		4.84	2.21	4.57	
1-5		4.61	2.22		
0-6		4.23	2.03	4.13	
0-7		3.54	1.80	3.40	
1-8		2.77	1.31	2.59	

There is an increase in the shifts with increasing frequency which is the opposite of that expected unless there is a large $x_e\omega_e''$ term. No vibrational analysis has been found which satisfies this observed isotope effect. The 0-6 band is shown in Plate 9.

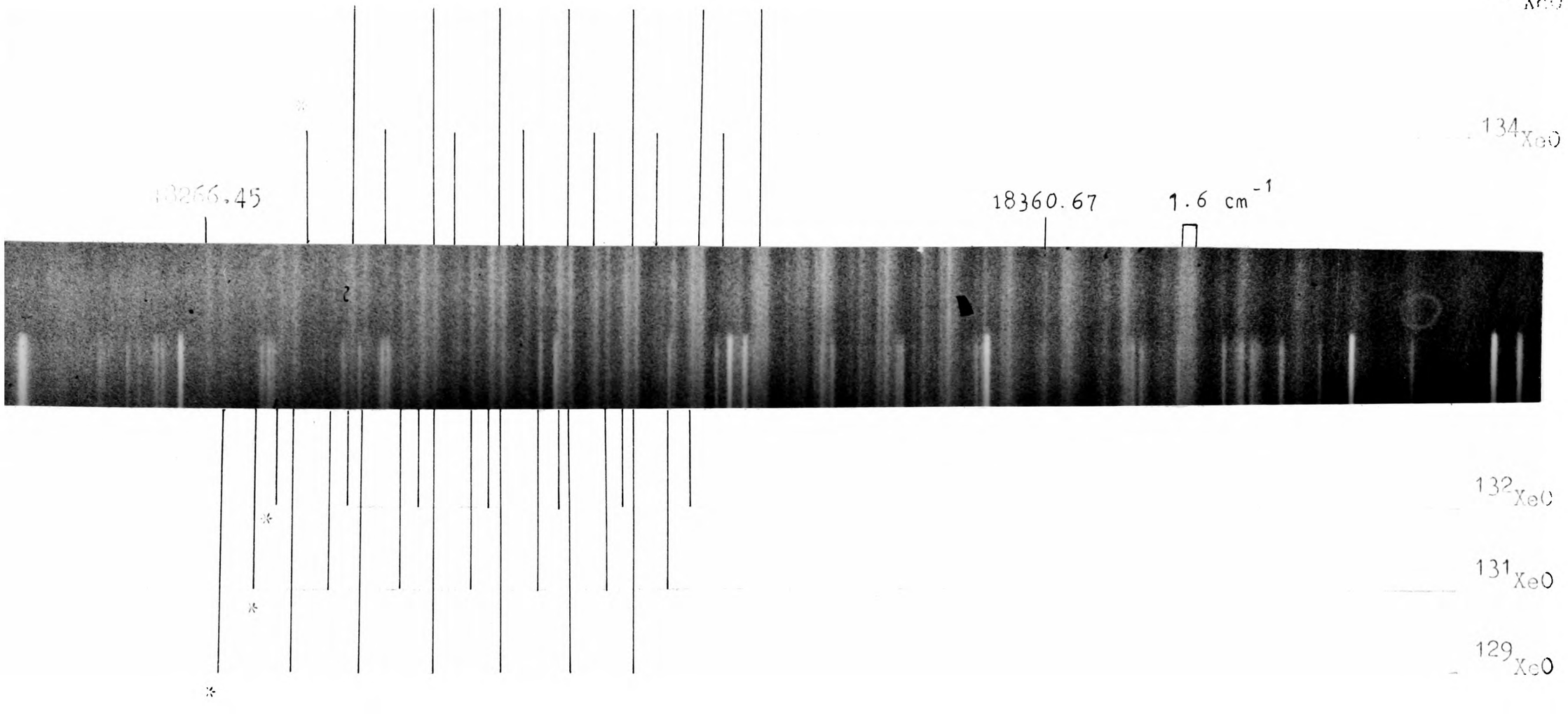

Fig 9. 0-0 Band of XeO with part of the suggested isotope [illegible] lines with the assigned values.

Discussion

All the rotational structure is adequately explained by the assignment as R or P lines of the 5 main isotopic species. The transition therefore has $\Delta\Omega = 0$, XeO being presumably described by case-c. The states may be derived as follows:

$Xe(^1S_0) + O(^1S_0)$ gives only $^1\Sigma^+$ for the upper state

$Xe(^1S_0) + O(^1D_2)$ gives $^1\Sigma^+$, $^1\Pi$ or $^1\Delta$ for the ground state.

The electron configuration of the ground state, with 2 more electrons than TeO, is probably $\sigma^2\pi^4\pi^{*4}$ giving only $^1\Sigma^+$. The transition is thus confirmed as $^1\Sigma^+ - {}^1\Sigma^+$. The first excited configuration is presumably $\ldots\sigma^2\pi^4\pi^{*3}\sigma^*$ giving $^3\Pi$, $^1\Pi$. The 0^+ component of $^3\Pi$ is then the upper state and since σ^* is more anti-bonding than π^*. B' should be smaller than B".

These arguments are tentative; studies of the chemical shifts of the xenon fluorides and oxyfluorides[86] show that the bonds are quite ionic, involving F(2p) and Xe(5p) orbitals and also probably some d-hybridisation. The main qualitative contribution to bonding comes from the polarizability of Xe and the high electronegativity of O and F. The smaller polarizabilities of Kr and Ar are then responsible for the relative instability of their oxides and the greater diffuseness of their spectra.

The present study raises more problems than it solves. Future work is planned using a more powerful r/f generator and a faster spectrograph giving higher dispersion; the use of $^{17}O_2$ could also confirm the isotope effect. The limit to analysis will always be set, however, by the diffuseness and scarcity of lines in a branch.

APPENDIX B

THEORETICAL ORDER-SORTING FOR AN EBERT SPECTROGRAPH

The Theoretical Performance of an Ebert Spectrograph

The aim of this section is to indicate the basis of the equations used in the computation of wavelengths at the camera of an Ebert spectrograph recently acquired by this laboratory. Several papers have been published[60-64] which give details of the possible optical arrangements of a spectrograph using a plane grating and a concave mirror or mirrors. In the present case the results are derived for a single mirror "in line" design in which the slit is mounted vertically above the camera, since this is the layout used in the Oxford 3.4 metre Jarrell-Ash spectrograph. The grating of this instrument has relatively few (7620) lines to the inch, but is blazed at about 57,000 Å so that in the visible region it is used at about 10th Order. This means, however, that the orders must be separated before the light enters the Ebert slit.

There are two methods for doing this: in the first the light is dispersed, by a fore-prism, across the Ebert slit so that the different wavelengths fall at different heights and hence the orders occur at different heights on the camera; this is made possible by the stigmatic nature of the instrument and has been discussed by Jarrell[63]. In the second the light is dispersed parallel to the Ebert slit so that only those wavelengths falling on the slit pass into the instrument. The second method has been adopted here.

The use of an Ebert instrument is essentially simple, since to change the wavelength region the grating is merely rotated, but the fore-optics must also be changed so that only the light of a single order gets on to the grating.

The wavelength equation for a diffraction grating is

$n\lambda = d(\sin\beta + \sin\alpha)$ where β is diffraction angle
α is incidence angle, i.e. grating angle
n is order
d is line-spacing .

At the centre of the camera $\alpha = \beta$ and so the wavelength is given by

$$\lambda_c = \frac{2d \sin\alpha}{n}$$

For a mirror of focal length f, the linear dispersion at the camera centre is given by

$$\frac{d\lambda}{dx} = \frac{d\lambda}{d\beta}\cdot\frac{1}{f} = \frac{d\cos\beta}{nf} = \frac{d\cos\alpha}{nf}$$

The wavelength range at the camera is found as follows:

$$\frac{d\lambda}{dx} = \frac{d\cos\beta}{nf}$$

but $\cos\beta = \sqrt{1 - (\frac{n\lambda}{d} - \sin\alpha)^2}$

let $\frac{n\lambda}{d} - \sin\alpha = \sin\theta$ then $\cos\beta = \cos\theta$

and $\frac{n}{d}\cdot d\lambda = \cos\theta\, d\theta$

Thus $d\lambda = \frac{d\cos\theta\, d\theta}{n} = \frac{d\cos\beta\, dx}{nf} = \frac{d\cos\theta\, dx}{nf}$

$\therefore \quad dx = f.d\theta$

$$\therefore \int dx = f \int d\theta$$

$$\therefore \quad x = f[\theta] \quad \text{where } x \text{ is linear displacement along the camera}$$

$$\therefore \quad \frac{x}{f} = \sin^{-1}\left(\frac{n\lambda}{d} - \sin\alpha\right) - C \quad \text{where } C \text{ is a constant}$$

$$\therefore \quad \sin\left(\frac{x}{f} + C\right) = \frac{n\lambda}{d} - \sin\alpha$$

Let $x = 0$ when $\lambda = \lambda_c$

$$\text{then} \quad \sin c = \frac{n\lambda_c}{d} - \sin\alpha = \frac{2nd\sin\alpha}{nd} - \sin\alpha$$

$$\therefore \quad \sin c = \sin\alpha$$

$$\therefore \quad \frac{n\lambda}{d} = \sin\alpha + \sin\left(\frac{x}{f} + \alpha\right)$$

$$\therefore \quad \lambda = \frac{d}{n}\left\{\sin\alpha + \sin\left(\frac{x}{f} + \alpha\right)\right\}$$

This equation is very useful for the calculation of the wavelengths of spectral lines at the camera by interpolation between standards. It may be rewritten

$$\lambda = \frac{d}{n}\sin\alpha + \frac{d}{n}\sin\frac{x}{f}\cos\alpha + \frac{d}{n}\cos\frac{x}{f}\sin\alpha$$

i.e. $\lambda = A + B\sin\frac{x}{f} + C\cos\frac{x}{f}$.

In this form the constants A, B and C can be determined by a least squares method using the values of λ obtained by measuring the positions x of the standard lines.

The maximum and minimum values of λ for each order are computed from $x = \pm\frac{1}{2}$ (camera length) and the difference, the Range, is computed.

The problem of order-sorting lies in the selection of wavelengths between λ_{max} and λ_{min} for a given order, and only allowing these to pass through the Ebert slit. The fore-optics consist of a fore-slit, a lens and a 90° Pellin-Broca prism, and the fore-prism is rotated until light of wavelength λ_c is focussed on to the slit. The wavelength range around λ_c is then determined by the linear dispersion due to the fore-prism across the slit and by the width of the fore-slit. Since the fore-slit width s is always much greater than the Ebert slit width, s is given by

$$s = \frac{z.\delta\lambda.d\theta/d\lambda}{2m}$$

where z is the distance from fore-prism to fore-slit, m is the magnification produced by the lens used for focussing, $\delta\lambda$ is the selected range and $d\theta/d\lambda$ is the dispersion of the fore-prism for the given λ_c.

At present, however, the Jarrell-Ash instrument is only in best focus over 12" at the short wavelength end of the 20" camera. A single plate can be used in this position but the order-sorting is slightly different. λ_{max} has therefore been derived for x=50.8 mm. and λ_{min} for x=-25.4 mm., and the fore-slit width has been calculated for the plate centre λ_0. If D is defined as $\lambda_{min}(n) - \lambda_{max}(n+1)$ then the optimum value of $\delta\lambda$ depends on the sign of D. If D is positive there is no overlap between successive orders and some allowance can be made for error in the fore-prism angle by putting $\delta\lambda$ = Range + D. If D is negative,

for maximum use of the plate the best $\delta\lambda$ is Range, but the long wavelength end of the plate is slightly overlapped.

These conditional clauses are included in the programme to compute $\delta\lambda$, which is the optimum wavelength range for a given order n, i.e. for a given value of λ_o.

For a Spectrosil lens the refractive index for a given wavelength λ in microns is given by Rodney and Spindler[59],

$$n^2 = 2.979864 + \frac{0.008777808}{(\lambda^2-0.010609)} - \frac{84.06224}{96.0000-\lambda^2}$$

$$\therefore \frac{dn}{d\lambda} \doteq -\frac{0.008777808}{(\lambda^2-0.010609)^2} \cdot \frac{\lambda}{n}$$

$$\text{also } \frac{d\theta}{dn} = \frac{2\sin\sigma/2}{(1-n^2\sin^2\sigma/2)^{\frac{1}{2}}}$$

where σ is the dispersion angle, i.e. 60° for a Pellin-Broca prism.

Thus $\frac{d\theta}{d\lambda}$ can be found, being equal to $\frac{dn}{d\lambda} \times \frac{d\theta}{dn}$.

Using these equations it is possible to calculate how much the fore-prism should be rotated, $\theta/2$, to bring a given λ_o on to the slit, starting at a reference point. In the present case the above formulae only hold for $\lambda < 13{,}800$ Å and so this was taken as the reference point, i.e.

$$\theta = \int_{13800}^{\lambda_o} \left(\frac{d\theta}{dn} \times \frac{dn}{d\lambda}\right) d\lambda$$

The integration was computed by the Gauss method.

One final problem, discussed by Minkowsky[65], is that the spectrum lines formed by a plane grating are curved convex towards shorter wavelengths. Also in the "in line" arrangement all rays meet the grating at an angle above the horizontal. The result is spectrum lines which are segments of much longer lines, taken at some distance from their apices. The lines are substantially straight but if the slit is vertical, they will be tilted over at an angle to the vertical. If this angle is small and constant over the width of the camera, the slit may be tilted in the opposite direction to compensate. When using an order sorter as previously described, it is very important to have the fore-slit and the Ebert slit exactly parallel if the order sorting is to be efficient and so it is convenient to know the angle of tilt. At the centre of the camera the relevant equation for the spectral line is $q = \frac{h^2}{f}\tan\beta$

where β = angle of diffraction = α
f = focal length
h = distance of image off axis in vertical direction
q = displacement of spectral line

Thus the line-slope is given by $\frac{dq}{dh} = \frac{2h\tan\alpha}{f}$. This value was also computed.

The output of the computer was arranged as a series of pages, each page giving the required information for a given grating angle. Thus for each value of n, the following were printed: λ_c, λ_{max}, λ_{min}, Range, Angstrom Dispersion, Wavenumber Dispersion, Foreslit Width,

Prism Rotation, Slit-tilt. A print-out of the programme is given in Appendix C.

The order-sorter was designed according to the specification indicated by these figures, and the dimensions of its parts were chosen to match the aperture of the Ebert spectrograph. While detailed results have not yet been obtained, preliminary evidence suggests that the order-sorting is satisfactory.

APPENDIX C

ALGOL COMPUTER PROGRAMMES

(1) Klein Curve Calculation

(2) Mbert Spectrograph Settings

CHANDLER KLEIN CURVE→

```
begin library A0,A6;
comment this program calculates rmax and rmin for each
vibrational level from experimental data by the Klein
method, as adapted by Richards.  data is added at the end
as follows: title, last vib. level for which data is
known n , reduced mass mA , delta G values from 0 to n-1,
B values from 0 to n inclusive,   these are separated
as usual by ;

real af,bf,ag,bg,f,g,max,min,mA,C,pi,I1f,I2f,I3f,I1g,I2g,
        I3g,X,SUM1f,SUM2f,SUM1g,SUM2g;
integer n,m,p,i,q,j,J,O;
open(20); open(10);

writetext(10,[[cc]]);
copytext(20,10,[;]);
writetext(10,[[cc]n*****r*min****r*max[cc]]);
O:=read(20);

begin array A,B,F1,F2,G1,G2,F[0:O+2];
procedure TOTALS (r) term:(t) order:(N) result:(y);
  value N; integer r,N; real t,y;
  begin real s; s:=0;  for r:=1 step 1 until N do
        s:=s+t;
        y:=s;
  end;

real procedure SIM (a,b);
  value a; integer a; array b;
  begin real s; integer i;
  s:=(b[1] - b[a])/2;
  for i:=1 step 2 until a-2 do
  s:=s + 2×b[i+1] + b[i+2];
  SIM:=2×s/3;
  end;


pi:=3.1415926;
mA:=read(20);
for j:=1 step 1 until O do A[j-1]:=read(20);
for J:=1 step 1 until O+1 do B[J]:=read(20);

C:=sqrt((66.234 × 60.251)/(8 × pi↑2 × 2.99776 × mA));
```

...continued

```
for n:=8 step 1 until 0 do
begin for m:=1 step 1 until n do TOTALS(i,A[i-1],m,F[m]);

      for p:=1 step 1 until n-3 do
        begin F1[p]:=1/(sqrt(F[n] - (if p=1 then 0 else
                            F[p-1])));
              G1[p]:=F1[p] × B[p]/C↑2;
end;    end;

if n/2 - n÷2 < 0.1 then goto EVEN else goto ODD;

EVEN:   I2f:=SIM(n-3,F1);
        I2g:=SIM(n-3,G1);
        I1f:=(3×F1[1] - F1[2])/4;
        I1g:=(3×G1[1] - G1[2])/4;
        goto CONTINUE;

ODD:    for p:=1 step 1 until n-3 do
        begin F2[p+1]:=F1[p];
              G2[p+1]:=G1[p];
        end;

        F2[1]:=F2[2]+F2[3]-F2[4];
        G2[1]:=G2[2]+G2[3]-G2[4];
        I2f:=SIM(n-2,F2);
        I2g:=SIM(n-2,G2);
        I1f:=-(3×F2[2] - F2[3])/4;
        I1g:=-(3×G2[2] - G2[3])/4;


CONTINUE:       SUM1f:=SUM2f:=SUM1g:=SUM2g:=0;
        for q:=n-3 step 1 until n do
        begin SUM1f:=SUM1f + (n-q)×(F[n] - F[q]);
              SUM1g:=SUM1g + (n-q)×(F[n] - F[q]) × C↑4/
                                        B[q+1]↑2;

              SUM2f:=SUM2f + (n-q)↑2×(F[n] - F[q]);
              SUM2g:=SUM2g + (n-q)↑2×(F[n] - F[q]) ×
                                      C↑4/B[q+1]↑2;
        end;


af:=(SUM1f×98 - SUM2f×36)/76;
bf:=(SUM2f×14 - SUM1f×36)/76;

ag:=(SUM1g×98 - SUM2g×36)/76;
bg:=-(SUM2g×14 - SUM1g×36)/76;
```

...continued

```
I3f:=(abs(ln(8xbf/af +1 + sqrt((8xbf/af +1)↑2 -1))))/
                                        sqrt(bf);
f:=Cx(I1f + I2f + I3f);
if bg<0 then goto NEG;
X:=1 - 8xbg/ag;
I3g:=(1.5707963 - arctan(X/sqrt(1.0-X↑2)))/sqrt(bg);
goto OUT;

NEG: bg:=-bg;
     I3g:=(abs(ln(8xbg/ag +1+sqrt((8xbg/ag +1)↑2 -1))))/
                                        sqrt(bg);

OUT: g:=Cx(I1g + I2g + I3g);


max:=sqrt(f/g + f↑2) + f;
min:=sqrt(f/g + f↑2) - f;

write(10,format([ndsss]),n);
write(10,format([d.ddddsss]),min);
write(10,format([d.ddddc]),max);

end;
end;
close(10); close(20);
end→
```

CHANDLER GRATING SETTINGS→

```
begin library A0,A6;
comment This program calculates wavelengths at a 12 inch
plate for the 3400 mm Ebert, optimum foreslit widths,
micrometer setting for fore-prism, slit tilt of Ebert;
real M,f,A,Summax,Summin,AngsDisp,Range,D,Lc,dL,Lo,T,a,
     b,h,SUM,pi,r;
integer p,q,m,n,F,i;
comment Data is added so that first number is Magnification M,
        second is prism-to-foreslit distance f in mms, third
        is length of turntable arm  a  in inches, fourth is
        armlength of Ebert slit-tilt  b  in inches, fifth
        is distance off axis h of plate centre in inches,
        thereafter grating incidence angle A in degrees to
        4 decimal places concluding with 10↑4;

array x,w[0:10];

real procedure Prisum(L); value L; real L;
begin r:=sqrt(2.979864+0.008777808/((Lx10↑-4)↑2-0.010609)
        -84.06224/(96.0-(Lx10↑-4)↑2));
Prisum:=10↑-4x(2x(Lx10↑-4)xsin(pix30/180)x0.0 8777808)/
   (rx((Lx10↑-4)↑2-0.010609)↑2xsqrt(1-r↑2x(sin(pix30/180))↑2));
end;


open(30);
open(20); M:=read(20); f:=read(20); a:=read(20); b:=read(20);
          h:=read(20); pi:=3.1415926;

NEW ANGLE:      A:=read(20); if A>10↑3 then goto FINISH
        else goto START;

START:  writetext(30,[[pss]angle**]);
write(30,format([dd.ddddccc]),A);
writetext(30,[order**mid-camera***angst-disp****range
        ****plate-min***plate-max***nos-disp***
        foreslit****prism***slit-tilt[cc]]);
q:=0;
A:=pixA/180;
```

...continued

```
for m:=1 step 1 until 6 do
begin for p:=1 step 1 until 5 do
begin n:=q+p;
        Lc:=2₁₀5×sin(A)/(3×n);
        if Lc>13800 then goto LARGE else if
        Lc<2000 then goto LARGE;
        write(30,format([sndssss]),n);
        F:=format([snddd.ds]);
        write(30,F,Lc);
        AngsDisp:=cos(A)/(0.102×n);
        write(30,format([sssnd.ddddsssss]),AngsDisp);
        Summax:=₁₀5×(sin(A+50.8/3400)+sin(A))/3;
        Summin:=₁₀5×(sin(A-254/3400)+sin(A))/3;
        Range:=Summax/n-Summin/n;
        write(30,format([nddd.dssss]),Range);
        write(30,F,Summin/n);
        writetext(30,[*-*]);
        write(30,F,Summax/n);
        write(30,format([3snd.dddd]),₁₀8×AngsDisp/Lc↑2);
        D:=Summin/n-Summax/(n+1);
        Lo:=(Summax/n+Summin/n)/2;
        dL:=if D>0 then Range+D else Range;
        write(30,format([4s-d.ddds]),f×Prisum(Lo)×dL/(2×M));

        SUM:=0;
        x[5]:=-0.14887 43390; x[6]:=-x[5];
        x[4]:=-0.43339 53941; x[7]:=-x[4];
        x[3]:=-0.67940 95683; x[8]:=-x[3];
        x[2]:=-0.86506 33667; x[9]:=-x[2];
        x[1]:=-0.97390 65285; x[10]:=-x[1];

        w[1]:=w[10]:=0.06667 13443;
        w[2]:=w[9]:=0.14945 13492;
        w[3]:=w[8]:=0.21908 63625;
        w[4]:=w[7]:=0.26926 67193;
        w[5]:=w[6]:=0.29552 42247;

        for i:=1 step 1 until 10 do
        SUM:=SUM+w[i]×(Prisum((13800-Lo)×x[i]/2+(1380 +Lo)/2));
        T:=(13800-Lo)×SUM/2;
        write(30,format([4snd.ddddds]),a×T/2);
        write(30,format([4sd.ddd]),(2×b×h×25.4×sin(A))/
        (3400×cos(A)));
        LARGE:   writetext(30,[[c]]);
        end;  q:=q+5; writetext(30,[[c]]);
end;  goto NEW ANGLE;
FINISH:          close(20);      close(30);
end→
```

APPENDIX D

VACUUM WAVE NUMBERS OF LINES FOR ANALYSED BANDS OF Se_2

Emission Bands page 158

Absorption Bands page 167

Δ_2F'' for v''=0, F_1-F_1 bands of $^{78}Se_2$

J	v'=21	20	19	18	17	16	15	14	13	12	11	10	8	m.v.
7	2.73	.76	.77	.75	.80	.76	.75	.76	.75	.78		.73		2.755
9	3.24	.56	.56	.52	.51	.48	.51	.51	.48	.49	.49		.46	3.490
11	4.03	.36	.19	.28	.21	.23	.25	.24	.24	.24	.26	.26	.21	4.240
13	4.73	5.02	5.05	.94	.93	.93	.96	.98	.96	.98	.97	.97	.90	4.960
15	5.32	.69	.75	.78	.71	.72	.71	.73	.74	.70	.70	.71	.67	5.710
17	6.24	.34	.52	.49	.43	.44	.43	.45	.45	.43	.45	.44	.40	6.440
19	7.06	.16	.18	.21	.22	.23	.18	.16	.18	.17	.18	.24	.16	7.180
21	7.89	.91	.94	.91	.90	.92	.91	.91	.94	.91	.90	.92	.92	7.920
23	8.70	.70	.71	.55	.67	.65	.64	.61	.64	.64	.65	.62	.63	8.630
25	9.34	.36	.39	.41	.37	.44	.38		.38	.38	.38	.33	.37	9.370
27	10.17	.16	.14	.11	.07	.15	.13	.12	.13	.21	.10	.09	.09	10.120
29	10.84	.83	.88	.82	.82	.80	.85	.84	.88	.86	.86	.81	.85	10.850
31	11.51	.57	.66	.57	.60	.66	.61	.57	.62	.62	.60	.55	.59	11.590
33	12.39	.33	.35	.32	.38	.28	.34	.31	.35	.32	.33	.26	.35	12.320
35	13.04	.08	.12	.04	.10	.07	.03	.00	.07	.08	.07	.01	.10	13.060
37	13.74	.89	.72	.76	.75	.81	.82		.79	.82	.83	.78	.80	13.810
39	14.63	.61	.53	.51	.58	.62	.53		.55	.54	.55	.53	.54	14.540
41	15.12	.31	.29	.22	.23	.34	.26	.21	.28	.27	.27	.27	.29	15.270
43	16.13	.12	.10	.99	.91	.04	.01	.02	.01	.99	.01	.03	.03	16.010
45	16.67	.77	.68	.72	.71	.68				.73	.74	.76	.77	16.750
47	17.46	.49	.48	.50	.40	.43	.49	.47	.47	.46	.46	.47	.49	17.470
49	18.20	.18	.30	.23		.24	.20	.21	.20	.22	.20	.26	.22	18.220
51		18.97	.88	.96		.94		.94	.95	.95	.93	.97	.95	18.950
53		19.62	.73	.87		.69		.67	.70	.68		.66	.69	19.680
55		20.49	.46	.44		.50		.41		.41		.43	.42	20.420
57		21.17	.11	.10		.07		.14		.15		.13	.15	21.140
59		21.83	.91	.97		.96		.81		.88		.83	.91	21.860
61								22.62		.61		.62	.61	22.615
63								23.36		.31	.35	.33		23.340
65								24.11			.07	.07	.13	24.090
67								24.84		.85	.79	.85	.79	24.820
69								25.54		.54	.50	.50		25.520
71								26.28		.28	.23			26.260
73									26.98	.99				26.985
75									27.73	.75	.73	.76		27.740
77									28.47	.47	.47	.49		28.475
79									29.19	.18	.23	.22		29.205
81									29.95			.94		29.945
83									30.66			.65		30.655
85									31.39			.38		31.385
87									32.09			.08		32.085

N.B. only v' for 8 to 15 inclusive used for m.v.

(5-28) Band — $^{80}Se_2$

J	R_{22}	P_{22}	J	R_{33}	P_{33}
61	16570.40	16553.91	62	16569.97	16553.12
63	67.06	50.05	64	66.63	49.29
65	63.55	46.07	66	63.05	45.31
67	59.70	41.92	68	61.14	41.08
69	57.25	37.40	70	56.48	38.52
71	52.92	34.31	72		33.19
73		29.33			

(5-29) Band — $^{80}Se_2$

J	R_{22}	P_{22}	J	R_{33}	P_{33}
61	16240.96	16224.47	62	16240.57	16223.72
63	37.68	20.68	64	37.31	19.96
65	34.27	16.76	66	33.82	16.05
67	30.49	12.69	68	32.00	11.91
69	28.14	08.27	70	27.39	09.44
71	23.89	05.26	72		04.20
73		00.38			

New analysis of the last few lines of v'=5 indicating predissociation

(5-2) Band

$^{78}Se_2$

J	R_{11}	P_{11}
8	26350.12	26347.75
10	49.60	46.65
12	48.90	45.40
14	48.03	43.96
16	47.01	42.37
18	45.80	40.60
20	44.42	38.67
22	42.87	36.54
24	41.19	34.30
26	39.29	31.86
28	37.25	29.24
30	35.04	26.46
32	32.65	23.51
34	30.07	20.37
36	27.36	17.11
38	24.46	13.65
40	21.40	10.03
42	18.16	06.24
44	14.75	02.27
46	11.15	298.13
48	07.40	93.80
50	03.47	89.32
52	299.36	84.66
54	95.05	79.83
56	90.59	74.80
58	85.92	69.59
60	81.09	64.21
62	75.97	58.62
64	70.53	52.80
66	64.39	46.64
68	56.63	39.73
70		31.27
72	(50.72)	
74	44.21	24.03
76	(37.79)	16.66
78	(31.36)	09.54
80	(24.86)	(02.38)
82	(18.08)	(195.13)
84	(11.24)	(87.66)
86	(04.21)	(80.06)
88	(197.02)	(72.36)
90	(89.67)	(64.40)
92	(82.30)	(56.27)
94		(48.01)

Mean values for abs. and em.; ( ) indicate abs. only observed.

	6 - 1 Band	$^{78}Se_2$	6 - 2 Band	$^{78}Se_2$
J	R_{11}	P_{11}	R_{11}	P_{11}
0				
2				
4	26973.39		26586.85	26585.63
6	73.18		86.70	84.84
8	72.74	26970.47	86.29	83.90
10	72.26	69.31	85.77	82.82
12	71.45	67.95	85.01	81.56
14	70.61	66.56	84.17	80.12
16	69.53	64.91	83.13	78.51
18	68.28	63.13	81.93	76.72
20	66.90	61.12	80.51	74.79
22	65.23	58.96	78.94	72.64
24	63.49	56.55	77.20	70.32
26	61.55	54.11	75.26	67.86
28	59.44	51.44	73.20	65.21
30	57.11	48.59	70.90	62.42
32	54.56	45.54	68.46	59.44
34	51.99	42.34	65.84	56.25
36	49.11	38.94	63.07	52.90
38	46.14	35.39	60.18	49.37
40	42.96	31.70	57.02	45.70
42	39.59	27.73	53.70	41.85
44	36.07	23.67	50.22	37.82
46		19.38	46.57	33.60
48			42.74	29.20
50			38.73	24.64
52			34.55	19.92
54			30.18	15.00
56	11.15	895.31	25.63	09.90
58	06.32	89.98	20.90	04.63
60			15.99	499.18
62			10.88	93.55
64				87.71

Predissociated at ___

6 - 3 Band $^{78}Se_2$

J	R_{11}	P_{11}
0		
2		
4	26202.73	
6	02.59	26200.69
8	02.17	199.83
10	01.64	98.73
12	00.98	97.47
14	00.10	96.07
16	199.07	94.46
18	97.87	92.69
20	96.49	90.77
22	94.95	88.68
24	93.25	86.39
26	91.35	83.94
28	89.31	81.34
30	87.10	78.56
32	84.68	75.58
34	82.13	72.48
36	79.33	69.16
38	76.44	65.67
40	73.37	62.03
42	70.10	58.22
44	66.68	54.26
46	63.11	50.09
48	59.28	(45.77)
50	(55.35)	41.25
52	51.19	(36.59)
54	46.99	31.84
56	42.43	26.76
58	37.80	(21.55)
60	33.03	

Predissociated at ___

Mean values for abs. and em.; ( ) indicate abs. only observed.

11 - 3 Band $^{78}Se_2$

J	R_{11}	P_{11}
0		
2		
4		
6		
8		
10	27347.80	27344.99
12	47.10	43.63
14	46.17	42.16
16	44.99	40.48
18	43.63	38.61
20	42.16	36.55
22	40.48	

11 - 2 Band $^{78}Se_2$

J	R_{11}	P_{11}
0		
2		
4		
6	27733.17	27731.26
8	32.64	30.30
10	32.02	29.10
12	31.26	27.82
14	30.30	26.27
16	29.10	24.55
18	27.82	22.71
20	26.27	20.65
22		18.36

11 - 4 Band $^{78}Se_2$

J	R_{11}	P_{11}
0		
2		
4		
6	26966.56	
8	66.26	26963.96
10	65.69	62.83
12	64.91	61.55
14	63.96	60.05
16	62.83	58.37
18	61.55	56.55
20	60.05	54.56
22	58.37	52.27
24	56.55	49.87
26	54.56	47.35
28		44.69

12 - 6 Band $^{78}Se_2$

J	R_{11}	P_{11}
42	26396.01	
44	92.37	26380.36
46	88.58	76.01
48	84.62	71.52
50	80.36	66.79
52	76.01	61.87
54		56.80

12 - 4 Band $^{78}Se_2$

J	R_{11}	P_{11}
42	27153.39	
44	49.61	27137.57
46	45.74	33.12
48	41.68	28.47
50	37.57	23.67
52	33.12	18.74
54		13.55
56		08.17

13 - 6 Band $^{78}Se_2$

J	R_{11}	P_{11}
0		
2		
4	26649.38	26648.14
6	49.14	47.39
8	48.74	46.44
10	48.14	45.34
12	47.39	44.00
14	46.44	42.51
16	45.34	40.83
18	44.00	38.99
20	42.51	36.97
22	40.83	34.76
24		32.37

Predissociated

1$ - 5 Band $^{78}Se_2$

J	R_{11}	P_{11}
0		
2		
4	27027.73	27026.46
6	27.45	25.67
8	27.03	24.75
10	26.46	23.56
12	25.67	22.24
14	24.75	20.78
16	23.56	19.07
18	22.24	17.19
20	20.78	15.26
22	19.07	

13 - 4 Band $^{78}Se_2$

J	R_{11}	P_{11}
0		
2		
4		
6		
8		
10	27406.71	274
12	05.87	02.38
14	04.92	00.87
16	03.73	399.19
18	02.38	97.30
20	00.87	95.30
22	399.19	93.02
24		90.56

Predissociated

13 - 3 Band $^{78}Se_2$

J	R_{11}	P_{11}
0		
2		
4	27790.18	27788.87
6	89.93	88.05
8	89.47	87.09
10	88.87	85.92
12	88.05	84.62
14	87.09	83.05
16	85.92	81.34
18	84.62	79.46
20	82.98	77.36
22	81.21	75.06
24		72.56

Predissociated

$^{80}Se_2$

J	(0-7) Band R_{11}	(0-7) Band P_{11}	(1-8) Band R_{11}	(1-8) Band P_{11}
16			23140.20	23135.62
18			39.29	34.11
20		Perturbation	38.20	32.46
22			36.99	30.67
24	23261.05		35.62	28.77
26	59.56	23252.11	34.11	26.71
28	57.88	49.93	32.46	24.50
30	56.11	47.56	30.67	22.16
32	54.17	45.10	28.77	19.69
34	52.11	42.50	26.71	17.06
36	49.93	39.73	24.50	14.30
38	47.56	36.85	22.16	11.40
40	45.10	33.80	19.69	08.35
42	42.50	30.63	17.06	05.17
44	39.73	27.30	14.30	01.86
46	36.85	23.84	11.40	098.40
48	33.80	20.25	08.35	94.79
50	30.63	16.52	05.17	91.07
52	27.30	12.65	01.86	87.18
54	23.84	08.61	098.40	83.15
56	20.25	04.45	94.77	78.99
58	16.52	00.14	91.03	74.66
60	12.65	195.71	87.09	70.23
62	08.61	91.11	83.03	65.62
64	04.45	86.44	78.81	60.87
66		81.51	74.33	55.97
68			71.01	50.82
70			65.90	46.81
72	186.52		61.08	40.99
74	81.66	60.83	56.16	35.50
76	76.66	55.27	51.13	29.85
78	71.54	49.58	45.98	24.13
80	66.25	43.79	40.67	18.27
82	60.83	37.79	35.24	12.25
84	55.27	31.66	29.66	06.08
86	49.58	25.41	23.95	
88	43.79	19.03	18.09	
90		12.46	12.07	
92			05.92	

	(3-4) Band		(2-5) Band	$^{80}Se_2$
J	R_{11}	P_{11}	R_{11}	P_{11}
10			24499.29	
12			98.67	24495.20
14			97.92	93.90
16	Perturbation		97.07	92.47
18	25111.79		96.03	90.88
20	10.42	25104.87	94.86	89.15
22	08.99	02.81	93.54	87.27
24	07.43	00.67	92.04	85.24
26	05.71	098.39	90.42	83.05
28	03.85	95.97	88.64	80.72
30	01.83	93.39	86.72	78.24
32	099.66	90.68	84.63	75.61
34	97.35	87.81	82.41	72.81
36	94.88	84.77	80.04	69.88
38	92.26	81.60	77.52	66.81
40	89.46	78.27	74.84	63.57
42	86.54	74.78	72.02	60.18
44	83.45	71.15	69.03	56.65
46	80.20	67.36	65.90	52.97
48	76.80	63.39	62.62	49.12
50	73.24	59.28	59.19	45.14
52	69.54	55.02	55.61	41.01
54	65.68	50.60	51.87	36.74
56	61.65	46.02	48.00	32.31
58	57.45	41.30	43.96	27.74
60	53.13	36.40	39.79	22.99
62	48.65	31.36	35.46	18.14
64	43.99	26.16	30.98	13.11
66	39.18	20.81	26.36	07.92
68	34.21	15.31	21.57	02.61
70	29.10	09.65	16.66	397.13
72	23.85	03.82	11.58	91.49
74	18.42	24997.88	06.35	85.71
76	12.84	91.75	00.96	79.77
78	07.10	85.47	395.43	73.68
80	01.20	79.02	89.73	67.43
82	24995.17	72.44	83.91	61.06
84	88.97		77.89	54.49
86	82.59		71.74	47.78
88	76.05		65.43	40.92
90	69.39		58.93	
92			52.24	
94			45.29	
96			38.39	

(7-1) Band $^{80}Se_2$

J	R_{11}	P_{11}
0		
2		
4		
6	27192.28	
8	91.94	27189.63
10	91.38	88.51
12	90.66	87.27
14	89.76	85.82
16	88.69	84.23
18	87.45	82.45
20	86.05	80.48
22	84.46	78.35
24	82.69	76.05
26	80.76	73.58
28	78.64	70.92
30	76.36	68.10
32	73.91	65.11
34	71.29	61.94
36	68.47	58.59
38	65.49	55.06
40	62.33	51.37
42	59.00	47.49
44	55.49	43.47
46	51.79	39.23
48	47.94	34.83
50	43.91	30.24
52	39.68	25.49
54	35.27	20.56
56	30.70	15.45
58	25.93	10.15
60	20.97	04.67
62	15.81	099.00
64	10.48	93.14
66	04.90	87.11
68	099.07	80.79
70	92.93	74.26
72		67.39

perturbation

$^{80}Se_2$

J	(8-0) Band R_{11}	(8-0) Band P_{11}	(8-1) Band R_{11}	(8-1) Band P_{11}
0				
2				
4				
6	27804.69		27421.27	27419.51
8	04.31	27802.02	20.90	18.59
10	03.71	00.90	20.36	17.49
12	02.95	799.62	19.60	16.22
14	02.02	98.14	18.70	14.78
16	00.90	96.49	17.60	13.14
18	799.62	94.66	16.32	11.33
20	98.14	92.64	14.87	09.36
22	96.49	90.47	13.25	07.18
24	94.66	88.08	11.45	04.85
26	92.64	85.50	09.47	02.32
28	90.47	82.80	07.31	399.62
30	88.08	79.89	04.97	96.75
32	85.50	76.80	02.45	93.69
34	82.80	73.53	399.75	90.47
36	79.89	70.06	96.86	87.04
38	76.80	66.41	93.83	83.48
40	73.53	62.61	90.61	79.70
42			87.17	75.75
44			83.58	71.64
46			79.81	67.33
48			75.85	62.84
50			71.68	58.15
52			67.38	53.28
54			62.84	48.22
56				42.99

perturbation

	(9-1) Band		(9-2) Band		$^{80}Se_2$
J	R_{11}	P_{11}	R_{11}	P_{11}	
0					
2					
4					
6	27647.98				
8	47.56	27645.30	27266.14		
10	47.02	44.19	65.52	27262.75	
12	46.25	42.87	64.76	61.45	
14	45.30	41.41	63.85	60.00	
16	44.19	39.73	62.75	58.35	
18	42.87	37.92	61.45	56.52	
20	41.41	35.85	60.00	54.54	
22	39.73	33.71	58.35	52.35	
24	37.92	31.30	56.52	50.01	
26	35.85	28.75	54.54	47.42	
28	33.61	25.99		44.69	
30	31.19	23.04			
32	28.63	19.90			
34	25.81	16.58			
36	22.86	13.11			
38	19.65	09.43			
40	16.31	05.56			
42	12.72	01.46			
44	08.97	597.20			
46	05.07	92.72			
48	00.96	88.10			

$^{80}Se_2$

J	(10-0) Band R_{11}	(10-0) Band P_{11}	(10-1) Band R_{11}	(10-1) Band P_{11}
		perturbation		perturbation
36			27848.81	
38	28228.63		45.74	27835.46
40	25.39	28214.53	42.47	31.59
42	21.95	10.52	39.08	27.62
44	18.37	06.34	35.46	23.52
46	14.53	01.96	31.74	19.27
48	10.52	197.44	27.79	14.78
50	06.34	92.75	23.65	10.12
52	01.96	87.88	19.32	05.23
54	197.44	82.83	14.85	00.20
56	92.65	77.52	10.18	794.99
58	87.73	72.05	05.29	89.62
60	82.58	66.40	00.24	84.04
62	77.25	60.56	794.99	78.27
64	71.70	54.49	89.49	72.29
66	65.88	48.22	83.75	66.10
68		41.67		59.64
70		perturbation		
72				
74				
76				
78				
80			40.12	18.64
82			33.03	11.08
84			25.77	03.28
86			18.34	695.34
88			10.72	87.16
90			02.92	78.82
92			694.94	70.31
94			86.74	61.58
96			78.38	52.70
98			69.80	43.62

$^{80}Se_2$

J	(11-0) Band R_{11}	(11-0) Band P_{11}	(11-1) Band R_{11}	(11-1) Band P_{11}
0				
2				
4				
6	28477.64	28475.93	28094.26	
8	77.21	74.94	93.84	28091.57
10	76.60	73.80	93.23	90.44
12	75.80	72.47	92.46	89.12
14	74.83	70.96	91.48	87.62
16	73.67	69.27	90.35	85.95
18	72.32	67.39	89.03	84.09
20	70.79	65.31	87.52	82.06
22	69.08	63.07	85.83	79.82
24	67.18	60.65	83.98	77.42
26	65.11	58.03	81.92	74.85
28	62.83	55.23	79.68	72.07
30	60.39	52.25	77.26	69.13
32	57.75	49.08	74.66	66.00
34	54.93	45.73	71.88	62.68
36	51.91	42.19	68.92	59.18
38	48.72	38.47	65.77	55.51
40	45.35	34.55	62.45	51.65
42	41.78	30.45	58.90	47.60
44	38.03	26.18	55.21	43.37
46	34.08	21.70	51.33	38.97
48	29.94	17.04	47.25	34.35
50	25.61	12.20	42.97	29.55
52	21.07	07.16	38.49	24.59
54				
56			perturbation	
58				
60	01.53	385.68		
62	396.01	79.51		
64	90.39	73.24		
66	84.54	66.89		
68	75.52	60.34		
70	72.25	53.58		
72	65.85	46.64		
74	59.23	39.50		
76	52.32	32.16		
78		24.62		

perturbation

(12-0) Band

(12-1) Band $^{80}Se_2$

J	R_{11}	P_{11}	R_{11}	P_{11}
		perturbation		perturbation
44	28657.91		28275.04	
46	53.72	28641.59	70.91	28258.79
48	49.41	36.66	66.66	53.94
50	44.94	31.64	62.27	48.97
52	40.32	26.47	57.71	43.87
54	35.51	21.14	52.96	38.60
56	30.50	15.61	48.03	33.14
58	25.33	09.90	42.92	27.51
60	19.85	03.99	37.53	21.67
62	14.42	597.79	32.18	15.57
64	08.64	91.65	26.46	09.50
66	02.65	85.15		03.09
68		78.44		
70	590.29			
72	83.76	64.69		
74	77.01	57.44		
76	69.90	49.96		
78	62.86	42.15		
80		34.40		

$^{80}Se_2$

	(13-0) Band		(13-1) Band	
J	R_{11}	P_{11}	R_{11}	P_{11}
0				
2				
4	28914.44	29813.31		
6	14.16	12.45	28530.74	28529.07
8	13.71	11.47	30.31	28.07
10	13.04	10.25	29.68	26.92
12	12.23	08.93	28.85	25.55
14	11.23	07.38	27.87	24.03
16	10.01	05.65	26.69	22.33
18	08.62	03.73	25.30	20.41
20	07.04	01.62	23.76	18.34
22	05.27	899.31	21.99	16.05
24	03.30	96.80	20.08	13.60
26	01.09	94.13	17.92	10.94
28	898.78	91.25	15.61	08.08
30	96.44	88.15	13.11	05.05
32	93.46	84.91	10.40	01.81
34	90.55	81.43	07.51	498.41
36	87.45	77.82	04.42	94.79
38	84.11	73.95	01.14	91.00
40	80.54	69.92	497.64	87.00
42	77.25	65.66	94.38	82.80
44	73.01	61.61	90.21	78.82
46	68.90	56.69	86.15	73.93
48	64.59	51.86	81.89	69.17
50	60.11	46.84	77.46	64.20
52	55.38	41.63	72.82	59.04
54	50.45	36.21	67.95	53.69
56	45.27	30.59	62.83	48.11
58		24.68		
60	34.93			
62	29.14	12.88		
64	23.28	06.44		
66	17.11	799.81		
68	10.73	92.93		
70	03.72	85.80		
72		78.09		
:				
84	757.32			
86	48.64	26.72		
88	40.01	17.34		
90	31.42	07.96		
92	22.49	698.62		
94	13.56	89.00		
96		79.37		

(14-0) Band — $^{80}Se_2$

J	R_{11}		P_{11}	
0				
2				
4	29128.49		29127.26	
6	28.18		26.51	
8	27.70		25.46	
10	27.08		24.30	
12	26.21		22.94	
14	25.11		21.36	
16	23.86		19.58	
18	22.26	23.43	17.60	
20		21.01	15.29	16.48
22		19.12	12.78	13.31
24		17.10		10.70
26		14.84		07.93
28		12.43		05.00
30		09.76		01.85
32		06.85		098.46
34				94.83
36	00.80			
38	097.54		87.31	
40	93.87		83.33	
42	89.94		78.96	
44	85.88		74.32	
46	81.21		69.50	
48			64.16	
50				
52				
54		64.80		
56				44.90
58	54.44			
60	48.32		33.08	
62	42.52		26.29	
64	36.69		19.78	
66		30.21	13.26	
68		23.65		06.09
70		17.13		28998.78
72		10.40		91.54
74		03.31		84.13
76		28996.83		76.30
78				69.09

___ marks last sharp line

(15-0) Band — $^{80}Se_2$

J	R_{11}		P_{11}	
0				
2				
4				
6				
8	29339.35			
10	38.59		29335.91	
12	37.67		34.44	
14	36.57		32.81	
16	35.28		31.03	
18	33.80		29.00	
20	32.07		26.79	
22			24.36	
24		28.16		
26		26.11		18.99
28		23.55		16.25
30		20.74		12.97
32		17.62		09.40
34	15.24			05.63
36	11.77		02.39	
38	08.53		298.31	
40	04.76		94.36	
42	00.90	00.76	89.89	
44	297.47	296.96	85.30	85.16
46		93.64	81.12	80.62
48		87.97		75.56
50				70.22

___ marks last sharp line

	(16-0) Band $^{80}Se_2$		(17-0) Band $^{80}Se_2$	
J	R_{11}	P_{11}	R_{11}	P_{11}
0				
2				
4	29548.69	29547.55	29754.13	29752.90
6	48.35	46.67	53.77	52.11
8	47.82	45.65	53.27	51.08
10	47.14	44.41	52.55	49.87
12	46.28	43.03	51.62	48.42
14	45.18	41.43	50.48	46.79
16	43.87	39.65	49.19	44.96
18	42.41	37.59	47.68	42.89
20	40.70	35.37	45.90	40.65
22	38.79	32.93	44.02	38.21
24	36.68	30.37	41.86	35.54
26	34.40	27.56	39.52	32.72
28	31.90	24.55	36.95	29.63
30	29.21	21.31	34.21	26.35
32	26.31	17.93	31.26	22.91
34	23.27	14.33	28.06	19.23
36	19.94	10.50	24.70	15.34
38	16.44	06.48	21.15	11.27
40	12.79	02.30	17.38	06.94
42	08.84	497.88	13.41	02.49
44	04.72	93.26	09.19	697.80
46	00.43	88.45	04.86	92.94
48	495.96	83.47	00.27	87.78
50	91.24	78.19	695.49	82.54
52	86.39		90.41	76.99
54				71.26

J	(18-0) Band $^{80}Se_2$		(19-0) Band $^{80}Se_2$	
	R_{11}	P_{11}	R_{11}	P_{11}
0				
2				
4	29955.91	29954.79	30153.68	30152.55
6	55.55	53.95	53.32	51.60
8	55.02	52.86	52.77	50.59
10	54.33	51.63	51.98	49.32
12	53.38	50.19	51.06	47.92
14	52.27	48.55	49.84	46.20
16	50.90	46.68	48.47	44.30
18	49.31	44.58	46.93	42.20
20	47.54	42.32	45.05	39.86
22	45.52	39.81	43.00	37.29
24	43.35	37.12	40.77	34.59
26	40.99	34.22	38.34	31.68
28	38.39	31.09	35.64	28.46
30	35.54	27.78	32.80	25.10
32	32.53	24.25	29.69	21.53
34	29.30	20.48	26.38	17.70
36	25.85	16.55	22.91	13.65
38	22.20	12.37	19.14	09.42
40	18.38	08.05	15.17	05.00
42	14.31	03.49	11.05	00.32
44	10.02	898.68	06.66	095.44
46	05.56	93.68	02.02	90.35
48	00.89	88.47	097.29	85.04
50	895.97	83.11	92.31	79.54
52	90.83	77.51	87.08	73.75
54	85.53	71.67	81.61	67.95
56	79.96		76.00	61.68
58	74.22		70.03	
60			63.98	

	(20-0) Band $^{80}Se_2$		(21-0) Band $^{80}Se_2$	
J	R_{11}	P_{11}	R_{11}	P_{11}
0				
2				
4				
6	30346.04			
8	45.42	30343.47		
10	44.75	42.06		
12	43.75	40.63	30529.75	30526.73
14	42.53	38.86	28.44	24.98
16	41.10	36.92	26.97	23.00
18	39.47	34.84	25.26	20.76
20	37.58	32.46	23.37	18.29
22	35.48	29.84	21.14	15.62
24	33.22	27.02	18.80	12.74
26	30.64	24.00	16.13	09.67
28	27.90	20.79	13.39	06.31
30	24.92	17.31	10.28	02.74
32	21.80	13.67	06.98	98.94
34	18.37	09.75	03.42	94.89
36	14.70	05.66	499.71	90.67
38	10.86	01.31	95.68	86.22
40	06.84		91.47	81.50
42	02.58		87.01	76.58
44			82.33	71.38
46			77.46	66.05
48			72.28	60.38
50			66.91	54.62
52			61.35	48.53
54			55.50	42.22
56			49.48	

(0-9) Band

$^{80}Se_2$

J	R_{22}	P_{22}	J	R_{33}	P_{33}
1			2		
3			4		
5			6		
7			8		
9			10		
11			12	22079.87	
13			14	79.26	22075.14
15	22078.79	22074.45	16	78.51	73.86
17	77.99	73.06	18	77.63	72.40
19	77.02	71.52	20	76.63	70.82
21	75.91	69.85	22	75.48	69.10
23	74.67	68.06	24	74.20	67.26
25	73.29	66.15	26	72.80	65.30
27	71.77	64.04	28	71.23	63.18
29	70.12	61.83	30	69.57	60.95
31	68.35	59.48	32	67.76	58.56
33	66.42	57.01	34	65.80	56.05
35	64.37	54.39	36	63.73	53.41
37	62.19	51.65	38	61.51	50.62
39	59.86	48.75	40	59.17	47.73
41	57.38	45.71	42	56.69	44.67
43	54.78	42.56	44	54.07	41.48
45	52.04	39.25	46	51.31	38.17
47	49.16	35.81	48	48.43	34.72
49	46.14	32.24	50	45.40	31.13
51	43.00	28.53	52	42.25	27.41
53	39.70	24.67	54	38.94	23.56
55	36.28	20.68	56	35.51	19.58
57	32.70	16.57	58	31.93	15.43
59	28.97	12.30	60	28.22	11.18
61	25.12	07.90	62	24.34	06.77
63	21.11	03.34	64	20.33	02.20
65	16.96	21998.63	66	16.13	21997.50
67	12.63	93.78	68	11.76	92.60
69	08.10	88.75	70	07.06	87.51
71	03.30	83.53	72	01.84	82.11
73		78.02	74		76.21

(1-9) Band

$^{80}Se_2$

J	R_{22}	P_{22}	J	R_{33}	P_{33}
1			2		
3			4		
5			6		
7			8		
9			10	22324.25	22321.31
11	22323.96	22320.73	12	23.73	20.20
13	23.37	19.58	14	23.08	19.02
15	22.62	18.27	16	22.30	17.66
17	21.74	16.84	18	21.37	16.17
19	20.73	15.26	20	20.31	14.54
21	19.58	13.55	22	19.11	12.79
23	18.27	11.71	24	17.76	10.84
25	16.84	09.70	26	16.24	08.85
27	15.26	07.57	28	14.63	06.69
29	13.55	05.31	30	12.93	04.36
31	11.71	02.88	32	11.05	01.91
33	09.70	00.33	34	09.03	299.34
35	07.57	297.64	36	06.86	96.61
37	05.31	94.81	38	04.57	93.75
39	02.88	91.84	40	02.13	90.77
41	00.33	88.70	42	299.57	87.64
43	297.64	85.46	44	96.86	84.38
45	94.81	82.09	46	94.01	80.96
47	91.84	78.57	48	91.03	77.42
49	88.70	74.90	50	87.91	73.75
51	85.46	71.09	52	84.66	69.95
53	82.09	67.16	54	81.27	66.01
55	78.57	63.11	56	77.73	61.91
57	74.90	58.88	58	74.07	57.70
59	71.09	54.52	60	70.25	53.32
61	67.15	50.01	62	66.30	48.82
63	63.05	45.34	64	62.22	44.18
65	58.82	40.57	66	57.98	39.37
67	54.42	35.62	68	53.58	34.48
69	49.87	30.53	70	49.01	29.34
71	45.16	25.30	72	44.25	24.07
73	40.26	19.90	74	39.24	18.64
75	35.14	14.26	76		12.94
77	29.71	08.50			
79		02.36			

(1-8) Band

$^{80}Se_2$

J	R_{22}	P_{22}	J	R_{33}	P_{33}
1			2		
3			4		
5			6		
7			8		
9			10		
11			12		
13	22693.13		14		
15	92.36	22688.04	16	22692.02	22687.40
17	91.46	86.58	18	91.08	85.90
19	90.44	84.98	20	89.99	84.26
21	89.23	83.27	22	88.78	82.49
23	87.93	81.39	24	87.40	80.57
25	86.48	79.35	26	85.90	78.50
27	84.87	77.18	28	84.26	76.30
29	83.12	74.91	30	82.49	73.97
31	81.22	72.46	32	80.57	71.48
33	79.21	69.87	34	78.50	68.85
35	77.05	67.14	36	76.30	66.10
37	74.74	64.26	38	73.97	63.20
39	72.29	61.24	40	71.48	60.15
41	69.68	58.09	42	68.85	56.97
43	66.95	54.79	44	66.10	53.65
45	64.06	51.35	46	63.24	50.20
47	61.04	47.76	48	60.20	46.60
49	57.84	44.03	50	57.03	42.86
51	54.56	40.18	52	53.72	39.00
53	51.10	36.18	54	50.24	34.97
55	47.50	32.03	56	46.64	30.81
57	43.76	27.74	58	42.90	26.51
59	39.89	23.30	60	39.00	22.08
61	35.86	18.71	62	34.97	17.49
63	31.70	13.98	64	30.81	12.75
65	27.38	09.10	66	26.51	07.88
67	22.89	04.09	68	22.03	02.85
69	18.26	598.92	70	17.37	597.68
71	13.46	93.58	72	12.52	92.33
73	08.39	88.09	74	07.41	86.78
75	03.26	82.31	76		80.98
77	597.73	76.51			
79		70.31			

	(1-8) Band		(0-7) Band	$^{78}Se_2$
J	R_{11}	P_{11}	R_{11}	P_{11}
10				
12				
14	23105.77	23101.62		
16	04.96	00.23		
18	03.99	098.70		
20	02.89	97.01		
22	01.62	95.18		
24	00.23	93.21	perturbed	
26	098.70	91.10		
28	97.01	88.84	23223.84	
30	95.18	86.44	22.04	23213.18
32	93.21	83.88	20.04	10.73
34	91.10	81.21	17.90	08.04
36	88.84	78.36	15.67	05.21
38	86.44	75.39	13.27	02.25
40	83.88	72.26	10.80	199.13
42	81.21	69.01	08.11	95.87
44	78.36	65.59	05.29	92.48
46	75.39	62.05	02.30	88.90
48	72.26	58.36	199.20	85.25
50	69.01	54.53	95.96	81.43
52	65.59	50.55	92.56	77.45
54	62.05	46.44	89.01	73.34
56	58.36	42.20	85.31	69.11
58	54.53	37.80	81.50	64.67
60	50.55	33.24	77.52	60.14
62	46.40	28.55	73.40	55.44
64	42.14	23.70	69.11	50.61
66	37.74	18.69	64.67	45.60
68	33.14	13.55	60.41	40.45
70	28.42	08.22	55.59	35.47
72	23.50	02.79	50.74	29.94
74		22997.17	45.75	24.39
76			40.65	18.69
78			35.34	12.85
80			29.94	06.86
82			24.39	00.76
84			18.69	094.47
86			12.85	88.06
88			06.86	81.50
90			00.76	74.78
92			094.47	67.94
94			88.06	60.96

$^{78}Se_2$

	(3-4) Band		(2-5) Band	
J	R_{11}	P_{11}	R_{11}	P_{11}
10	25103.89		24480.66	
12	03.24	25099.70	80.09	24476.52
14	02.45	98.36	79.34	75.20
16	01.51	96.85	78.43	73.74
18	00.41	95.18	77.37	72.08
20	099.14	93.36	76.18	70.32
22	97.72	91.37	74.81	68.39
24	96.13	89.23	73.29	66.31
26	94.38	86.91	71.62	64.08
28	92.45	84.44	69.81	61.68
30	90.35	81.79	67.83	59.13
32	88.03	78.96	65.70	56.42
34		75.91	63.42	53.58
36			60.99	50.56
38	81.23		58.38	47.41
40	78.24	66.95	55.64	44.09
42	75.17	63.24	52.75	40.62
44	71.98	59.45	49.69	37.01
46	68.63	55.53	46.50	33.21
48	65.14	51.45	43.13	29.29
50	61.49	47.24	39.61	25.21
52	57.69	42.85	35.93	20.98
54	53.73	38.33	32.11	16.59
56	49.62	33.64	28.12	12.04
58	45.34	28.79	24.00	07.35
60	40.89	23.77	19.72	02.51
62	36.29	18.59	15.28	397.49
64	31.54	13.26	10.69	92.34
66	26.61	07.75	05.94	87.04
68	21.52	02.09	01.04	81.58
70	16.26	24996.26	396.00	75.95
72	10.84	90.26	90.78	70.18
74	05.26	84.10	85.41	64.24
76	24999.52	77.78	79.90	58.15
78	93.60	71.26	74.21	51.91
80	87.52	64.61	68.40	45.48
82	81.24		62.40	
84	74.88		56.24	
86	68.30		49.94	
88	61.54		43.45	

$^{78}Se_2$

J	(7-1) Band R_{11}	(7-1) Band P_{11}	(4-3) Band R_{11}	(4-3) Band P_{11}
0				
2				
4				
6	27207.03			
8	06.66	27204.27		
10	06.07	03.17	25726.91	25723.84
12	05.35	01.86	26.22	22.71
14	04.41	00.36	25.41	21.32
16	03.32	198.72	24.41	19.77
18	02.05	96.89	23.24	18.05
20	00.59	94.89	21.95	16.18
22	198.96	92.70	20.50	14.14
24	97.15	90.34	18.82	11.89
26	95.16	87.79	17.03	09.55
28	92.99	85.07	15.06	07.01
30	90.64	82.17	12.91	04.31
32	88.11	79.09	10.60	01.45
34	85.41	75.84	08.14	698.39
36	82.52	72.38	05.51	95.22
38	79.45	68.77	02.70	91.87
40	76.21	64.98	699.74	88.33
42	72.78	61.01	96.62	84.61
44	69.17	56.84	93.30	80.77
46	65.38	52.50	89.83	76.71
48	61.42	47.98	86.21	72.52
50	57.27	43.28	82.35	68.15
52	52.93	38.38	78.34	63.59
54	48.41	33.31	74.14	58.86
56	43.71	28.08	69.62	53.90
58	38.81	22.62	64.72	48.70
60	33.73	17.01	62.89	43.06
62	28.42	11.24	57.33	40.49
64		05.21	52.07	34.20
66		099.00	46.81	28.25
68		92.60	41.48	22.29
70			35.99	16.17
72			30.34	09.97
74			24.87	03.61
76			18.65	597.44
78			12.51	90.45
80			06.24	83.61
82			599.79	
84			93.19	
86			86.40	

	(8-0) Band		(8-1) Band		$^{78}Se_2$
J	R_{11}	P_{11}	R_{11}	P_{11}	
0					
2					
4					
6	27826.96				
8	26.55	27824.23	27438.30	27435.98	
10	25.98	23.09	37.69	34.79	
12	25.19	21.77	36.91	33.47	
14	24.23	20.29	35.98	31.99	
16	23.09	18.56	34.86	30.32	
18	21.77	16.69	33.57	38.46	
20	20.29	14.61	32.09	26.41	
22	18.56	12.37	30.42	24.20	
24	16.69	09.93	28.56	21.80	
26	14.61	07.32	26.53	19.22	
28	12.37	04.52	24.32	16.45	
30	09.93	01.52	21.92	13.51	
32	07.32	798.34	19.33	10.37	
34	04.52	94.97	16.58	07.07	
36	01.52	91.42	13.61	03.56	
38	798.34	87.72	10.47	399.87	
40	94.97	83.80	07.15	96.00	
42	91.42	79.68	03.64	91.94	
44	87.66	75.39	399.93	87.69	
46	83.70	70.89	96.04	83.27	
48	79.58	66.21	91.98	78.63	
50	75.25	61.36	87.72	73.83	
52	70.72	56.30	83.27	68.85	
54	66.00	51.04	78.63	63.67	
56	61.09	45.58	73.79	58.30	
58	55.99	39.94	68.75	52.72	
60	50.67	34.08	63.50	46.95	
62	45.13	28.06	58.06	40.98	
64	39.40	21.73	52.40	34.81	
66	33.38	15.27	46.51	28.40	
68		08.59		21.79	

	(9-1) Band		(9-2) Band	$^{78}Se_2$
J	R_{11}	P_{11}	R_{11}	P_{11}
0				
2				
4				
6	27668.05	27666.11		27279.96
8	67.50	65.18	27281.33	79.02
10	66.90	63.99	80.73	77.86
12	66.11	62.65	79.96	76.53
14	65.18	61.12	79.09	75.05
16	63.99	59.44	77.86	73.37
18	62.65	57.54	76.53	71.51
20	61.12	55.46	75.05	69.45
22	59.44	53.20	73.37	67.20
24	57.54	50.72	71.51	64.70
26	55.46	48.02	69.45	62.10
28	53.20	45.22		59.35
30	50.72	42.28		
32	48.02	39.10		
34	45.22	35.68		
36	42.28	32.05		
38		28.30		

$^{78}Se_2$

J	(10-0) Band R_{11}	(10-0) Band P_{11}	(10-1) Band R_{11}	(10-1) Band P_{11}
12	28281.54	28270.14	27893.36	27889.85
14	80.60	76.57	92.44	88.43
16	79.47	74.89	91.33	86.73
18	78.23	73.03	90.06	84.89
20	76.69	70.99	88.58	82.91
22	74.99	68.77	86.92	80.70
24	73.12	66.37	85.09	78.31
26	71.08	63.79	83.06	75.74
28	68.83	60.99	80.86	72.98
30	66.40	58.02	78.48	70.05
32	63.79	54.85	75.91	66.95
34	60.99	51.53	73.14	63.61
36	58.02	47.98	70.19	60.14
38	54.85	44.24	67.07	56.47
40	51.53	40.32	63.86	52.59
42	47.98	36.26	60.31	48.63
44	44.24	31.95	56.62	44.40
46	40.32	27.48	52.74	40.00
48	36.26	22.85	48.70	35.40
50	31.95	18.00	44.40	30.60
52	27.43	12.98	40.00	25.62
54	22.78	07.77	35.40	20.46
56	17.89	02.35	30.60	15.09
58	12.82	196.76	25.62	09.55
60	07.60	90.98	20.46	03.79
62	02.13	84.98	15.09	797.91
64	196.49	78.80	09.55	91.81
66	90.70	72.42	03.79	85.53
68	84.59	65.85	797.82	79.05
70		59.09		72.35
72				
74	65.75		79.18	
76	58.87	37.99	72.41	51.54
78	51.85	30.38	65.51	44.04
80	44.68	22.63	58.43	36.37
82	37.28	14.74	51.15	28.59
84	29.73	06.63	43.69	20.56
86	21.96	098.35	36.03	12.38
88	14.01	89.88	28.19	04.00
90	05.90	81.20	20.13	695.42
92	097.55	72.33	11.92	86.66
94	89.03	63.27	03.48	77.71
96	80.30	54.02	694.87	68.56
98	71.35	44.56	86.04	59.23
100	62.32	34.91	77.06	49.68
102	52.97	25.09	67.88	40.02
104	43.44	15.06	58.49	30.13
106	33.71	04.80	48.90	20.03

	(11-0) Band		(11-1) Band	$^{78}Se_2$
J	R_{11}	P_{11}	R_{11}	P_{11}
0				
2				
4	28507.83	28506.55		
6	07.57	05.78	28119.37	28117.48
8	07.10	04.79	18.82	16.50
10	06.49	03.61	18.19	15.34
12	05.65	02.23	17.39	14.01
14	04.64	00.68	16.40	12.45
16	03.43	498.94	15.21	10.72
18	02.05	96.98	13.87	08.81
20	00.46	94.87	12.31	06.70
22	498.71	92.56	10.59	04.43
24	96.75	90.06	08.65	01.97
26	94.59	87.37	06.55	099.32
28	92.27	84.49	04.23	96.45
30	89.75	81.41	01.75	93.44
32	87.02	78.15	099.08	90.21
34	84.11	74.69	96.21	86.79
36	81.02	71.04	93.16	83.19
38	77.72	67.19	89.88	79.40
40	74.23	63.17	86.47	75.44
42	70.54	58.96	82.84	71.27
44	66.66	54.53	79.01	66.90
46	62.57	49.92	75.00	62.32
48	58.32	45.11	70.79	57.59
50	53.84	40.12	66.39	52.65
52		34.91		47.55
54				
56				
58				
60				
62	23.58		36.55	
64	17.66	00.23	30.71	13.30
66	11.61	393.59	24.73	06.72
68	05.36	86.82	18.58	00.02
70	398.91	79.86	12.21	27993.13
72	92.26	72.68	05.63	86.03
74	85.36	65.27	27998.83	78.72
76	78.22	52.63	91.77	71.18
78	70.81	49.75	84.50	63.44
80		41.58		55.43

$^{78}Se_2$

J	(12-0) Band R_{11}	(12-0) Band P_{11}	(12-1) Band R_{11}	(12-1) Band P_{11}
0				
2				
4	28729.63		28341.33	
6	29.37	28727.60	41.10	28339.27
8	28.94	26.62	40.65	38.32
10	28.32	25.45	40.07	37.16
12	27.50	24.08	39.27	35.82
14	26.47	22.52	38.26	34.25
16	25.27	20.77	37.08	32.56
18	23.86	18.84	35.71	30.65
20	22.28	16.69	34.12	28.53
22	20.49	14.37	32.32	26.22
24	18.49	11.85	30.38	23.72
26	16.43	09.11	28.35	21.03
28	14.11	06.22	26.07	18.17
30	11.54	03.25	23.54	15.24
32	08.79	699.92	20.85	11.96
34	05.85	96.47	17.93	08.56
36	02.71	92.77	14.82	04.91
38	699.35	88.89	11.49	01.07
40	95.81	84.81	08.02	297.03
42	92.06	80.54	04.34	92.80
44	88.13	76.07	00.45	88.38
46	84.01	71.40	296.38	83.78
48	79.69	66.55	92.11	78.97
50	75.16	61.47	87.66	73.97
52	70.44	56.21	82.98	68.77
54	65.50	50.76	78.14	63.40
56	60.35	45.09	73.03	57.79
58	55.06	39.20	67.84	51.98
60	49.44	33.18	62.29	46.03
62	43.67	26.83		39.77
64		20.36		
66	32.04			
68	25.64	07.19	38.82	20.37
70	19.05	00.10	32.33	13.38
72	12.22	592.77	25.59	06.16
74	05.28	85.24	13.73	198.70
76	597.98	77.53	11.51	91.09
78	90.24	69.51	03.90	83.17
80		61.06		74.80

$^{78}Se_2$

J	(13-0) Band R_{11}	(13-0) Band P_{11}	(13-1) Band R_{11}	(13-1) Band P_{11}
0				
2				
4		28947.79	28560.60	28559.40
6	28948.76	46.99	60.34	58.59
8	48.27	46.00	59.90	57.59
10	47.63	44.79	59.20	56.40
12	46.78	43.39	58.40	55.03
14	45.71	41.82	57.38	53.46
16	44.49	40.01	56.17	51.68
18	43.05	38.04	54.73	49.73
20	41.43	35.87	53.11	47.59
22	39.58	33.49	51.32	45.24
24	37.54	30.94	49.32	42.70
26	35.30	28.16	47.09	39.96
28	32.92	25.17	44.78	37.01
30	30.31	22.04	42.17	33.93
32	27.47	18.69	39.37	30.63
34	24.41	15.12	36.35	27.10
36	21.33	11.34	33.35	23.33
38	17.85	07.54	29.92	19.54
40	14.22	03.30	26.33	15.38
42	10.37	898.94	22.52	11.07
44	06.34	94.36	18.54	06.55
46	02.08	89.61	14.31	01.84
48	897.62	84.61	09.93	496.93
50	92.90	79.42	05.27	91.76
52	88.01	73.97	00.40	86.39
54		68.31		80.81
56	78.30			
58	72.64	57.18		
60	66.81	50.75		
62	60.63	44.17		
64	54.30	37.23		
66		30.20		
68				
70				
72			445.11	
74			37.92	418.23
76	17.06		30.46	10.29
78	09.41	788.59	22.90	02.10
80	01.58	80.22	15.97	393.82
82	793.53	71.63	07.23	85.36
84	85.28	62.87	399.08	76.69
86	76.96	53.89	90.81	67.85
88		44.87		58.70

(14-0) Band $^{78}Se_2$

J	R_{11}	P_{11}
0		
2		
4	29165.47	29164.28
6	65.20	63.48
8	64.73	62.45
10	64.03	61.22
12	63.15	59.79
14	62.07	58.17
16	60.76	56.34
18	59.25	54.31
20	57.51	52.09
22	55.48	49.60
24		46.87
26	52.23	
28	49.19	42.11
30	46.17	38.35
32	43.14	34.60
34	39.78	30.83
36		26.78
38		
40	31.00	
42	25.86	15.79
44		09.84
46	17.97	
48	13.86	00.50
50	09.03	095.65
52	04.02	90.09
54	098.45	84.35
56	93.66	78.04
58	87.73	72.52
60	82.31	65.92
62	76.75	59.69
64	69.86	53.39
66	63.57	45.75
68	57.24	38.73
70	51.54	31.70
72		25.26

___ marks last sharp line

(15-0) Band $^{78}Se_2$

J	R_{11}		P_{11}	
0				
2	29379.01		29378.32	
4	78.90		77.70	
6	78.61		76.89	
8	78.11		75.85	
10	77.40		74.60	
12	76.46		73.15	
14	75.23		71.50	
16		74.30	69.52	
18		72.68		67.87
20		70.90		65.50
22		68.89		62.99
24	67.17			60.25
26	64.60		57.79	
28	61.78		54.47	
30		59.44	50.93	
32		56.03		47.83
34	53.23			43.69
36	50.04		40.20	
38	46.45		36.22	
40	42.89		31.92	
42	38.77		27.63	
44	34.63		22.76	
46	30.34		17.81	
48	25.72		12.85	
50	20.97		07.52	
52	15.85		01.94	
54	10.73		296.42	
56	05.45		90.54	
58	299.90		84.38	
60	94.15		78.09	
62	88.09		71.44	
64	81.96		65.01	
66	76.00		57.95	

___ marks last sharp line

	$^{78}Se_2$ (16-0) Band		$^{78}Se_2$ (17-0) Band	
J	R_{11}	P_{11}	R_{11}	P_{11}
0				
2		29589.04		29796.25
4	29589.65	88.35	29796.82	95.59
6	89.31	87.58	96.49	94.74
8	88.78	86.51	95.94	93.74
10	88.07	85.30	95.21	92.43
12	87.13	83.84	94.37	91.00
14	86.04	82.20	93.12	89.34
16	84.69	80.32	91.76	87.41
18	83.17	78.25	90.20	85.33
20	81.42	75.94	88.42	82.98
22	79.45	73.50	86.43	80.52
24	77.34	70.80	84.22	77.76
26	74.95	67.90	81.77	74.85
28	72.35	64.80	79.14	71.70
30	69.68	61.55	76.38	68.32
32	66.62	58.02	73.34	64.78
34	63.44	54.34	70.02	60.96
36	60.06	50.37	66.56	56.92
38	56.53	46.25	62.94	52.81
40	52.66	41.91	59.02	48.36
42	48.62	37.32	54.90	43.79
44	44.37	32.58	50.59	38.99
46	39.93	27.69	46.14	33.88
48	35.37	22.50		28.74
50	30.47	17.13		
52	25.44	11.53		
54	20.28	05.75		
56	14.62	499.78		
58	09.07	93.55		
60	03.46	87.11		
62	497.31	80.57		

J	(18-0) Band $^{78}Se_2$		(19-0) Band $^{78}Se_2$	
	R_{11}	P_{11}	R_{11}	P_{11}
0				
2				
4	30000.44		30199.53	
6	00.08	29998.39	99.12	30197.43
8	29999.55	97.31	98.63	96.36
10	98.85	96.03	97.78	95.07
12	97.81	94.57	96.86	93.59
14	96.70	92.87	95.61	91.81
16	95.26	90.91	94.21	89.86
18	93.59	88.77	92.48	87.69
20	91.84	86.38	90.63	85.30
22	89.71	83.93	88.58	82.69
24	87.54	81.16	86.22	79.87
26	85.04	79.13	83.69	76.83
28	82.36	74.93	80.95	73.55
30	79.46	71.54	77.98	70.07
32	76.34	67.89	74.76	66.32
34	73.06	64.02	71.39	62.41
36	69.44	60.02	67.63	58.27
38	65.70	55.68	63.88	53.91
40	61.77	51.19	59.77	49.35
42	57.59	46.55	55.57	44.48
44	53.17	41.60	50.96	39.47
46	48.57	36.45	46.31	34.28
48	43.75	31.07	41.39	28.83
50	38.66	25.52	36.16	23.09
52	33.44	19.70	30.74	17.28
54	27.84	13.57	25.11	11.01
56	22.14	07.40	19.27	04.65
58	16.29	01.04	13.26	098.16
60			06.90	91.35
62			00.52	84.23

	(20-0) Band $^{78}Se_2$		(21-0) Band $^{78}Se_2$	
J	R_{11}	P_{11}	R_{11}	P_{11}
0				
2	30393.45			
4	93.32	30392.15		
6	92.91	91.32		
8	92.35	90.18		
10	91.52	88.79		
12	90.48	87.16		
14	89.22	85.46		
16	87.68	83.53	30573.42	30569.76
18	85.98	81.34	71.68	67.18
20	84.06	78.82	69.76	64.62
22	81.93	76.15	67.50	61.87
24	79.52	73.23	64.96	58.80
26	77.00	70.16	62.29	55.62
28	74.09	66.84	59.27	52.12
30	71.03	63.26	56.08	48.43
32	67.73	59.46	52.67	44.57
34	64.24	55.40	49.04	40.28
36	60.57	51.16	45.09	36.00
38	56.54	46.68	40.91	31.35
40	52.36	41.93	36.50	26.28
42	47.96	37.05	32.06	21.38
44	43.27	31.84	26.96	15.93
46	38.34	26.50	21.91	10.29
48	33.13	20.85	16.64	04.45
50	27.85	14.94	10.96	498.44
52	22.23	08.88	05.00	
54	16.55	02.61	499.03	
56	10.62	296.06		
58	04.26	89.45		
60	297.75	82.43		
62	91.08	75.06		
64	84.19	67.90		
66		60.08		

(0-9) Band

$^{78}Se_2$

J	R_{22}	P_{22}	J	R_{33}	P_{33}
1			2		
3			4		
5			6		
7			8		
9			10	22037.34	
11			12	36.84	22033.19
13	22036.48		14	36.23	32.09
15	35.78	22031.31	16	35.46	30.68
17	34.89	29.87	18	34.57	29.21
19	33.92	28.29	20	33.54	27.59
21	32.82	26.61	22	32.37	25.86
23	31.52	24.77	24	31.07	23.94
25	30.11	22.77	26	29.64	21.94
27	28.58	20.66	28	28.05	19.80
29	26.91	18.40	30	26.33	17.50
31	25.08	15.99	32	24.49	15.06
33	23.11	13.45	34	22.49	12.50
35	21.03	10.78	36	20.37	09.80
37	18.78	07.96	38	18.11	06.96
39	16.41	05.01	40	15.71	03.97
41	13.89	01.91	42	13.18	00.86
43	11.22	21998.67	44	10.51	21997.60
45	08.42	95.29	46	07.70	94.21
47	05.48	91.79	48	04.75	90.69
49	02.41	88.12	50	01.67	87.02
51	21999.18	84.33	52	21998.45	83.21
53	95.81	80.39	54	95.07	79.28
55	92.32	76.31	56	91.58	75.20
57	88.67	72.10	58	87.93	70.99
59	84.89	67.74	60	84.15	66.64
61	80.95	63.25	62	80.23	62.14
63	76.88	58.61	64	76.16	57.51
65	72.67	53.85	66	71.97	52.75
67	68.33	48.91	68	67.63	47.84
69	63.82	43.85	70	63.12	42.77
71	59.18	38.63	72	58.49	37.56
73	54.38	33.26	74	53.68	32.19
75	49.40	27.74	76	48.65	26.66
77	44.25	22.06	78	43.39	20.94
79	38.84	16.19	80		14.96
81	33.10				

(1-9) Band

$^{78}Se_2$

J	R_{22}	P_{22}	J	R_{33}	P_{33}
1			2		
3			4		
5			6		
7			8		
9			10		
11			12		
13			14		
15			16		
17			18		
19			20		
21			22		
23			24		
25			26	22276.46	22269.00
27	22275.41	22267.59	28	74.80	66.65
29	73.63	65.25	30	73.00	64.25
31	71.74	62.74	32	71.05	61.75
33	69.69	60.13	34	69.00	59.09
35	67.50	57.38	36	66.77	56.31
37	65.16	54.46	38	64.41	53.36
39	62.68	51.40	40	61.92	50.29
41	60.05	48.19	42	59.27	47.06
43	57.30	44.86	44	56.51	43.71
45	54.38	41.37	46	53.59	40.21
47	51.35	37.74	48	50.53	36.58
49	48.19	33.99	50	47.32	32.79
51	44.79	30.08	52	43.99	28.89
53	41.32	26.02	54	40.50	24.82
55	37.70	21.84	56	36.87	20.63
57	33.95	17.50	58	33.10	16.29
59	30.04	13.02	60	29.20	11.81
61	25.97	08.40	62	25.15	07.20
63	21.77	03.63	64	20.95	02.43
65	17.42	198.72	66	16.60	197.53
67	12.92	93.67	68	12.10	92.47
69	08.26	88.45	70	07.44	87.26
71	03.46	83.07	72	02.60	81.88
73	198.46	77.55	74	197.53	76.33
75	93.28	71.86	76		70.55
77	87.81	65.94			
79		59.78			

(1-8) Band

$^{78}Se_2$

J	R_{22}	P_{22}	J	R_{33}	P_{33}
1			2		
3			4		
5			6		
7			8		
9			10		
11			12		
13			14		
15	22657.28	22652.90	16		
17	56.39	51.39	18		
19	55.32	49.74	20	22654.81	22648.89
21	54.08	47.94	22	53.54	47.05
23	52.70	45.99	24	52.16	45.07
25	51.19	43.89	26	50.59	42.93
27	49.52	41.65	28	48.89	40.68
29	47.69	39.27	30	47.05	38.27
31	45.75	36.74	32	45.07	35.72
33	43.64	34.09	34	42.93	33.00
35	41.41	31.26	36	40.68	30.17
37	39.02	28.29	38	38.27	27.19
39	36.49	25.19	40	35.72	24.07
41	33.81	21.94	42	33.00	20.80
43	30.99	18.54	44	30.17	17.37
45	28.03	15.02	46	27.19	13.84
47	24.92	11.34	48	24.07	10.15
49	21.67	07.51	50	20.80	06.32
51	18.27	03.54	52	17.37	02.33
53	14.72	599.43	54	13.84	598.21
55	11.04	95.16	56	10.15	93.92
57	07.20	90.75	58	06.32	89.51
59	03.23	86.19	60	02.33	84.96
61	599.08	81.49	62	598.21	80.26
63	94.80	76.65	64	93.92	75.42
65	90.37	71.67	66	89.51	70.43
67	85.77	66.52	68	84.92	65.29
69	81.05	61.24	70	80.17	60.00
71	76.13	55.78	72	75.25	54.54
73	71.07	50.18	74	70.10	48.91
75	65.79	44.39	76		43.04
77	60.24	38.41			
79		32.13			

APPENDIX E

VACUUM WAVE NUMBERS OF LINES FOR ANALYSED BANDS OF ^{128}TeO

(0-4) Band $0^+ - 0^+$ $^{128}Te0$

J	R	P	J	R	P
17	24913.61	24894.35	63	24668.65	24600.01
18	11.52	91.28	64	59.87	590.18
19	09.26	87.99	65	50.89	80.18
20	06.88	84.57	66	41.83	70.01
21	04.49	81.02	67	32.52	59.72
22	01.90	77.30	68	23.17	49.28
23	899.17	73.45	69	13.63	38.66
24	96.12	69.45	70	03.86	27.96
25	93.18	65.32	71	594.06	16.97
26	89.97	61.03	72	84.03	05.93
27	86.58	56.60	73	73.84	494.73
28	83.09	52.01	74	63.49	83.38
29	79.50	47.28	75	53.12	71.84
30	75.72	42.38	76	42.40	60.20
31	71.82	37.38	77	31.60	48.37
32	67.69	32.19	78	20.76	36.40
33	63.54	26.90	79	09.56	24.24
34	59.09	21.51	80	498.36	11.98
35	54.65	15.90	81	86.96	399.60
36	49.93	10.08	82	75.40	87.01
37	45.13	04.25	83	63.72	74.30
38	40.20	798.28	84	51.75	61.40
39	35.12	92.11	85	39.72	48.44
40	29.89	85.78	86	27.56	35.12
41	24.55	79.30	87	15.27	21.72
42	18.92	72.76	88	02.75	08.15
43	13.29	66.02	89	389.99	294.51
44	07.47	59.11	90	77.01	80.82
45	01.38	52.04	91	64.48	66.74
46	795.43	44.90	92	51.35	52.27
47	89.10	37.49	93	37.91	38.56
48	82.71	30.06	94	24.54	24.03
49	76.13	22.39	95	10.86	09.37
50	69.47	14.62	96	297.05	194.62
51	62.54	06.67	97	83.04	79.72
52	55.55	698.62	98	69.01	64.64
53	48.40	90.39	99	54.75	49.23
54	41.07	82.01	100	40.36	33.78
55	33.66	73.60	101	25.77	18.22
56	26.07	64.82	102	10.94	02.55
57	18.33	56.03	103	196.19	086.47
58	10.46	47.06	104	80.91	70.55
59	02.43	37.96	105	65.71	54.39
60	694.17	28.69	106	50.29	37.93
61	85.81	19.28	107	34.72	21.40
62	77.32	09.73			

(0-5) Band $0^+ - 0^+$ ^{128}TeO

J	R	P
9	24167.24	
10	66.46	
11	65.40	24152.71
12	64.27	50.60
13	63.04	48.26
14	61.66	45.80
15	60.13	43.12
16	58.48	40.34
17	56.62	37.43
18	54.68	34.45
19	52.57	31.27
20	50.29	27.90
21	47.91	24.42
22	45.41	20.85
23	42.75	17.13
24	39.94	13.23
25	37.02	09.23
26	33.97	05.03
27	30.75	00.78
28	27.34	096.30
29	23.89	91.73
30	20.25	86.99
31	16.47	82.14
32	12.50	77.11
33	08.51	71.99
34	04.31	66.73
35	00.00	61.24
36	095.52	55.70
37	90.90	50.02
38	86.07	44.17
39	81.14	38.17
40	76.11	32.02
41	70.96	25.76
42	65.61	19.33
43	60.14	12.82
44	54.53	06.12
45	48.71	23999.28
46	42.83	92.32
47	36.78	85.22
48	30.60	77.95
49	24.25	70.54
50	17.80	63.02
51	11.18	55.37
52	04.43	47.50
53	23997.55	23939.53
54	90.47	31.42
55	83.29	23.16
56	75.97	14.73
57	68.47	06.17
58	60.86	897.51
59	53.08	88.69
60	45.16	79.72
61	37.12	70.65
62	28.91	61.37
63	20.55	51.95
64	12.06	42.40
65	03.46	32.68
66	894.62	22.86
67	85.66	12.92
68	76.63	02.74
69	67.42	792.48
70	58.02	81.98
71	48.46	71.46
72	38.80	60.74
73	28.90	49.80
74	19.00	38.86
75	08.96	27.70
76	798.62	16.43
77	88.21	04.94
78	77.60	693.36
79	66.90	81.59
80	56.05	69.70
81	44.91	57.71
82	33.86	45.52
83	22.44	33.20
84	11.10	20.67
85	699.43	08.04
86	87.63	595.18
87	75.71	82.23
88	63.68	69.13
89	51.44	55.88
90	38.73	42.54
91		28.88
92		14.89

Perturbation continued overleaf

(0-5) Band (continued)

J	R	P
	(perturbed branches)	
91	23626.82	
92	13.92	
93	01.06	23501.63
94	588.02	487.47
95	74.81	73.27
96	61.49	58.98
97	48.11	44.54
98	34.35	29.86
99	20.59	15.03
100	06.62	00.07
101	492.45	385.03
102	78.22	69.78
103	63.82	54.39
104	49.21	38.80
105	34.43	23.08
106	19.55	07.19
107	04.47	291.14
108	389.23	74.94
109	73.83	58.57
110	58.25	42.03
111	42.58	25.35
112	26.63	08.54
113	10.69	191.45
114	294.32	74.23
115	77.90	56.93
116		39.38
117		21.73

(0-6) Band $0^+ - 0^+$ ^{128}TeO

J	R	P	J	R	P
12	23415.03	23401.38	54	47.77	88.75
13	13.86	399.01	55	40.86	80.73
14	12.47	96.62	56	33.81	72.59
15	11.03	94.08	57	26.61	64.29
16	09.40	91.35	58	19.29	55.89
17	07.64	88.51	59	11.75	47.33
18	05.76	85.57	60	04.16	38.63
19	03.79	82.52	61	196.35	29.81
20	01.65	79.24	62	88.42	20.85
21	399.37	75.88	63	80.37	11.72
22	96.97	72.37	64	72.18	02.51
23	94.39	68.75	65	63.84	093.10
24	91.75	64.97	66	55.35	83.57
25	88.91	61.08	67	46.75	73.87
26	85.94	57.03	68	37.97	64.08
27	82.87	52.87	69	29.07	54.13
28	79.63	48.55	70	20.04	44.03
29	76.29	44.07	71	10.82	33.81
30	72.77	39.50	72	01.49	23.44
31	69.16	34.83	73	092.03	12.90
32	65.41	29.95	74	82.40	02.26
33	61.48	24.98	75	72.65	22991.52
34	57.44	19.84	76	62.73	80.55
35	53.25	14.57	77	52.65	69.42
36	48.92	09.16	78	42.46	58.22
37	44.48	03.63	79	32.13	46.88
38	39.92	297.96	80	21.64	35.37
39	35.25	92.19	81	11.02	23.72
40	30.35	86.24	82	00.19	11.93
41	25.36	80.17	83	22989.24	899.97
42	20.23	73.97	84	78.28	87.85
43	14.94	67.63	85	67.04	75.64
44	09.55	61.14	86	55.65	63.22
45	04.00	54.59	87	44.17	50.67
46	298.32	47.77	88	32.60	37.99
47	92.50	40.86	89	20.71	25.12
48	86.54	33.81	90	08.47	12.29
49	80.43	26.61	91	896.94	799.07
50	74.21	19.29	92	84.54	85.54
51	67.82	11.91	93	72.02	72.72
52	61.31	04.32	94	59.41	58.96
53	54.59	196.59	95	46.77	45.23

continued

(0-6) Band (continued)

J	R	P
96	22833.91	22731.34
97	20.88	17.34
98	07.81	03.20
99	794.38	688.88
100	80.85	74.40
101	67.25	59.79
102	53.48	45.02
103	39.54	30.12
104	25.45	15.05
105	11.20	599.83
106	696.80	84.42
107	82.26	68.91
108	67.50	53.20
109	52.63	37.38
110	37.59	21.37
111	22.48	05.22
112	07.07	488.87
113	591.54	72.40
114	75.87	55.75
115	60.09	38.99
116		22.03
117		04.91

(0-7) Band $0^+ - 0^+$ ^{128}TeO

J	R	P	J	R	P
9	22676.42		57	92.74	30.47
10	75.66		58	85.68	22.34
11	74.76	22662.14	59	78.46	14.05
12	73.75	60.10	60	71.12	05.65
13	72.61	57.83	61	63.61	397.11
14	71.32	55.46	62	56.02	88.40
15	69.96	52.98	63	48.22	79.60
16	68.41	50.33	64	40.36	70.67
17	66.75	47.56	65	32.34	61.63
18	64.98	44.72	66	24.19	52.39
19	63.03	41.71	67	15.87	43.04
20	60.97	38.62	68	07.45	33.50
21	58.80	35.31	69	398.87	23.92
22	56.44	31.93	70	90.11	14.16
23	54.00	28.41	71	81.27	04.27
24	51.47	24.73	72	72.30	294.28
25	48.79	20.97	73	63.16	84.09
26	45.91	17.07	74	53.90	73.78
27	42.98	12.99	75	44.48	63.33
28	39.88	08.81	76	34.87	52.75
29	36.62	04.51	77	25.26	42.03
30	33.32	00.10	78	15.44	31.17
31	29.84	595.48	79	05.48	20.18
32	26.24	90.78	80	295.37	08.99
33	22.48	85.94	81	85.13	197.70
34	18.60	80.97	82	74.72	86.32
35	14.59	75.87	83	64.23	74.76
36	10.43	70.66	84	53.54	63.07
37	06.16	65.28	85	42.68	51.25
38	01.76	59.79	86	31.76	39.25
39	597.20	54.22	87	20.59	27.16
40	92.52	48.47	88	09.46	14.88
41	87.74	42.57	89	197.95	02.47
42	82.77	36.55	90	86.18	090.02
43	77.72	30.39	91	75.05	77.20
44	72.51	24.12	92	63.07	64.14
45	67.16	17.71	93	51.11	51.73
46	61.72	11.17	94	38.97	38.44
47	56.10	04.48	95	26.72	25.18
48	50.36	497.69	96	14.35	11.73
49	44.52	90.75	97	01.72	21998.22
50	38.50	83.68	98	089.02	84.57
51	32.34	76.47	99	76.23	70.78
52	26.09	69.14	100	63.24	
53	19.69	61.65	101	50.06	
54	13.14	54.07	102	36.78	
55	06.48	46.34	103	23.29	
56	499.67	38.46	104	09.69	

(1-4) Band $0^+ - 0^+$ ^{128}TeO

J	R	P
19	25353.26	25332.19
20	50.77	28.67
21	48.00	24.90
22	45.12	21.00
23	42.09	16.84
24	39.00	12.65
25	35.63	08.25
26	32.19	03.72
27	28.67	299.02
28	24.90	94.20
29	21.00	89.27
30	16.93	84.10
31	12.72	78.84
32	08.35	73.43
33	03.85	67.89
34	299.19	62.15
35	94.36	56.29
36	89.35	50.18
37	84.27	43.96
38	78.96	37.56
39	73.54	31.15
40	67.99	24.57
41	62.15	17.71
42	56.29	10.83
43	50.18	03.65
44	43.96	196.42
45	37.56	88.99
46	31.07	81.38
47	24.39	73.63
48	17.55	65.73
49	10.55	57.68
50	03.36	49.44
51	196.07	41.10
52	88.61	32.58
53	80.97	23.91
54	73.17	15.14
55	65.24	06.09
56	57.24	096.99
57	48.95	87.66
58	40.59	78.24
59	32.03	68.61
60	23.40	58.82

J	R	P
61	14.53	49.03
62	05.46	38.93
63	096.28	28.77
64	86.98	18.32
65	77.55	07.80
66	67.96	24997.18
67	58.23	86.40
68	48.44	75.50
69	38.45	64.27
70	28.37	53.21
71	18.24	41.85
72	07.97	30.46
73	24997.63	18.96
74	87.15	07.28
75	76.67	895.56
76	66.15	83.83
77	55.54	72.00
78	44.81	60.07
79	34.07	48.09
80	23.31	36.11
81	12.34	24.11
82	01.39	11.94
83	890.34	799.62
84	79.12	87.35
85	67.69	74.97
86	56.17	62.54
87		49.65
88		36.81

Perturbation

(1-5) Band $0^+ - 0^+$ ^{128}TeO

J	R	P
18	24598.92	
19	96.66	24575.72
20	94.06	72.21
21	91.48	68.55
22	88.85	64.64
23	85.82	60.62
24	82.79	56.54
25	79.51	52.27
26	76.28	47.86
27	72.77	43.30
28	69.22	38.65
29	65.39	33.83
30	61.48	28.80
31	57.43	23.63
32	53.17	18.36
33	48.84	12.96
34	44.31	07.29
35	39.69	01.63
36	34.89	495.81
37	29.93	89.75
38	24.84	83.56
39	19.62	77.25
40	14.18	70.75
41	08.60	64.16
42	02.92	57.37
43	497.03	50.44
44	91.02	43.39
45	84.80	36.20
46	78.54	28.79
47	72.16	21.31
48	65.44	13.59
49	58.68	05.78
50	51.75	397.83
51	44.68	89.70
52	37.45	81.44
53	30.06	73.04
54	22.55	64.48
55	14.97	55.74
56	07.08	46.87
57	399.10	37.91
58	90.98	28.64
59	82.73	19.33
60	74.30	09.86
61	65.74	00.18
62	57.05	290.40
63	48.21	80.52
64	39.16	70.47
65	30.06	60.26
66	20.74	49.89
67	11.35	39.43
68	01.83	28.84
69	292.24	18.11
70	82.45	07.21
71	72.61	196.34
72	62.67	85.22
73	52.65	73.99
74	42.53	62.70
75	32.42	51.37
76	32.27	39.94
77	12.03	28.50
78	01.75	17.00
79	191.42	05.38
80	80.91	093.78
81	70.27	82.14

(1-6) Band $0^+ - 0^+$ ^{128}TeO

J	R	P
33	23801.91	
34	797.54	
35		23755.01
36	88.21	49.27
37	83.57	43.46
38	78.65	37.42
39	73.56	31.29
40	68.50	25.03
41	63.03	
42	57.39	
43	51.92	05.28
44	46.04	
45	40.18	691.40
46		84.28
47		
48	21.38	
49		61.96
50		54.14
51	01.35	46.39
52	694.29	38.29
53	87.26	30.18
54		21.90
55	72.58	
56	64.98	04.76
57	57.35	
58		587.09
59	41.48	78.03
60	33.20	68.87
61	25.05	59.49
62	16.70	50.02
63	08.04	40.34
64		30.62
65	590.54	20.79
66	81.58	10.78
67	72.48	00.63
68	63.23	490.31
69	54.01	79.88
70		69.31
71	35.02	
72	25.40	47.95
73	15.64	37.10
74		26.15
75		15.03

(0-3) Band 1 - 1 ^{128}TeO

J	$R_{e\ \&\ d}$	$P_{e\ \&\ d}$
1		
2		
3		
4		
5		
6		
7		
8		
9		
10		
11		
12		
13		
14		
15		
16	25283.64	
17	81.77	
18	79.79	
19	77.61	25256.15
20	75.30	52.56
21	72.91	49.04
22	70.32	45.32
23	67.52	41.52
24	64.72	37.67
25	61.63	33.42
26	58.45	29.14
27	55.17	24.83
28	51.74	20.17
29	48.15	15.41
30	44.44	10.61
31	40.47	05.60
32	36.48	00.46
33	32.33	195.27
34	28.04	89.74
35	23.58	84.29
36	18.96	78.52
37	14.20	72.68
38	09.25	66.66
39	04.29	60.57

..continued

(0-3) Band (continued)

J	R_c	P_c	R_d	P_d
40	25199.14	25154.25	25199.14	25154.25
41	93.75	47.82	93.75	48.07
42	88.18	41.48	88.18	41.48
43	82.69	34.49	82.69	34.82
44	76.82	27.68	76.92	27.96
45	70.93	20.65	71.15	20.98
46			65.16	13.82
47			58.76	06.52
48	52.38		42.38	099.05
49	45.83	091.41		91.33
50	39.21	83.53	39.77	83.64
51	32.30	75.55	32.96	
52	24.95	67.47	25.94	
53		59.28	18.70	60.00
54		50.48	11.67	51.70
55	03.86	42.88	04.29	43.28
56	096.28	34.15	096.74	34.65
57	88.64	25.41	89.14	25.89
58	80.76	16.45	81.28	16.99
59	72.74	07.36	73.36	07.97
60	64.58	24998.15	65.29	24998.83
61	56.24	88.70	57.10	89.58
62	47.66	79.21	48.79	80.22
63	38.99	69.43	40.22	70.52
64	30.39	59.63	31.53	60.66
65	21.40	49.70	22.71	50.84
66	12.31	39.51	13.77	40.80
67	03.01	29.12	04.66	30.46
68	24993.48	18.63	24995.38	20.23
69	83.68	07.96	85.81	09.75
70	73.87	897.09	76.40	899.17
71	63.56	86.07	66.68	88.30
72	53.44	74.77	56.72	77.30
73	42.89	63.27	46.72	66.32
74	31.94	51.58	36.64	55.04
75	20.96	39.72	26.32	43.76
76		27.45	15.84	32.23
77			05.15	20.47
78			894.35	08.60
79			83.51	796.70
80			72.37	84.57
81				72.22
82				59.57

(0-4) Band 1 - 1 ^{128}TeO

J	$R_{c\ \&\ d}$	$P_{c\ \&\ d}$
1		
2		
3		
4		
5	24528.28	24522.20
6	27.96	20.77
7	27.62	19.31
8	27.07	17.67
9	26.36	15.85
10	25.53	13.93
11	24.52	11.84
12	23.43	09.59
13	22.20	07.29
14	20.77	04.79
15	19.31	02.19
16	17.67	499.39
17	15.85	96.54
18	13.93	93.48
19	11.84	90.30
20	09.59	86.99
21	07.29	83.51
22	04.79	79.89
23	02.19	76.20
24	499.39	72.36
25	96.54	68.29
26	93.48	64.16
27	90.30	59.86
28	86.99	55.41
29	83.51	50.86
30	79.89	46.12
31	76.20	41.28
32	72.36	36.30
33	68.29	31.15
34	64.16	25.90
35	59.86	20.49
36	55.41	15.07
37	50.86	09.40
38	46.12	03.47
39	41.28	397.47

...continued

(0-4) Band (continued)

J	R_c	P_c	R_d	P_d
40	24436.40	24391.56	24436.40	24391.56
41	31.15	85.44	31.15	85.44
42	25.90	79.03	25.90	79.03
43	20.49	72.48	20.49	72.48
44	14.88	65.74	15.07	66.03
45	09.25	58.93	09.40	59.20
46	03.47	51.99	03.47	52.28
47		44.88	397.47	45.19
48	91.27	37.65	91.27	37.91
49	85.02	30.54		30.54
50	78.56	22.83	79.03	22.97
51	71.94	15.13	72.48	
52	64.85	07.31	65.74	08.15
53		299.33	58.93	00.18
54		90.80	51.99	292.04
55	44.54	83.49	44.88	83.85
56	37.21	75.01	37.65	75.46
57	29.75	66.47	30.30	66.99
58	22.22	57.82	22.83	58.40
59	14.50	49.02	15.13	49.64
60	06.59	40.05	07.31	40.77
61	298.54	30.99	299.33	31.70
62	90.40	21.76	91.24	22.61
63	82.00	12.33	82.94	13.28
64	73.51	02.86	74.63	03.85
65	64.85	193.14	66.08	194.19
66	56.01	83.30	57.46	84.51
67	47.05	73.28	48.63	74.63
68	37.85	63.04	39.73	64.64
69	28.45	52.71	30.62	54.52
70	18.93	42.16	21.42	44.20
71	09.12	31.45	12.03	33.78
72	199.13	20.57	02.53	23.20
73	88.90	09.40	192.83	12.50
74	78.39	098.07	82.99	01.58
75	67.80	86.47	73.05	090.60
76	56.75	74.59	63.04	79.42
77	45.41	62.61	52.71	68.12
78	33.97	50.30	42.37	56.70
79		37.61	31.72	45.04
80			20.85	33.26
81				21.40

(0-5) Band 1 - 1 ^{128}TeO

J	$R_{c\,\&\,d}$	$P_{c\,\&\,d}$
1		
2		
3		
4		
5	23769.69	
6	69.45	
7	69.04	23760.74
8	68.50	59.04
9	67.87	57.39
10	67.14	55.43
11	66.22	53.43
12	65.17	51.28
13	63.96	48.98
14	62.65	46.56
15	61.18	43.99
16	59.64	41.32
17	57.93	38.49
18	56.05	35.55
19	54.11	32.44
20	52.04	29.24
21	49.80	25.89
22	47.36	22.44
23	44.91	18.79
24	42.21	15.03
25	39.42	11.10
26	36.53	07.12
27	33.47	02.97
28	30.27	698.71
29	26.96	94.29
30	23.50	89.70
31	19.92	85.02
32	16.24	80.20
33	12.34	75.24
34	08.35	70.17
35	04.25	64.98
36	699.98	59.63
37	95.57	54.14
38	91.04	48.49
39	86.38	42.71

...continued

(0-5) Band (continued)

J	R_c	P_c	R_d	P_d
40	23681.59	23636.82	23681.59	23636.82
41	76.66	30.76	76.66	30.85
42	71.58	24.54	71.58	24.70
43	66.37	18.25	66.37	18.45
44	61.02	11.80	61.02	12.00
45	55.53		55.53	05.36
46	50.25		49.95	598.65
47	44.23		44.23	91.80
48	38.36		38.23	84.81
49	32.22	577.63		77.63
50	26.02	70.25	26.58	70.25
51	19.61	62.81	20.14	
52	12.73	55.24	13.65	55.88
53		47.49	07.03	48.11
54		39.23	00.31	40.34
55	593.17	32.11	593.50	32.37
56	86.14	23.90	86.49	24.31
57	78.97	15.64	79.42	16.12
58	71.67	07.26	72.16	07.78
59	64.20	498.72	64.78	499.30
60	56.60	90.07	57.25	90.73
61	48.91	81.25	49.59	81.99
62	40.99	72.35	41.77	73.17
63	32.96	63.22	33.85	64.13
64	24.72	53.99	25.78	54.98
65	16.37	44.54	17.56	45.72
66	07.78	35.04	09.22	36.28
67	499.16	25.35	00.73	26.74
68	90.31	15.51	492.14	17.02
69	81.25	05.48	83.37	07.23
70	71.97	395.24	74.44	397.26
71	62.60	84.91	65.43	87.15
72	52.94	74.29	56.25	76.92
73	43.03	63.54	46.92	66.53
74	32.94	52.51	37.44	56.00
75	22.59	41.31	27.82	45.34
76	11.99	29.95	18.14	34.53
77	01.07	18.20	08.26	23.64
78	389.93	06.19	398.22	12.57
79	78.59	294.00	88.06	01.40
80	66.94	81.54	77.74	289.97
81		68.91	67.38	78.50
82		55.97		66.85
83				55.19

(0-6) Band 1 - 1 ^{128}TeO

J	$R_{e\,\&\,d}$	$P_{e\,\&\,d}$
1		
2		
3		
4		23014.04
5	23019.06	12.90
6	18.77	11.60
7	18.44	10.11
8	17.97	08.54
9	17.35	06.81
10	16.63	04.98
11	15.76	02.99
12	14.78	00.93
13	13.66	22998.71
14	12.44	96.36
15	11.02	93.86
16	09.56	91.27
17	07.89	88.50
18	06.17	85.66
19	04.30	82.66
20	02.26	79.53
21	00.19	76.25
22	22997.86	72.89
23	95.46	69.42
24	92.91	65.74
25	90.26	61.97
26	87.46	58.08
27	84.57	54.04
28	81.50	49.88
29	78.28	45.63
30	75.00	41.20
31	71.56	36.68
32	68.03	32.01
33	64.30	27.21
34	60.47	22.30
35	56.50	17.22
36	52.43	12.05
37	48.20	06.73
38	43.85	01.29
39	39.38	895.71

...continued

(0-6) Band (continued)

J	R_c	P_c	R_d	P_d
40	22934.78	22889.99	22934.78	22889.99
41	29.93	84.15	29.93	84.15
42	25.18	78.19	25.18	78.19
43	20.17	72.02	20.17	72.13
44	15.00	65.79	15.00	65.90
45	09.71	59.41	09.80	59.55
46	04.07	52.87	04.39	53.10
47	898.92	46.24	898.83	46.50
48	93.21	39.24	93.05	39.67
49	87.34	32.73		32.73
50	81.36	25.63	81.90	25.63
51	75.17	18.45	75.64	
52	68.51	11.13	69.45	11.79
53	63.11	03.61	63.22	04.25
54	56.48	795.61	56.69	796.68
55	49.82	88.79	50.09	89.03
56	43.02	80.85	43.37	81.24
57	36.15	72.86	36.54	73.29
58	29.11	64.73	29.55	65.23
59	21.93	56.49	22.46	57.05
60	14.63	48.10	15.21	48.72
61	07.18	39.54	07.81	40.23
62	799.58	30.92	00.34	31.71
63	91.86	22.14	792.73	22.98
64	83.96	13.19	84.95	14.16
65	75.87	04.17	77.06	05.21
66	67.70	694.87	69.04	696.11
67	59.32	85.48	60.85	86.84
68	50.76	75.99	52.54	77.51
69	42.06	66.29	44.09	68.00
70	33.15	56.44	35.54	58.35
71	24.07	46.41	26.83	48.60
72	14.76	36.11	17.98	38.62
73	05.21	25.72	09.05	28.68
74	695.47	15.05	699.93	18.50
75	85.48	04.19	90.67	08.21
76	75.22	593.14	81.38	597.76
77	64.67	81.78	71.79	87.16
78	54.00	70.20	62.14	76.52
79	42.98	58.34	52.31	65.65
80		46.23	42.36	54.67
81		33.96		43.56
82				32.34

Perturbation

..continued

(0-6) Band (continued)

J	R_c	P_c	R_d	P_d
81	22636.62	22533.96	22632.47	22543.56
82	26.15		22.15	32.34
83	15.56	24.94	11.80	20.99
84	04.86	13.14	01.33	09.40
85	594.04	01.22	590.68	497.69
86	83.09	489.24	79.87	85.89
87	72.03	77.10	68.91	73.98
88	60.79	64.84	57.85	61.91
89	49.42	52.46	46.55	49.58
90	37.75	39.93	35.06	37.19
91	26.09	27.22		24.61
92		14.33		11.80
93		01.35		

(0-7) Band 1 - 1 ^{128}TeO

J	$R_{e\ \&\ d}$	$P_{e\ \&\ d}$
1		
2		
3		
4		
5	22276.49	22270.29
6	76.26	68.99
7	75.93	67.56
8	75.51	66.01
9	74.97	64.35
10	74.27	62.57
11	73.47	60.65
12	72.54	58.61
13	71.50	56.44
14	70.29	54.17
15	68.99	51.74
16	67.56	49.21
17	66.01	46.52
18	64.35	43.73
19	62.57	40.84
20	60.65	37.90
21	58.61	34.74
22	56.44	31.46
23	54.17	28.10
24	51.74	24.55
25	49.21	20.90
26	46.52	17.12
27	43.73	13.21
28	40.84	09.12
29	37.76	05.00
30	34.58	00.71
31	31.28	196.32
32	27.87	91.80
33	24.29	87.18
34	20.59	82.41
35	16.82	77.52
36	12.93	72.51
37	08.86	67.33
38	04.69	62.10
39	00.38	56.69

...continued

(0-7) Band (continued)

J	R_c	P_c	R_d	P_d
40	22195.96	22151.11	22195.96	22151.11
41	91.40	45.51	91.40	45.51
42	86.74	39.76	86.74	39.76
43	81.95	33.82	81.95	33.93
44	77.00	27.77	77.00	27.94
45	71.92	21.63	71.95	21.79
46	66.51	15.37	66.78	15.52
47	61.61	08.90	61.46	09.11
48	56.09	02.17	55.88	02.59
49	50.48	095.91	49.53	095.91
50	44.72	89.02	45.19	89.02
51	38.81	82.09	39.25	81.25
52	32.39	74.99	33.29	75.63
53	27.16	67.72	27.16	68.33
54	20.87	60.02	21.03	61.04
55	14.48	53.33	14.74	53.65
56	07.98	45.78	08.24	46.07
57	01.35	38.04	01.72	38.44
58	094.60	30.22	095.00	30.63
59	87.71	22.18	88.20	22.72
60	80.69	14.11	81.25	14.67
61	73.50	05.89	74.13	06.53
62	66.19	21997.56	66.91	21998.22
63	58.77	89.07	59.61	89.87
64	51.18	80.42	52.13	81.38
65	43.45	71.74	44.55	72.74
66	35.54		36.78	
67	27.50		28.99	
68	19.28		20.98	
69	10.89		12.89	
70	02.29		04.64	
71	21993.57		21996.29	
72	84.57		87.82	
73	75.45		79.22	
74			70.50	

References

1. Messerschmitt, J., Z.Wiss.Photogr., 1907, 5, 249.
2. Rosen, B. and Désirant, M., Bull.Acad.Roy.Belg., 1935, 21, 223, 436 and 723.
3. Rosen, B. and Montfort, F., Physica, 1936, 4, 257.
4. Rosen, B., Désirant, M. and Neven, L., Nature, 1936, 137, 498.
5. Minne, A., Bull.Soc.Roy.Sci.Liège, 1937, 6, 254.
6. Neven, L., Bull.Soc.Roy.Sci.Liège, 1937, 6, 257.
7. Asundi, R.K. and Parti, Y.P., Proc.Ind.Acad., 1937, 6A, 207.
8. Moraczewska, M., Z.Physik, 1930, 62, 270.
9. Olsson, E., Z.Physik, 1934, 90, 138.
10. Nevin, T.E., Phil.Mag., 1935, 20, 347.
11. Olsson, E., The Band Spectra of Sulphur, Selenium and Tellurium, 1938.
12. Rosen, B., Physica, 1939, 6, 205.
13. Davis, S.P., Thesis, University of California, Berkeley, 1954.
14. Davis, S.P. and Jenkins, F.A., Phys.Rev., 1951, 83, 1269.
15. Leelavathi, V. and Rao, P.T., Ind.J.Phys., 1955, 29, 1.
16. Chandler, G.G., Part II Thesis, Oxford, 1963.
17. Bhatnagar, S.S., Lessheim, H. and Khanna, M.L., Nature, 1937, 140, 152.
18. Kramers, H.A., Z.Physik, 1929, 53, 422.
19. Van Vleck, J.H., Phys.Rev., 1929, 33, 467.
20. Hebb, M.H., Phys.Rev., 1936, 49, 610.

21. Kovács, I., Phys.Rev., 1962, 128, 663.

22. Schlapp, R., Phys.Rev., 1937, 51, 342.

23. Barrow, R.F. and Deutsch, E.W., Proc.Phys.Soc., 1963, 82, 548.

24. Herman, L. and Herman, R., Nature, 1963, 199, 795.

25. Ittmann, G.P., Naturwiss, 1934, 22, 118.

26. Richards, W.G. and Barrow, R.F., Proc.Phys.Soc., 1964, 83, 1045.

27. Klein, O., Z.Physik, 1932, 76, 226.

28. Mulliken, R.S., J.Chem.Phys., 1960, 33, 247.

29. Oldenburg, O., Z.Physik, 1929, 56, 563.

30. Rice, O.K., Phys.Rev., 1930, 35, 1538 and 1551.

31. Schmid, R. and Gerö, L., Z.Physik, 1937, 104, 724.

32. Mörikofer, W., Dissertation, Basle, 1925.

33. Bengtsson-Knave, E. and Rydberg, R., Z.Physik, 1930, 59, 540.

34. Farkas, L., Z.Physik, 1931, 70, 733.

35. Herzberg, G. and Mundie, L.G., J.Chem.Phys., 1940, 8, 263.

36. Schmid, R. and Gerö, L., Csillagaszati Lapok, 1943, 6, 3.

37. Kovács, I. and Budó, A., J.Chem.Phys., 1947, 15, 166.

38. Herzberg, G., Lagerqvist, A. and Miescher, E., Canad.J.Phys., 1956, 34, 622.

39. Frackowiak, M., Bull.Acad.Polon.Sci., 1964, 12, 361.

40. Barrow, R.F. and Stamper, J.G., Proc.Roy.Soc., 1961, 263, 259.

41. du Parcq, R.P., Part II Thesis, Oxford, 1965.

42. Powell, F.X. and Lide, D.R.jr., J.Chem.Phys., 1964, 41, 1413.

43. Barrow, R.F. and Ketteringham, J., Canad.J.Phys., 1963, 41, 419.

44. Ketteringham, J., Thesis, Oxford, 1964.

45. Goldfinger, P., Jeunehomme, M. and Rosen, B., Nature, 1936, 138, 205.

46. Mulliken, R.S., Phys.Rev., 1940, 57, 500.

47. Mulliken, R.S., Rev.Mod.Phys., 1931, 3, 89.

48. Herzberg, G., Spectra of Diatomic Molecules, Van Nostrand, Toronto, 1963.

49. Townes, C.H. and Schlawlow, A.L., Microwave Spectroscopy, McGraw Hill, New York, 1955.

50. Choong, S-P., Ann.Phys.Paris, 1938, 10, 173.

51. Haranath, P.B.V., Rao, P.T. and Sivaramamurty, V., Z.Physik, 1959, 155, 507.

52. Purbrick, R.L., J.Chem.Phys., 1959, 30, 962.

53. Barrow, R.F. and Hurst, H.J., Nature, 1964, 201, 699.

54. Hurst, H.J., Thesis, Oxford, 1965.

55. Fry, P.W., Thesis, Oxford, 1964.

56. Barrow, R.F., Deutsch, J.L. and Travis, D.N., Nature, 1961, 191, 374.

57. Heimer, A., Z.Physik, 1935, 95, 328.

58. Milton, E.R.V., Dunford, H.B. and Douglas, A.E., J.Chem.Phys., 1961, 35, 1202.

59. Rodney, W.S. and Spindler, R.J., J.Res.Nat.Bur.Stds., 1954, 53, 185.

60. Richards, E.W.T., Thomas and Weinstein, A.E.R.E. C/R 2338, 2152 and 2163.

61. Thorne, R.P., Reid, C.D. and Robinson, I., U.K.A.E.A. (Capenhurst) DEG Report 141(CA)

62. Fastie, W.G., J.Opt.Soc.America, 1952, 42, 641.

63. Jarrell, R.J., J.Opt.Soc.America, 1955, 45, 259.

64. Pierce, A.K., J.Opt.Soc.America, 1957, 47, 6.

65. Minkowsky, Astrophys. J., 1942, 96, 306.

66. Gaydon, A.G., Dissociation Energies, Chapman & Hall, London, 1953.

67. Détry, D., Mémoire presenté au Concours Universitaire, 1963-64.

68. Massen, C.H., Weijts, A G.L.M. and Poulis, J.A., Trans.Far.Soc., 1964, 60, 317.

69. Moore, C.E., Circ.Nat.Bur.Stds., 1952, 467.

70. Jeunehomme, M., Thèse, Université Libre de Bruxelles, 1962.

71. Porter, R.F., J.Chem.Phys., 1963, 34, 583.

72. Crespin, D., Grandjean, J. and Sapin, G., Bull.Soc.Roy.Sci.Liège, 1937, 6, 261.

73. Rouppert, S., Compt.Rend., 1937, 204, 1723.

74. Heil, O., Z.Physik, 1932, 74, 18.

75. Benard, J., Physica, 1935, 2, 328.

76. Rompe, R., Z.Physik, 1936, 101, 214.

77. Rosen, B., Acta Physica Polonica, 1936, 5, 193.

78. Barrow, R.F. and du Parcq, R.P., Elemental Sulphur, ed. C.B. Meyer, John Wiley, New York, 1965.

79. Kenty, C., Phys.Rev., 1946, 69, 36.

80. Herman, R. and Herman, L., J.Phys.Rad., 1950, 11, 69.

81. Herman, R., Compt.Rend., 1946, 222, 492.

82. Tolnas, E.L., Bull.Am.Phys.Soc., 1959, 4, 67.

83. Cooper, C.D., Phys.Rev., 1958, 109, 2026.

84. Cooper, C.D., Cobb, G.C. and Tolnas, E.L., J.Mol.Spect., 1961, 7, 223.

85. Jacques, J.K., Thesis, Oxford, 1959.

86. Jameson, C.J. and Gutowsky, H.S., J.Chem.Phys., 1964, 40, 2285.

87. Templeton, D.H., Zalkin, A., Forrester, J.D. and Williamson, J.M., J.Am.Chem.Soc., 1963, 85, 242.

88. Jortner, J., Wilson, E.G. and Rice, S.A., J.Am.Chem.Soc., 1963, 85, 814.

89. Herman, R. and Herman, L., Nature, 1962, 193, 156.

90. Mulliken, R.S., Phys.Rev., 1930, 36, 1440.

91. Ketteringham, J.M. and Barrow, R.F., Proc.Phys.Soc., 1964, 83, 330.

92. Choong, S.P., Compt.Rend., 1936, 203, 239.

93. Migeotte, R., Bull.Soc.Roy.Sci.Liège, 1941, 10, 658.

94. Åslund, N., Arkiv för Fysik, to be published.

95. Cissane, W.J.M., Thesis, Oxford, 1965.

96. Haranath, P.B.V., J.Mol.Spect., 1964, 13, 168.

ACKNOWLEDGEMENT

The author wishes to thank the following:

Dr. R.F. Barrow for continual help and encouragement during his supervision of this work.

Dr. E.W.T. Richards of A.E.R.E. Harwell who kindly made available the use of his laboratory for some photographic work.

Catherine for patient help in the preparation and typing of this thesis.

D.S.I.R. for a maintenance grant.